REPUBLIQUE DU CAMEROUN

****

Paix-Travail-Patrie

****

Ecole Nationale Supérieure des Travaux Publics

****

DEPARTMENT DE GENIE CIVIL

DEPARTMENT OF CIVIL ENGINEERING

****

REPUBLIC OF CAMEROON

****

Peace-Work-Fatherland

****

UNIVERSITÀ DEGLI STUDI DI PADOVA

****

DEPARTMENT OF CIVIL, ARCHITECTURAL AND ENVIRONMENTAL ENGINEERING

****

ALTERNATIVE COST-EFFECTIVE SOLUTIONS FOR BRIDGE ABUTMENT CONSTRUCTION ON SOFT SOILS: CASE STUDY OF THE SECOND BRIDGE OVER THE WOURI RIVER

A thesis submitted in partial fulfilment of the requirement for the degree of Master of Engineering (MEng) in Civil Engineering

Curriculum: Geotechnical Engineering

Presented by:

AMBE Julius MFORLEM

Student Number: 16T21142

Supervised by:

Pr. Simonetta COLA

ACADEMIC YEAR: 2020-2021

To

My parents, Mr and Mrs Mforlem Emmanuel Ambe

ACKNOWLEDGEMENT

Words are inadequate to express my gratitude to the Almighty God, who is the ultimate source of wisdom and power. I am deeply indebted to my supervisor, **Pr. Simonetta COLA.** Her guidance and discussions added to my intellectual growth. Her valuable comments and suggestions on my project shaped my thinking greatly and helped make this work its best version.

Special thanks to:

- The President of the jury, for dedicating time to chairing this thesis defence.
- The Examiner of this thesis defence, for his availability and wise counsel, gave after going through this piece of work.
- **Pr. NKENG George ELAMBO**, Director of the National Advanced School of Public Works (NASPW) Yaoundé, for his unwavering commitment to providing standard engineering education.
- **Pr. MBESSA Michel**, the head of the Civil Engineering Department, for his effort to see that the work is completed on schedule and for his fatherly wise counsel.
- **Eng. POUEMI Parfait,** for his dedication, guidance, and commitment to making sure this piece of work becomes a reality.

My utmost appreciation and gratitude go to my siblings, Dr Che Gilbert Ambe, Mrs Ngwabie Odette nee Ambe, and Ms Ambe Mercy Ngum. They deserve special recognition for their selflessness, guidance, and unwavering support throughout my schooling and life. To all of my classmates and friends, thank you for the motivation and encouragement. We have been able to overcome mountains as a team.

LIST OF SYMBOLS

A_S	Area of stone column
c	Cohesion
c'	Effective cohesion
c_c	Compression index
c_r	Recompression index
c_s	Swelling index
c_u	Undrained shear strength
c_α	Coefficient of secondary consolidation
e	Void ratio
E	Young's Modulus
e_0	In situ void ratio
e_{eod}	Oedometric modulus
G	Shear modulus
H_0	Initial thickness of soil strata
k	Bulk modulus
k_0	Coefficient of at-rest earth pressure
k_h	Horizontal Permeability of stone column
k_{ac}	Active earth pressure generated by the material of the stone column
k_v	Vertical permeability of stone column
s_c	Secondary settlement
s_{eod}	Oedometric settlement
s_h	Horizontal settlement of stone column
s_i	Primary settlement
s_v	Vertical settlement of soil reinforced with stone column
s_α	Secondary consolidation
v	Poisson's ratio
z	Soil depth
γ	Unit weight of homogeneous soil
γ_{dry}	Dry unit weight of homogeneous soil
γ_w	Unit weight of water
σ'_o	Effective overburden pressure at the centre of the strata
σ'_h	Effective horizontal stress

σ'_v	Effective horizontal stress
$\Delta\sigma'_z$	Increase in pressure at the middle of the strata due to external loading
φ	Soil friction angle

LIST OF ABBREVIATIONS

ASTM	American society for testing and material
CAD	Computer-aided design
CPT	Cone penetrometer test
FEA	Finite element analysis
FEM	Finite element Method
LI	Liquidity Index
LL	Liquid limit
MSL	Mean sea level
OCR	Over consolidation ratio
PI	Plasticity index
PL	Plastic limit
PVD	Prefabricated vertical drains
SBT	Soil behaviour type
USCS	Unified soil classification system

ABSTRACT

The main objective of this thesis was to find a cost-effective way to stabilise the soft soil beneath the abutment wall of the second bridge over the Wouri River. Construction projects face difficulties when they encounter soft soil. Due to the high compressibility, poor shear strength, and low permeability of these soils with a consequence of long consolidation time, structures built on them crumble due to excessive settlement, which is sometimes differential. To meet project requirements, foundations built on these soils are frequently extremely expensive. To accomplish this objective, reinforcement of this soil with stone columns and prefabricated vertical drains (PVD) were adopted. To represent the abutment, an embankment load with surcharging was applied to the soft soil to estimate soil settlement before reinforcement was applied. The reinforcement using these methods was done to satisfy the serviceability use of the bridge. For this part of the structure, the fixed criteria consist of limiting the total settlement to less than 5 cm in 10 years. Analytical computation of settlement using MS Excel was used as a control method. The numerical computation was done using the finite element analysis software PLAXIS 2D V20.02. The interspacing between the stone column and PVD designs was chosen by fixing the consolidation time to less than 18 months. In the end, a cost-benefit analysis was conducted to determine which of the two soil reinforcement methods was most efficient. The soil settlement without reinforcement was 0.865 m, with a consolidation time of 2050 days. The rate of dissipation of the excess pore pressure increased when the soil sample was reinforced using prefabricated vertical drains, decreasing the settlement time for the project by 79.4% to 427 days. Soil reinforcement with stone columns kept soil settlement to a maximum of 4.46 cm (a 96% reduction from the initial settlement without any reinforcement). From the results of the cost-benefit analysis, employing columns to reinforce soil would cost 41% more than utilising PVDs to do so. Compared to prefabricated vertical drains, stone columns were 50% more effective at cutting down on construction time. From the results, PVDs are more effective when working on projects with severe budgetary restrictions, whereas stone column reinforcement is better for projects with limited time.

Keywords: Soil reinforcement, stone column, prefabricated vertical drains, consolidation

RESUME

L'objectif principal de cette mémoire de fin d'études était de trouver un moyen rentable de stabiliser le sol compressible sous la culée du second pont sur le fleuve Wouri. Les projets de construction sont confrontés à des difficultés lorsqu'ils rencontrent un sol compressible. En raison de la forte compressibilité, de la faible résistance au cisaillement et de la faible perméabilité de ces sols à laquelle s'associe une durée de consolidation longue, les ouvrages construits sur ces derniers s'effondrent en raison d'un tassement excessif. Pour répondre aux exigences du projet, les fondations construites sur ces sols sont souvent extrêmement coûteuses. Dans but d'atteindre de cet objectif, le renforcement de ces sols avec des colonnes de ballasts et des drains verticaux préfabriqués a été adopté. Pour représenter la culée, une charge de remblai avec surcharge a été appliquée au sol compressible pour estimer le tassement du sol avant le renforcement. Le renforcement en utilisant ces méthodes a été fait pour satisfaire l'état limite de service de l'ouvrage qui consiste en la limitation du tassement à 5 cm après 10 ans de vie de l'ouvrage. Le calcul analytique du tassement à l'aide de MS Excel a été effectué comme méthode de contrôle. Le calcul numérique a été effectué à l'aide du logiciel d'analyse d'éléments finis PLAXIS 2D V20.02. L'espacement entre les colonnes de ballasts et les drains verticaux préfabriqués a été choisi en fixant le temps de consolidation à moins de 18 mois. Finalement, une analyse coût-bénéfice a été menée pour déterminer laquelle des deux méthodes de renforcement du sol était la plus efficace. Le tassement du sol sans renforcement était de 0.865 m, avec une durée de consolidation de 2050 jours. Le taux de dissipation de l'excès de pression interstitielle a augmenté lorsque l'échantillon de sol a été renforcé à l'aide de drains verticaux préfabriqués, diminuant le temps de tassement du projet de 79,4 % à 427 jours. Le renforcement du sol par des colonnes ballasts a permis de maintenir le tassement du sol à un maximum de 4,46 cm (une réduction de 96 % au tassement initial sans traitement de terrain). D'après les résultats de l'analyse coût-bénéfice, l'utilisation de colonnes pour renforcer le sol coûterait 41% de plus que l'utilisation des drains verticaux préfabriqués pour le faire. Par rapport aux drains verticaux préfabriqués, les colonnes ballastées étaient 50% plus efficaces pour réduire la durée du projet. D'après les résultats, les drains verticaux préfabriqués sont plus efficaces lorsque l'on travaille sur des projets avec des restrictions budgétaires, tandis que le renforcement par des colonnes ballastées est préférable pour les projets à temps limité.

Mots clés : Renforcement du sol, colonne ballastée, drains verticaux préfabriqués, consolidation

LIST OF FIGURES

LIST OF TABLES

TABLE OF CONTENT

GENERAL INTRODUCTION

Construction on soft soil is a significant challenge in the field of geotechnical engineering. Due to the low shear strength and high compressibility of these soils, many engineering problems such as slope instability, bearing capacity failure, and excessive settlement could develop during or after the construction phase (Huat et al., 2005) (Mohamad et al., 2016). With the growing population, urbanisation, and economic activities, it is nearly impossible to avoid constructing structures on these types of soils. The City of Douala, like many coastal cities around the world, is built on soft soil deposits. As a result, the cost of construction in these areas has skyrocketed due to the numerous construction approaches required to bring the soil foundation up to project specifications. Deep foundations and piles have recently been employed as the foundation for several noteworthy constructions in the area, including the abutment wall built for the second bridge over the Wouri River. To lower the cost of buildings in these places, cost-effective foundation reinforcement techniques have been developed in recent years. Soil reinforcement techniques such as prefabricated vertical drains (PVD), stone column preloading, or a mix of some of these techniques are included. This strategy also reduces the amount of time required for construction. The main focus of this study will be to stabilise the soil beneath the abutment wall of Douala's second bridge over the Wouri River. The study's main reinforcement methods will be the use of PVD coupled with preloading and the usage of stone columns. Finally, a comparative analysis will be performed to determine which method is most suited for use in this area.

The study would be divided into three chapters to achieve the goals. The first chapter will be devoted to the literature review. The methodology of work will be expounded in the second chapter. The analytical and numerical approaches to the soil reinforcement techniques chosen (using PLAXIS 2D version 20.02) will be detailed. The third chapter culminates with a presentation of the site visit and project documentation outcomes, as well as the geometrical and geotechnical data gathered. The findings of the analytical and numerical designs will be presented in this section. The numerical design findings will provide information on how the embankment will behave in both unreinforced and reinforced circumstances. The evolution of the settlement for different situations, excess pore water pressure, and the study of consolidation end times will be the major data required to evaluate the efficacy of the proposed solution mentioned in this work.

CHAPTER 1. LITERATURE REVIEW

Introduction

Construction on soft soils has become inevitable due to the increasingly demanding economy and the continued increase in the population. Construction on these soils causes one of the greatest challenges in the field of geotechnical engineering. They have specific properties such as a large void ratio, high water content, high compressibility, low shear strength, low permeability, and special structural features that require significant attention for the analysis, design, and maintenance of geotechnical structures founded on them (Wang & Zhang, 2019). Among the different methods used to ameliorate the properties of these soils' consolidation time are soil reinforcement techniques. A proper study of these reinforcement techniques would require knowledge of some concepts. The following paragraphs in this chapter will cover an overview of soft soils, their characteristics and classification, and a review of soft soil stabilisation techniques. Moreover, a brief behaviour of abutment bridges on soft soils will be discussed eventually.

1.1. Soils

To the civil engineer, soil is any uncemmented or weakly cemented accumulation of mineral particles formed by the weathering of rocks as part of the rock cycle; the void space between the particles contains water and/or air. Weak cementation can be due to carbonates or oxides precipitated between the particles or due to organic matter (Knapetts & Criag, 2012). It is the unconsolidated material composed of solid particles produced by the disintegration of rocks. The void space between the particles may contain air, water, or both. Soil nature can be altered by the appropriate manipulation. Vibrations, for example, can transform loose sand into a dense one. Hence, the behaviour of soil in the field depends not only on the significant properties of individual constituents of the soil mass (Terzaghi et al., 1996).

1.1.1. Soil constituents

Soils are regarded as three-phase materials in geotechnical engineering, consisting of mineral particles, water, and air. As seen in figure 1.1, the soil void is the space between mineral particles that hold water and air. Gravel and sand fractions (coarse particles or granular particles), and silt or clay fractions (fine or cohesive particles) are present alone or mixed with organic matter in a limitless variety of compositions.

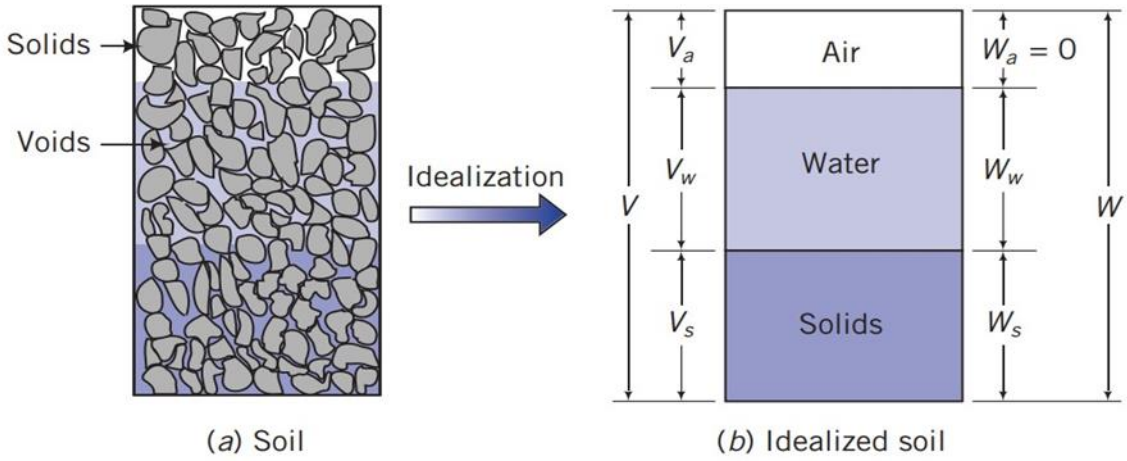

Figure 1.1. Soil phase diagram (Budhu, 2011)

1.1.1. Soil typology

Different soil types result from the weathering of rocks, which might be physical or chemical. Soils were determined based on the grain size distribution and the origin of the soils.

1.1.1.1. Soil classification using grain size distribution

Soil particles are characterised as cobbles, gravel, sand, silt, and clay based on their grain size. Gravel is made up of grains with sizes ranging from 4.75 mm to 76.2 mm. The soil is described as sand if the granules are visible to the human eye but are less than 4.75 mm in size. The lower limit of grain visibility for the naked eye is 0.075 mm. Silt refers to soil grains that are between 0.075 mm and 0.002 mm in size, whereas clay refers to soil grains that are finer than 0.002 mm (Murthy, 2003). Sands, gravels, and cobbles make up coarse-grained soils. Clays and silts are examples of fine-grained soils. Soils with coarse granules appear granular. Fine-grained soils appear to have a smooth surface, with the dominant minerals in fine-grained soils impacting their mechanical behaviour (Budhu, 2011).

1.1.1.2. Soil classification is based on the origin of the soil

Based on the origin of their constituents, soils can be divided into two large groups; residual soils and transported soils.

a. Residual soils

Residual soils are those that have remained at their formation site as a result of parent rock weathering. The depth of residual soil is mostly determined by climatic conditions and exposure duration. This depth could be significant in some regions. Residual soils in temperate zones are typically stiff and solid. The ambiguity of grain sizes is an important property of

residual soil. Because of the partially disintegrated condition, the amount passing through any given sieve size varies heavily on the time and energy used in shaking a leftover sample.

b. Transported soils

Soils that have been transported are those that have been discovered in sites that are far from where they were formed. Glaciers, wind, and water are the agents that move such soil. The soils are named for the kind of transportation used to transfer them. Alluvial soils are those that have been carried downstream by flowing water. Lacustrine soils are those that have been deposited in tranquil lakes. Marine soils are those that have been deposited in the sea. Aeolian soils are those that are carried and deposited by wind. Colluvial soils are those that are deposited predominantly by gravitational force, such as in landslides. The soils deposited by glaciers are known as glacial soils. Many of these transported soils are loose and soft to a depth of several hundred feet.

1.2. Soft Soils

Soft soil is a typical concept, that is generally referred to as soft plastic, or plastic soil with a large amount of water, high compressibility, low shear strength and weak bearing capacity (Zhao, 2018) (Wang et al., 2019). A clear description of soft soils can be done with the study of their properties and classification.

1.2.1. Properties of soft soils

Soft soil properties play a role when it comes to its engineering behaviour. The soil index properties, compression properties, strength properties and deformation properties play a great role in the behaviour of the soil under loading. Understanding these different properties is therefore essential in the study of soft soils.

1.2.1.1. Index Properties of soft soil

The index parameters are a measure of the physical behaviour of soil under different conditions. The index properties of soft soils are affected to some extent by the index parameters which are related to their geological history, mineralogical composition, the amount of clay fraction, the structure and distribution of the grains, and the texture of the grains (Kempfert & Gebreselassie, 2006). Table 1.1 shows the characteristic groups of index parameters. Index properties of soft soils share a common characteristic with other properties like the deformation and strength properties of soft soils. The undrained shear strength of clay can be computed from the liquidity index *(LI)* or the plasticity index *(PI),* while the compression index of shear strength can be obtained from the liquid limit *(LI).* The principal minerals in clay deposits tend

to influence their engineering behaviour. For example, the plasticity of clay soil is influenced by the amount of its clay fraction and the type of clay minerals present, since clay minerals greatly influence the amount of attracted water held in the soil. The amount of clay minerals present in clay influences the undrained shear strength.

Table 1.1. Characteristic index properties of fine-grained soils.(Kempfert & Gebreselassie, 2006)

Characteristics	Factors considered to have a relation with soil strength
Grain size	Grain size distribution, maximum grain size, mean grain size, coefficient of uniformity, shape of particles, content of fine fraction.
Density	Void ratio, relative density, dry density, specific gravity.
Plasticity	Liquid limit, plastic limit, shrinkage limit, plasticity index, consistency index, liquidity index.
Moisture	Natural moisture content and degree of saturation.
Texture	Type, proportion and structure of minerals and organic matter
Stress history	Age of deposition, number and magnitude of stress change experience, weathering, and physio-chemical effects

1.2.1.2. Compression properties of soft soil

Compression behaviour is a fundamental aspect of soil deformation, and modelling compression behaviour generally forms the basis of modelling the stress-strain relationships of soils. The compression behaviour of soft soils is somewhat different to that of coarse-grained soils (Terzaghi, 1943). Soft soils in the early stages of compression (viscous state) exhibit large strain and minimal pore pressure dissipation. As a result, the compression of soft soils at very low effective loads is determined by the initial water content of the soil (Win, 2015). Compression of soft soils can be grouped into the initial settlement, primary and secondary compression. The total settlement observed in soft soil over time is the sum of all 3 settlement stages represented in equation 1.1

$$S = S_i + S_c + S_\alpha \tag{1.1}$$

Where:

S_i is the immediate settlement

S_c is the primary consolidation settlement,

S_α is the secondary consolidation settlement.

a. Immediate settlement (S_i)

The immediate settlement (also known as the initial or undrained settlement) occurs soon after a load is applied, and if the soil is saturated, the shear strains beneath the loaded area generate continual volume deformation. When the clay has a low permeability, there is little drainage. Local yield (contained plastic flow) occurs when the shear stress in a spot of the soil mass is particularly high compared to the shear strength during undrained loading (Balasubramaniam & Brenner, 1981). The most common method for predicting immediate settlements is to use linear elastic theory. Christian and Carter proposed the computation of immediate settlement using the linear elastic theory. It is represented in equation 1.2. with its parameters read from a graph. A correction factor is applied to the fine soil layer to get the layer consolidation settlement (See appendix 1). The total immediate settlement is calculated by adding all the settlements of the different layers.

$$S_e = \mu_0 \mu_1 \frac{q_0 B}{E_u} \tag{1.2}$$

Where:

B, L is the Width and length of the footing,

q_o is the pressure at the foot base,

μ_0 is the coefficient function of D/B,

μ_1 is the coefficient function of H/B and L/B,

H is the thickness of the foundation layer,

D is the depth of the base,

E_u the young modulus in undrained condition.

b. Primary compression (consolidation settlement) (S_C)

Consolidation settlement arises because the hydraulic gradient of excess pore pressure set up by the applied load causes the water to drain out from the soil while the stress increment is transferred to the soil skeleton. Application of loads to a soft sample will cause a reduction in its volume caused by a reduction in the void ratio of particles in the soil. For soils that are saturated, the load is initially carried by the pore water which causes an excess pore pressure to develop. The excess pore pressure dissipates at a rate that depends on the permeability of the

soil mass, and the length of the maximum drainage path, and the load is eventually transferred to the soil structure. The component of such a deformation is described as irrecoverable or plastic. The ratio of the horizontal effective stress to the vertical effective stress is known as the coefficient of earth pressure at rest K_0, as represented in equation 1.3.

$$K_0 = \frac{\sigma_h'}{\sigma_V'} \tag{1.3}$$

Where:

$k_0 =$ earth pressure coefficient,

$\sigma_h' =$ effective horizontal stress,

$\sigma_v' =$ effective vertical stress.

The equation normally used for computing primary consolidation settlement S_c depends on the over consolidation ratio (OCR) of the compressed soil. OCR refers to the ratio between the highest soil stress state of the soil in the soil history to the present stress state of the soil. It is represented in equation 1.4.

$$S_C = \Delta H = \frac{\Delta e}{1+e_0} = \begin{cases} \frac{H_0}{1+e_0} C_c \, log \frac{\sigma_o' + \Delta\sigma_z'}{\sigma_o'} & if\ OCR = 1 \\ \frac{H_0}{1+e_0}\left(C_r \, log \frac{\sigma_c'}{\sigma_0'} + C_c \, log \frac{\sigma_o^i + \Delta\sigma_z'}{\sigma_o'}\right) & if\ OCR > 1 \end{cases} \tag{1.4}$$

Where:

e_0= in situ void ratio,

H_O=Initial thickness of soil strata,

σ_o'=effective overburden pressure at the centre of the strata,

$\Delta\sigma_z'$ =increase in pressure at the middle of the strata due to external loading from elastic theory,

C_r = recompression index,

The compression index C_c is determined in the laboratory or can be calculated using the formula in equation 1.5.

$$C_c = \frac{\Delta e}{\Delta \, log \, \sigma_{z'}} \tag{1.5}$$

To calculate the consolidation we need first calculate the stress increment $\Delta\sigma'_z$. Osterberg's formula provides a method for the calculation of the stress increment is represented in equation 1.6.

$$\Delta\sigma_z = \frac{q_o}{\pi}\left(\frac{B_1+B_2}{z}\right)(\alpha_1+\alpha_2) - \frac{B_1}{B_2}(\alpha_2) = Iq_0 \quad (1.6)$$

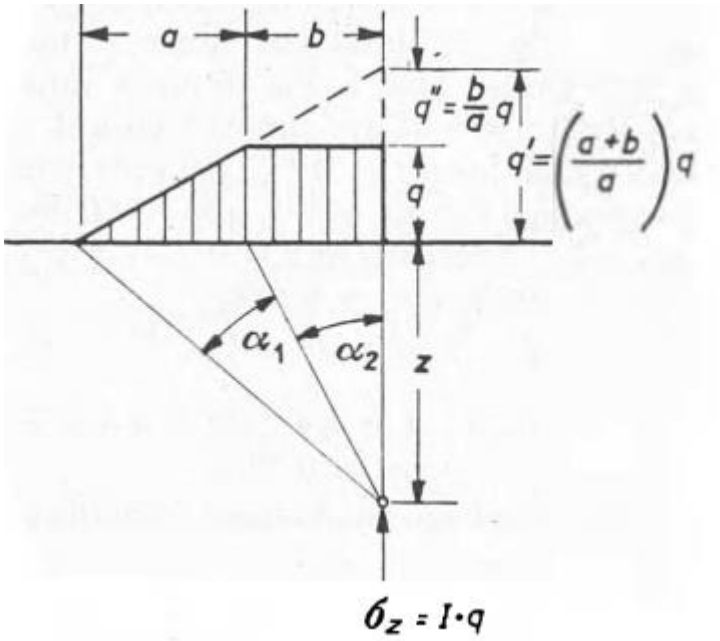

Figure 1.2. Influence of the embankment on consolidation settlement (Osterberg, 1957)

The correction factor proposed by (Skempton & Bjerrum, 1984) is used to correct the primary consolidation settlement represented in equation 1.7.

$$S_c = \beta S_{eod} \quad (1.7)$$

Where:

β depends on the type of soil, the foundation geometry and the H/B ratio,

H = layer thickness,

B = foundation width.

c. Secondary consolidation (creep)

Secondary consolidation may occur due to the rearrangement of soil particles or soil creep. Creep deformation is small compared to primary consolidation and is time dependent which is not caused exclusively by changes in effective stress. The relationship between void ratio and logarithm of time during secondary compression is usually linear for most soils over the time range after the completion of primary consolidation. The coefficient of secondary

compression is defined in equation 1.8. It begins theoretically at the end of the primary consolidation settlement but in reality, it begins at about the time when 95% of the primary consolidation has been done. The computation of secondary consolidation is represented analytically in equation 1.9. One of the main causes of the post-construction settlement is the creep of soil (Zhou et al., 2021). Some compression tests have shown that the creep coefficient decreases with the increase of OCR (Hu et al., 2014).

$$c_{\propto} = 0.0145.e_0^{1.555} \tag{1.8}$$

$$s_{\alpha} = \frac{H_0}{1+e_o} c_{\alpha}\ log\frac{t}{t_P} \tag{1.9}$$

1.2.1.3. Strength properties of soft soil

According to (Mitchell & Soga, 2005) the shearing resistance of a soil depends on many factors, and a complete equation might be of the form:(see equation 1.10)

$$\text{Shearing resistance} = f(e, \varphi, C, \sigma', c, H, T, \varepsilon, \dot{\varepsilon}, S) \tag{1.10}$$

Where:

e =Void ratio,

φ = soil friction angle,

C = Soil composition,

σ' = Soil effective stress,

c =cohesion,

H =soil stress history,

T =temperature,

ε =strain,

$\dot{\varepsilon}$ =strain rate,

S= soil structure,

Over time, many ways of measuring the strength of soft soils have developed. In most cases, a Mohr-Coulomb failure envelope, where shear strength is plotted as a function of the direct effective stress on the failure plane, or a modified Mohr diagram, in which maximum shear stress is plotted versus the average of the major and minor principal effective stresses at failure is used. The Mohr-Coulomb equation can be written as:

$$\tau = c + \sigma tan\,\varphi \tag{1.11}$$

Where:

τ= Shear strength,

c= Cohesion,

σ= Total compressive stress,

φ= Angle of internal friction.

This equation may also be written in the form of effective parameters as:

$$\tau = c' + \sigma' tan\, \varphi' \quad (1.12)$$

c'= Cohesion,

σ′= Effective compressive stress,

φ'= Soil friction angle,

shear strength increases with an increase in effective stress. Soil composition affects the friction angle, which is greatest for the non-clay mineral quartz, followed in descending order by kaolinite, iolite, and montmorillonite (Mitchell & Soga, 2005). The total strength of clay is composed of two distinct parts: a cohesion that depends only on the void ratio (water content), and a frictional contribution, dependent only on normal effective stress.

1.2.1.4. Deformation properties of soft soil

Soil deformation is one of the most important physical aspects in all geotechnical analyses The Young's modulus E, the Poisson's ratio v, the shear modulus G, and the bulk modulus K constitutes the material properties of soil responsible for deformation. The shear modulus G and the bulk modulus K can be written in terms of the young modulus E and Poisson's ratio represented in equations 1.13 and 1.14.

$$G = \frac{E}{2(1+v)} \quad (1.13)$$

$$K = \frac{E}{3(1+2v)} \quad (1.14)$$

1.2.2. Soft soil classification

There are many types of soil which range from hard, dense, rocks with large pieces, gravel, sand, silt, and clay to soft organic deposits and peat soil with high compressibility (Mitchell & Soga, 2005). While standards based on particle size distribution may apply to coarse-grained soils, the approach based exclusively on textural principles is ineffective in classifying fine-grained soils, where clay content and its mineralogy dictate the general properties (Moreno-Maroto et al., 2021). There are several systems and methods used in classifying soft soils. The most commonly used systems are the Unified Soil Classification System (USCS), and Piezocone Soil Classification.

1.2.2.1. Unified Soil Classification System (USCS)

The unified soil classification system is based on the engineering properties of soils and is most appropriate for earthwork construction. This system has evolved since its inception by Casagrande. The USCS emphasises particle size and uses the percentage retained on sieve No. 200(75 µm) to separate coarse-grained soils (more than 50% retained) from fine-grained soil. (More than 50% passing)(Park & Santamarina, 2017)(ASTM, 2011) The sub-classification of fine-grained soils into silt/clay or highly plastic/medium-plastic can conveniently be done by the use of Atterberg limits (Kim & Kim, 2018). Fine-grained soils are classified based on their coordinates of liquid limit (LL) and Plasticity Index (PI) on Casagrande's plasticity chart as seen in figure 1.3a. Figure 1.3b shows a chart that separates inorganic clay soils into zones above and below the A-line. The U-line specifies the possible upper limit based on the LL and PI. According to (ASTM, 2011), silts and clays can be further classified as high (H) or low (L) plasticity based on the exceedance of the liquid limit of 50%. Recognising the USCS symbols of classification gives an idea of the approximate permeability, shear strength, and volume change potential of the soil and how it may be affected by water, frost and other physical conditions. Table 1.2 presents a chart showing the classification of soils using the USCS symbols

Table 1.2. Classification of fine-grained soils and their symbols based on USCS (ASTM, 2017)

USCS Symbol	Description
ML	Inorganic silts, very fine sands, rock flour, silty or clayey fine sands
CL	Inorganic clays of low to medium plasticity, gravelly/sandy/lean clays
OL	Organic clays and organic silty clays of low plasticity
MH	Inorganic silt, micaceous or diatomaceous fine sands or silts, elastic silts
CH	Inorganic clays or high plasticity, fat clays
OH	Organic clays of medium to high plasticity

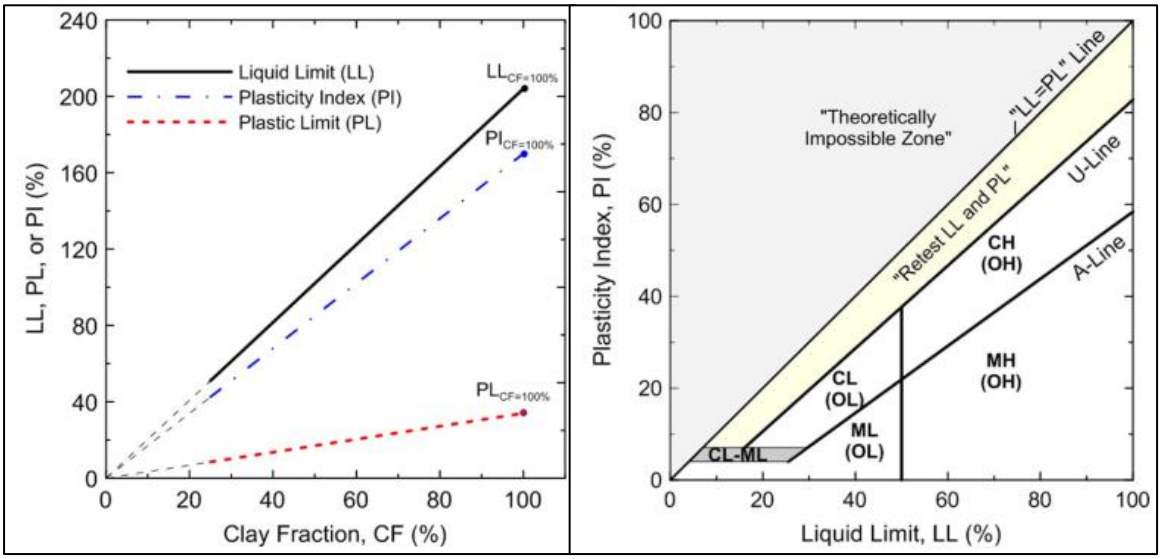

Figure 1.3. (A)Linearly proportional relationships of LL, PL, and PI with increasing Clay fractions. (B)Casagrande's plasticity chart and fine-grained soil classification. (Kim & Kim, 2018)

1.2.2.2. Soil classification based on penetrometer test results

The piezocone or cone penetrometer test is an in-situ soil testing method used to determine the geotechnical engineering properties of soil and assess subsurface stratigraphy, relative density, strength, and equilibrium groundwater pressure using the cone penetrometer test (CPT). One of the major applications of the CPT has been the determination of soil stratigraphy and the identification of soil (Robertson, 1989). Early charts using friction ratios were proposed by (Douglas & Olsen,1981) and (Cheng-hou et al., 1990) but the chart proposed by Robertson (1986) has become very popular. According to the CPT-bases proposed by (Robertson, 1989) charts are a prediction of soil behaviour type (SBT), given that the cone responds to the soil's in situ mechanical behaviour rather than grain size distribution and soil plasticity. CPT soil classification differentiates the soils according to the cone resistance of the soil and the soil's friction angle. Figure 1.4 shows the soil classification chart proposed by P.K. Robertson.

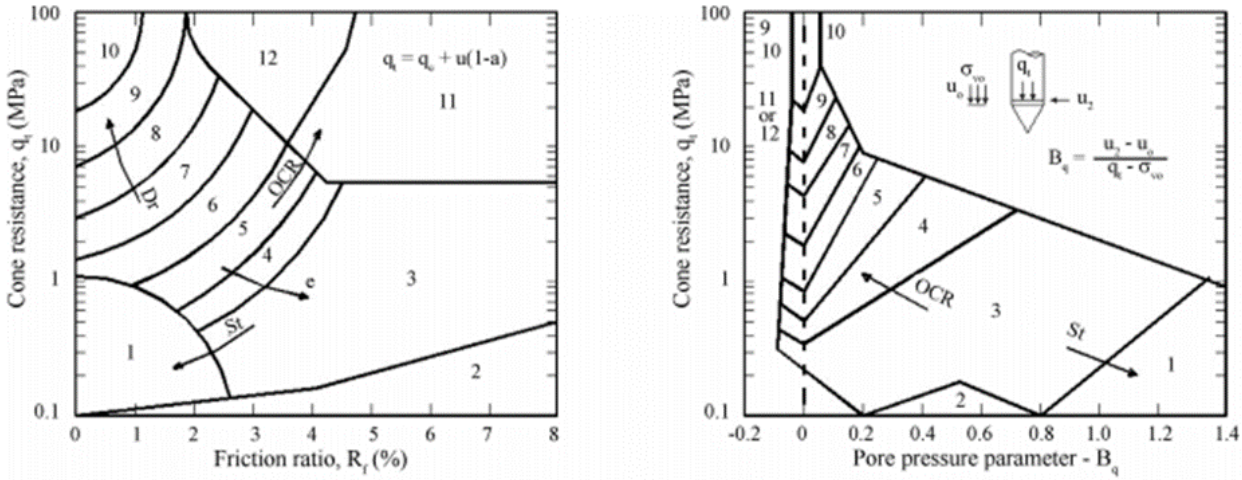

SBT	Soil behavior type
1	Sensitive fine grained
2	Organic material
3	Clay
4	Silty clay to clay
5	Clayey silt to silty clay
6	Sandy silt to clayey silt

SBT	Soil behavior type
7	Silty sand to sandy silt
8	Sand to silty sand
9	Sand
10	Gravelly sand to sand
11	Very stiff fine grained*
12	Sand to clayey sand*

* Overconsolidated or cemented

Figure 1.4. Soil classification chart for CPT interpretation proposed (Robertson, 1989)

1.3. Soil reinforcement

Reinforced soil is any soil or slope supporting system in which reinforcing elements are placed in a soil mass to improve its mechanical properties (Christopher et al., 1990). Reinforcing elements such as geotextile improve the engineering properties of the soil mass to meet project performance requirements by improving bearing capacity, increasing density, control of settlements and permeability, mitigating soil liquefaction and the increase slope stability. (Schaefer et al., 2017a)(Han, 2015). Typical ground improvement techniques may include preloading, vertical drains, deep mixing, stone columns and lightweight fills will be discussed in the following paragraphs.

1.3.1. Preloading

Pre-compression refers to the process of compressing foundation soil under applied vertical stress (preload) before placement or completion of the final permanent construction load. If the temporarily applied load exceeds the final loading, the amount in excess is referred to as a surcharge (Rixner et al., 1986). The surcharge is normally brought about by preloading, which involves the placement and removal of a surplus dead load. This compresses the

foundation soil thereby inducing settlement before construction (Bell 1993). Preloading can be grouped as either fill preloading or vacuum preloading.

1.3.1.1. Fill or conventional Preloading

Surcharging consists of applying load on the ground surface above that associated with the long-term development conditions to have accelerated consolidation. When the load is placed on the soft soil, it is initially carried by the pore water and this pore water pressure decreases gradually as the pore water flows away very slowly in the vertical direction (Bilal & Talib, 2016). Figure 1.5 gives a representation of this phenomenon. Pre-loading and surcharging are designed to ensure that Long-term primary and secondary consolidation settlements are acceptable. The treated ground has improved strength and stiffness properties that are consistent with design assumptions and project specifications. The treated ground has improved strength and density properties such that liquefaction potential is reduced to an acceptable level.

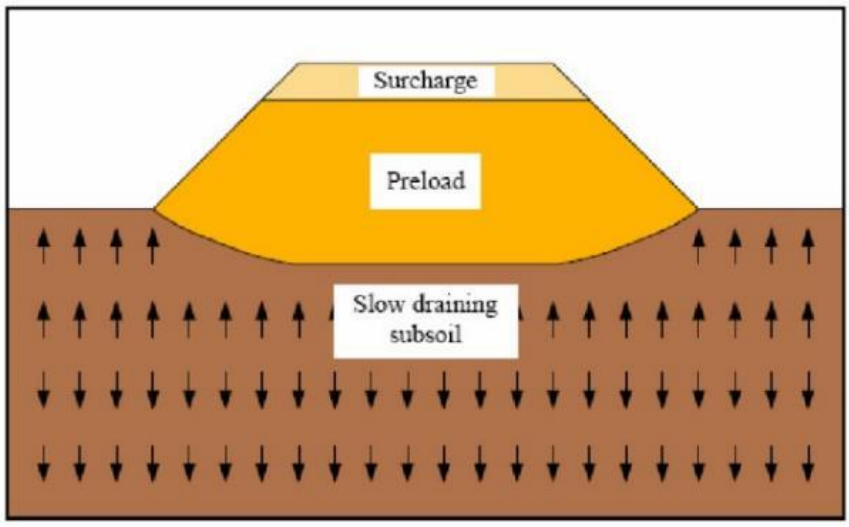

Figure 1.5. Fill or conventional preloading (Bilal & Talib, 2016)

Pre-compression can be utilised to reduce or eliminate post-construction settlements produced by primary consolidation of most compressible foundation soils. Surcharging can speed up the pre-compression process while also reducing settlements caused by secondary compression. As shown in figure 1.6, when loads are applied quickly to saturated cohesive soil, a settlement occurs that can be separated into three stages:

- In the initial or immediate settlement stage, there is a development of excess pore pressure in the underlying soil. For relatively thick layers of soils with low permeability, excess pore pressure develops leading to an initially undrained condition.
- As extra pore pressures dissipate, primary consolidation settlement develops. Water (pore pressures) transfers stress to the soil skeleton (effective stresses). The rate at which water drains from the soil layer controls the rate of primary consolidation. The rate of drainage is determined by the volume change and permeability of the soil.
- Secondary compression settlement is the continuing, long-term settlement that occurs after the excess pore pressures are essentially dissipated and the effective stresses are practically constant. These further volume changes and increased settlements are due to drained creep and are often characterised by a linear relationship between settlement and the logarithm of time.

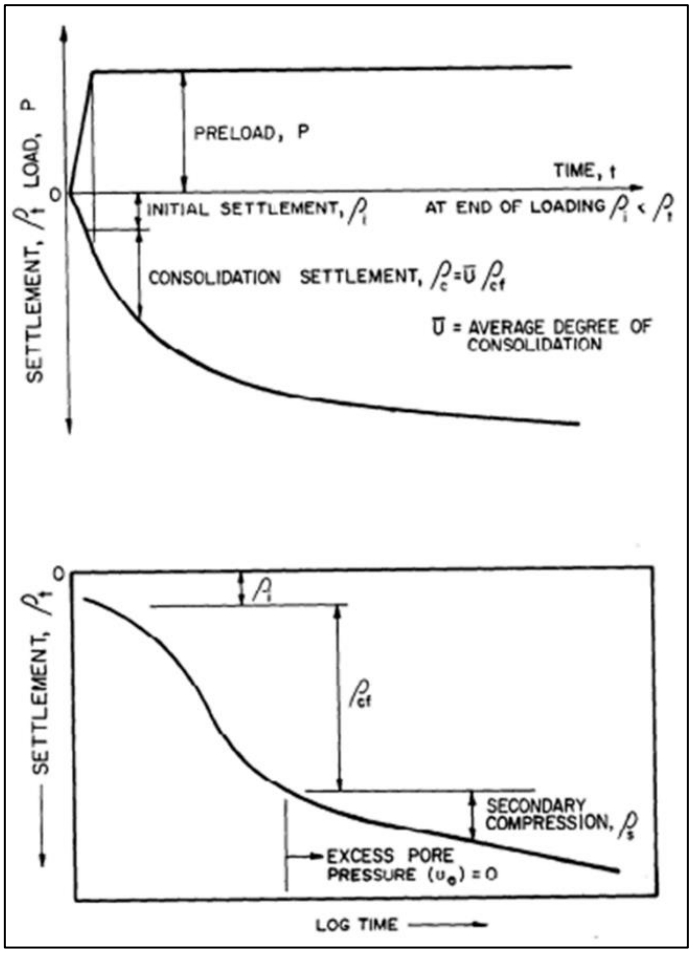

Figure 1.6. Idealised types of settlement under preload and surcharge(Rixner et al., 1986)

The objective of preloading for the length of time applied is to reduce the amount of settlement that occurs after the construction period has ended. This is represented in figure 1.7. The time required to produce a given amount of settlement under a particular preload is determined. The rate of time of settlement for one-dimensional primary consolidation can be obtained by using the method given by Terzaghi (1943). Where surcharging is involved in pre-compression, the degree of consolidation, $Uq + \Delta q$, developed under final loading conditions of q and surcharge Δq could be derived from equation 1.15.

$$U_{q+\Delta q} = \frac{\Delta H}{\Delta H_{q+\Delta q}} \tag{1.15}$$

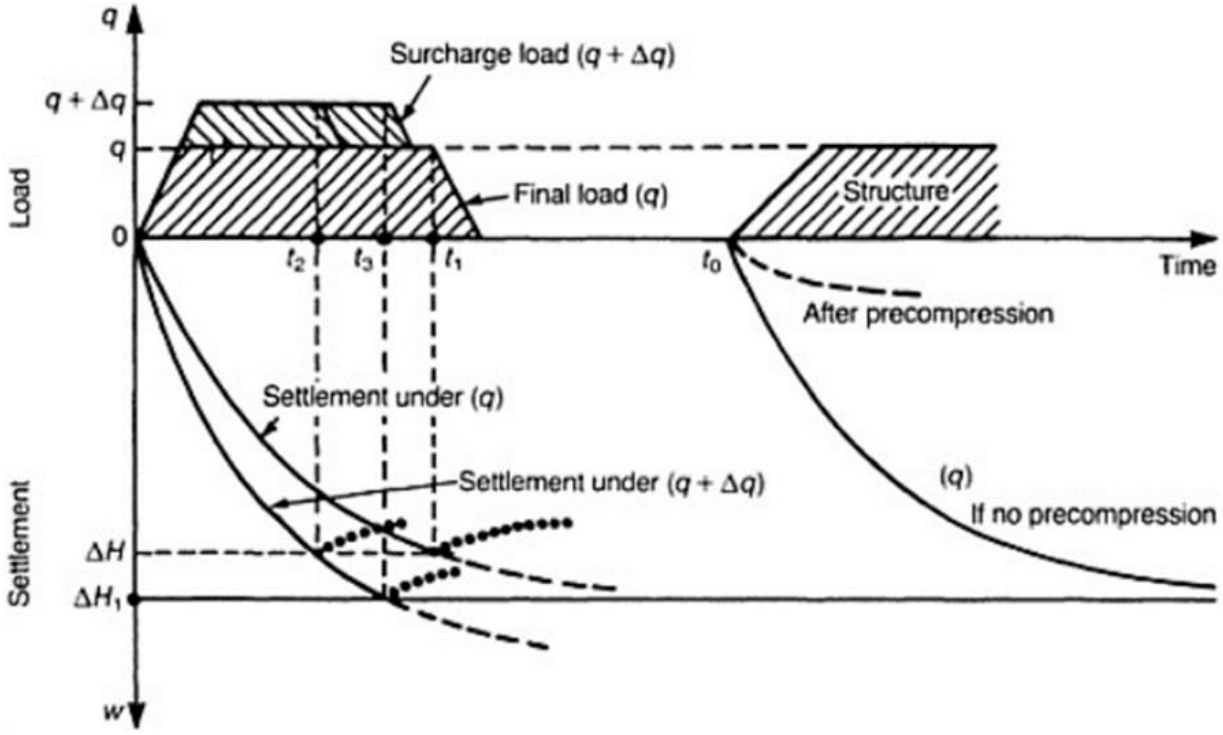

Figure 1.7. Principle of pre-compression using surcharge loading (Bell, 1993)

With the determination of the corresponding time factor Tv as represented in figure 1.8, the time, *t*, for surcharge removal is then derived after the degree of consolidation *U* has been determined for assumed values of permanent loading. As shown in equation 1.16.

$$t = \frac{T_V H^2}{C_v} \tag{1.16}$$

Where:

C_v is the coefficient of secondary consolidation,

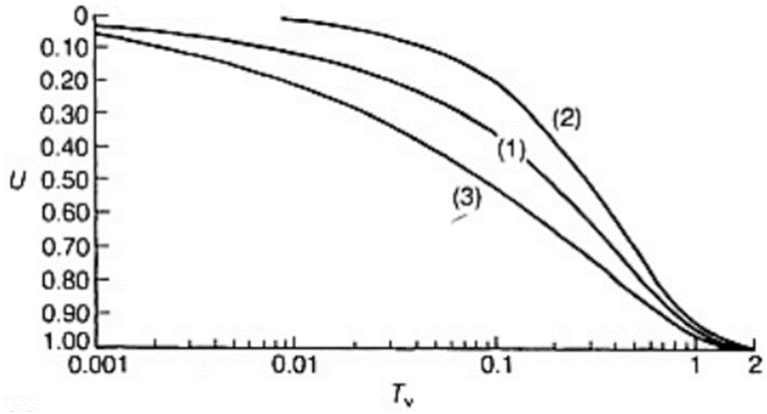

Figure 1.8. Time factor, Tv, versus degree of consolidation, U (Bell, 1993)

Reducing the water content of the soil through preloading significantly affects the compressibility and the shear strength of the soil. One common method for improving soft soil is to reduce the water content of the soil through consolidation. For consolidation to occur, there must be an increase in effective stress. This can be achieved by increasing the total stress or reducing the pore-water pressure (Chu et al, 2014). When a surcharge pressure is applied, the increase in the effective stress is dependent on the dissipation of excess pore-water pressures generated as a response to the application of this surcharge. For soft clays, the consolidation may take a longer time to complete due to their low permeability. If the time for preloading and construction of the structure exceeds the available time, vertical drains (VD) can be installed to shorten drainage distance thus accelerating the rate of consolidation and reducing the time for soil consolidation and settlement.

1.3.1.2. Vacuum preloading

When the ground is very soft or when the fill surcharge has to be applied in stages to maintain the stability of the fill embankment, the vacuum preloading method becomes a good alternative. Vacuum preloading is also used when there is no fill or the use of fill is costly, when there is no space on-site to place the fill and when slurry or soft soil is used as fill for reclamation. As proposed by Kjellman (1952), the basic idea of the vacuum preloading method is applying a vacuum suction into an isolated soil mass to reduce the atmospheric pressure and pore water pressure in the soil, resulting in soil consolidation and effective stress enhancement without changing the total stress. The whole vacuum preloading system consists of the drainage system, isolation system and vacuum pumps. Once generated in vacuum pumps, vacuum

suction rapidly spreads into soils along with the drainage systems, reducing atmosphere and pore water pressure and forming pressure differences between vertical drains and pore water in soils. This pressure difference causes the pore water to flow toward the vertical drain. Its principle is presented in figure 1.9. Atmospheric pressure pressurises the soft soils when the vacuum is imposed within the soil body. Vacuum pressure within the soil body is created by pumping through an interconnected network of a prefabricated vertical drain (PVD), horizontal filter pipes and sand blanket, forming a complete path for spreading the vacuum pressure and facilitating water flow.

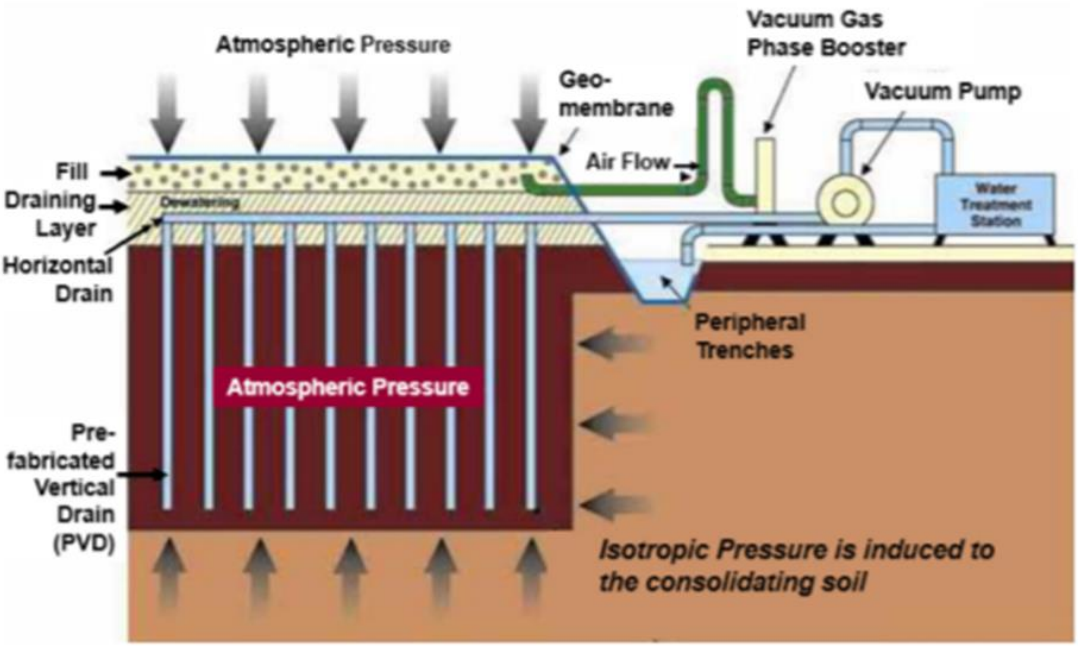

Figure 1.9. Principle of vacuum preloading (Gouw, 2020)

To be effective, an airtight isolation system is required to prevent leakage of water and air below it. The system consists of a geomembrane, and the soft clay itself. Figure 1.10 shows the whole configuration of the vacuum network. When there are sand lenses, a vertical slurry wall may be required to cut off the continuous sand lenses or else the vacuum may not work (Gouw, 2020)

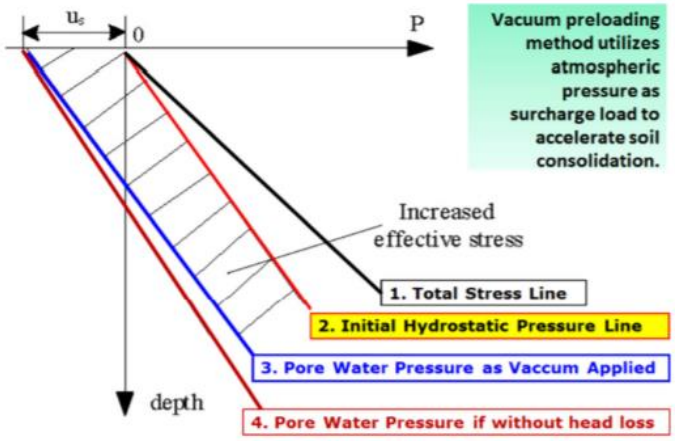

Figure 1.10. Configuration of the vacuum network

1.3.2. Vertical drains

Vertical drains along with pre-compression have the sole purpose of shortening the drainage path of the pore water, thereby accelerating the rate of primary consolidation. Vertical drains can also be used as pressure relief wells to reduce pore pressures due to seepage, such as below natural slopes. When used in conjunction with pre-compression vertical drains play a primary role in reducing the overall time required for primary consolidation due to preloading, reducing the amount of surcharge required to achieve the desired amount of pre-compression in the given time, and increasing the rate of strength gain. This section shall discuss the different types of vertical drains as well as the design approach used.

1.3.2.1. Types of vertical drains

Vertical drains can be classified into one of three general types: sand drains, fabric-encased sand drains, and prefabricated vertical (PV) drains. Each of the general types can be further divided into subtypes (see appendix 2).

a. Sand drains

These are vertical drains in which holes are created with rotary drilling and filled with highly permeable sand. The sand drain method involves the forming of fixed-diameter sand piles at a set distance apart in weak clayey soil above a uniform sand mat (Unizjersity, 1969). A steel casing pipe fitted with a lid is driven into the ground with a vibrating pile driver and withdrawal winch device to the required depth and filled with sand. This pipe is then withdrawn and a sand pile is formed (Tsuruoka & Yamakawa, 1996) as represented in figure 1.11.

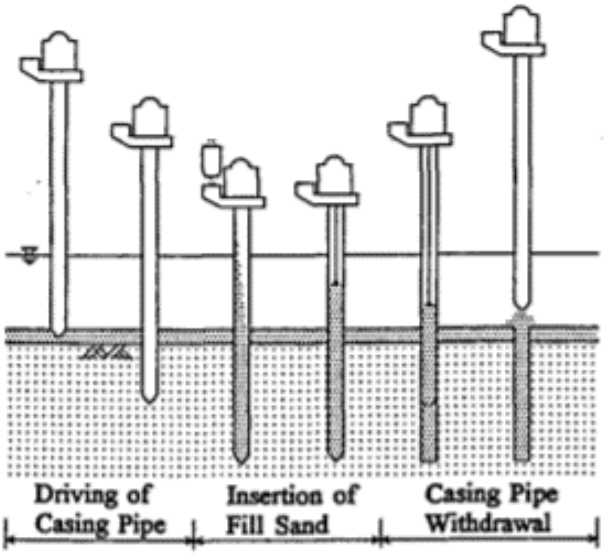

Figure 1.11. Sand pile placing process (Tsuruoka & Yamakawa, 1996)

b. Prefabricated Vertical Drains (PVD)

Prefabricated vertical drains, also known as wick drains, are made up of a channelled synthetic core wrapped in a geotextile fabric. They can be defined as any prefabricated material or product having the ability to be installed vertically into compressible subsurface soil strata under field conditions, the ability to permit pore water in the soil to seep into the drain, and a means by which the collected pore water can be transmitted up and down the length of the drain. Prefabricated vertical drains are often used to accelerate consolidation and gain strength in soft clayey soils. They are versatile, long-lasting, and inexpensive, and they have an advantage over sand drains in that they do not require drilling. The consolidation process depends on several uncertain parameters including the coefficients of consolidation and coefficient of permeability in vertical and horizontal directions, as well as the discharge capacity of the vertical drains (Hong & Shang, 1998).

1.3.2.2. Principle of function

The design of a PVD system consists of the selection of the type, spacing, and length of the drains to accomplish the required degree of consolidation within a specified time (Schaefer et al., 2017b). According to(Hansbo, 1987), the rate of consolidation U is expressed either as the ratio of the actual settlement (S) and calculated primary settlement (S_p) or in terms of pore pressure dissipation represented by equation 1.17. and equation 1.18.

$$U = \frac{S}{S_P} \tag{1.17}$$

$$U = \frac{1-\Delta U}{\Delta U_o} \tag{1.18}$$

Where:

U is the rate of consolidation,

ΔU is the remaining excess pore pressure,

ΔU_o initial excess pore pressure.

By definition, one-dimensional consolidation is considered to result from vertical drainage only, but consolidation theory can be applied to horizontal or radial drainage as well. Depending on the boundary conditions, consolidation may occur due to concurrent vertical and horizontal drainage. Experiments from (Hansbo, 1987),(Hong & Shang, 1998) and (Rixner et al., 1986) show that the rate of consolidation achieved in a vertically drained soil is a function of the excess pore pressure dissipation, both by pore-water flow in the vertical direction between drains, and horizontal direction towards the drains (radial drainage). The combination of the effects is represented in equation 1.19. and figure 1.12. In low permeability soils, the influence of the average degree of consolidation due to vertical drainage (U_v)is negligible with respect to the average degree of consolidation due to radial drainage(U_h) (Hansbo, 1987). The average consolidation of soil at depth z represented in figure 1.13 can be determined by the relation by Hansbo represented in equation 1.20,

$$U = U_h + U_v - U_h U_V \tag{1.19}$$

Where:

U = Overall average degree of consolidation.

U_h = Average degree of consolidation due to horizontal (or radial) drainage.

U_v = Average degree of consolidation due to vertical drainage.

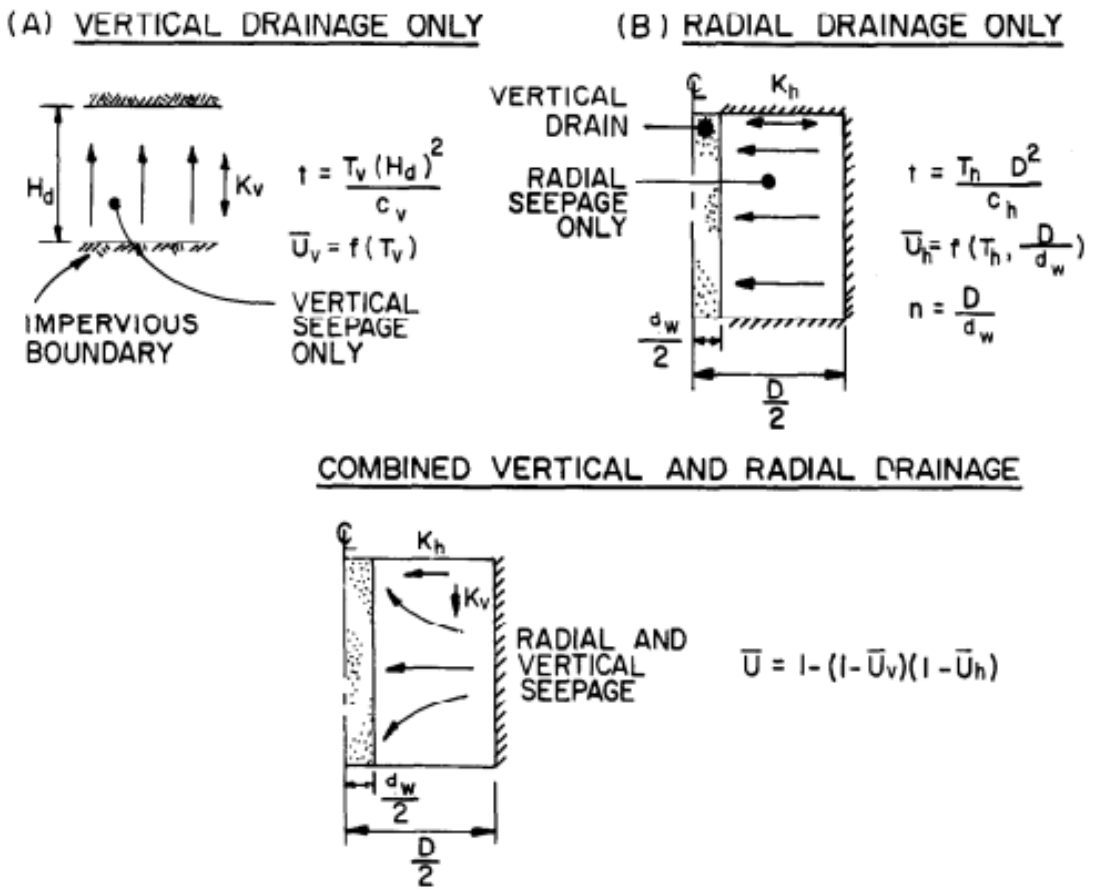

Figure 1.12. The combined effect of vertical and radial drainage in the overall consolidation effect (Rixner et al., 1986)

$$U_h = 1 - exp(-\frac{T_h}{\mu}) \tag{1.20}$$

$$T_h = \frac{C_h t}{D^2} \tag{1.21}$$

$$\mu = \frac{n^2}{n^2-1}\left[In\left(\frac{n}{s}\right) + \left(\frac{k_h}{k_s}\right) In(s) - 0.75\right] + \frac{s^2}{n^2-1}\left(1 - \frac{s^2}{4n^2}\right) + \left(\frac{k_h}{k_s}\right)\frac{1}{n^2-1}\left(\frac{s^4-1}{4n^2} - s^2 + 1\right) + \frac{n^2-1}{n^2}\pi z(2l - z)\left(\frac{k_h}{q_w}\right) \tag{1.22}$$

Where:

$n = \frac{D}{d}$

$s = \frac{d_s}{d}$

D= Diameter of soil cylinder dewatered by each drain,

d=Diameter of f=drain,

d_s=Diameter of smear zone,

k_h=Permeability of undisturbed soil in the horizontal direction,

k_s=Horizontal permeability in the zone of smear,

l= Length of drain if closed at the bottom (half-length of drain if open at both ends),

q_w= Water discharge capacity of the drain at hydraulic gradient $i = 1$ in the vertical direction,

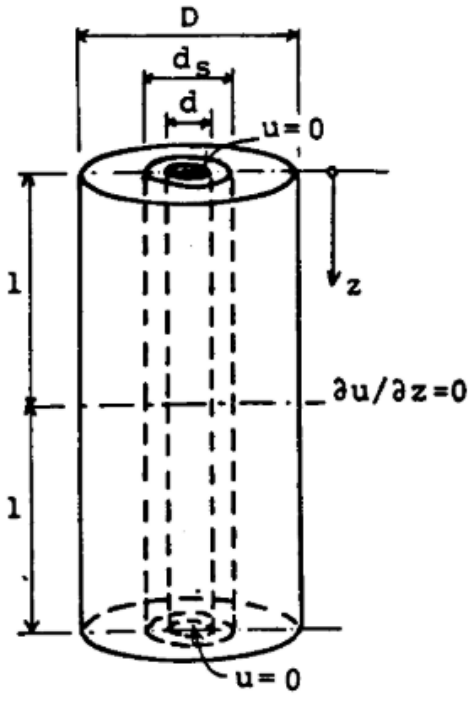

Figure 1.13. Representation of PVD using a vertical cylinder(Hansbo, 1987)

1.3.2.3.Radial drainage

The assumptions used in developing one-dimensional consolidation theory have been applied to the development of radial drainage theory related to vertical drains, which resulted in the relationship between time, drain diameter, spacing, coefficient of consolidation and the average degree of desired consolidation(Rixner et al., 1986a). It is represented in figure 1.23.

$$\boldsymbol{t = \frac{d_c^2}{8C_h}[F(n) + F_s + F_r]\, ln\left[\frac{1}{1-U_h}\right]} \quad (1.23)$$

where:

t = time required to achieve a desired average degree of consolidation U_h

U_h= average degree of consolidation due to horizontal drainage

d_c= diameter of the cylinder of influence of the drain (drain influence zone)

C_h= coefficient of consolidation for horizontal drainage

$F(n)$= drain spacing factor

F_s= Soil disturbance factor (smear zone)

F_r = Well resistance factor

The drain spacing factor F(n) is determined as in equation 1.24.

$$\boldsymbol{F(n) = \frac{D}{d} - \frac{3}{4}} \quad (1.24)$$

d= diameter of the drained circular path.

The radial consolidation equations include the drain diameter d. The equivalent diameter d_w of a vertical band-shaped drain is defined as the diameter of a circular drain that has the same theoretical radial drainage performance as the band-shaped drain. Under most conditions d_w can be assumed to be independent of subsurface conditions, soil properties and installation effects. It can be assumed to be a function of the drain geometry and configuration only. Equation 1.25 demonstrates the phenomenon.

$$\boldsymbol{d_w = \frac{2(a+b)}{\pi}} \quad (1.25)$$

Where:

a = width of a band-shaped drain cross-section,

b = thickness of a band-shaped drain cross-section.

1.3.2.4.Vertical Drain Effect

The construction of a vertical drain causes a disturbance in the surrounding soil. The extent of this disturbance depends on the executive technology of the installation of the drain and the type of soil in which it is inserted. The installation of the drains can be performed in different ways; inserting the draining fixtures without removal of material and inserting the drains made with material removal. If no material is removed, the dredging is affected by moving a volume of soil equal to that of the drain itself. The action exerted by the tool on the walls of the hole causes a rehash and a distortion of the ground (smear) which cause the

interruption of thin horizontal permeable layers or other horizontal drainage ways. This area of land reworked around the drain causes a local reduction in the horizontal permeability which, in the case of a consolidation, is equivalent to the reduction of the diameter of the same drain. If, on the other hand, the material is removed, regarding the jetting drilling, the walls of the hole are not in contact with the drilling nozzle which has a smaller diameter than the hole.

1.3.2.5. Smear effects.

The smear zone is a disturbed zone developed in the soil during PVD installations using a mandrel and characterises two main parameters; The extent ratio and the permeability ratio. The extend ratio signifies the extent of the soil damage due to mandrel penetration while, the permeability ratio κ represents the degree of disturbance to the soil permeability within the smear zone(Iskandar et al., 2018). The permeability reduction inhibits significantly the horizontal consolidation of the soft soil, known as the smear effects which eventually degrade the effectiveness of the PVD (Sharma & Xiao, 2000). Authors have come up with two propositions to delineate the smear zone. the two zones and the three-zone hypotheses as presented in Figure 1.14. The two-zone hypothesis, described among others by (Bergado et al., 1993)(Hansbo, 1987) and (Hawlader et al., 2002) divides the ground around the PVD into the smear zone and the undisturbed zone. The three-zone hypothesis, proposed among others (Sharma & Xiao, 2000) and (Kim et al., 2021) divides the ground around the PVD into 3 zones; the smear zone, the transition zone, and the undisturbed zone.

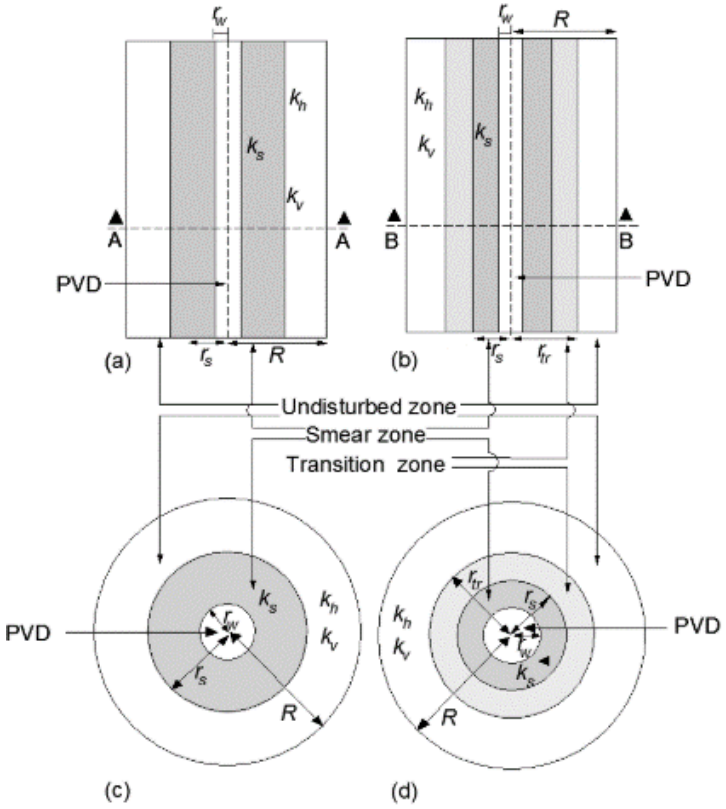

Figure 1.14. Schematic figures of a two-zone theory (a), a three-zone theory (b) a two-zone cross-section A-A (c), and a 3-zone cross-section B–B (d)

The main parameters proposed for characterising the smear zone are the extent ratio and the permeability ratio. The extent ratio ($s\ or\ s'$) is the ratio of the radius of the smear zone r_s to the radius of the drain r_w or the radius of the mandrel r_m respectively as represented in equation 1.26.

$$s = \frac{r_s}{r_w} \quad , s' = \frac{r_s}{r_m} \tag{1.26}$$

Where:

$s\ or\ s'$ represents the rate of disturbance due to the penetration of the mandrel on the treated ground.

The permeability ratio k is the ratio of the horizontal permeability k_h at the undisturbed location to that at the disturbed site k_s. k represents the degree of disturbance due to penetration of the mandrel on the soil permeability represented in equation 1.27.

$$k = \frac{k_h}{k_s} \tag{1.27}$$

These ratios become the two key values in PVD planning which will affect the rate and duration of consolidation. The values can be estimated using an analytical technique, field data back calculation (or numerical method), laboratory testing, or field testing.

1.3.3. Stone Columns

Stone columns are compacted columns of gravel or crushed rock installed into soft soils. Their diameter ranges from 0.6 m to 1.5 m and they provide vertical support to overlying structures and function as drains in soft soils(Mitchell, 1981). Stone columns are typically selected to increase bearing resistance, reduce settlement, accelerate consolidation time rate, increase shear strength, and reduce liquefaction potential. Their construction is accomplished by downhole vibratory methods. The technique of creating stone columns involves the introduction of backfill material into the soil so that dense and sometimes deep columns of aggregate are formed that are tightly interlocked with the surrounding soil improving the bearing capacity of the soil (Barksdale & Bachus, 1983).

1.1.1.1. Construction procedure

The improvement of soft soil with stone columns can be accomplished using two principal excavation and compaction techniques. Vibro replacement and Vibro-displacement. Where environmental concerns are strong, the dry process will typically be required. However, the wet process is more economical if environmental concerns are not as relevant to the project.

a. Vibro-replacement

Vibro-replacement refers to the wet, top feed process in which jetting water is used to aid the penetration of the ground by the vibrator. Due to the jetting action, part of the in situ soil is washed to the surface and therefore replaced by a backfill material(Schaefer et al., 2017b). A hole is formed in the ground by jetting a probe down to the desired depth. The encased hole is flushed out and then stone is added in 0.3-1.2 m increments and densified using an electrically or hydraulically actuated vibrator located near the bottom of the probe. Figure 1.15 shows the top feed Vibro replacement installation.

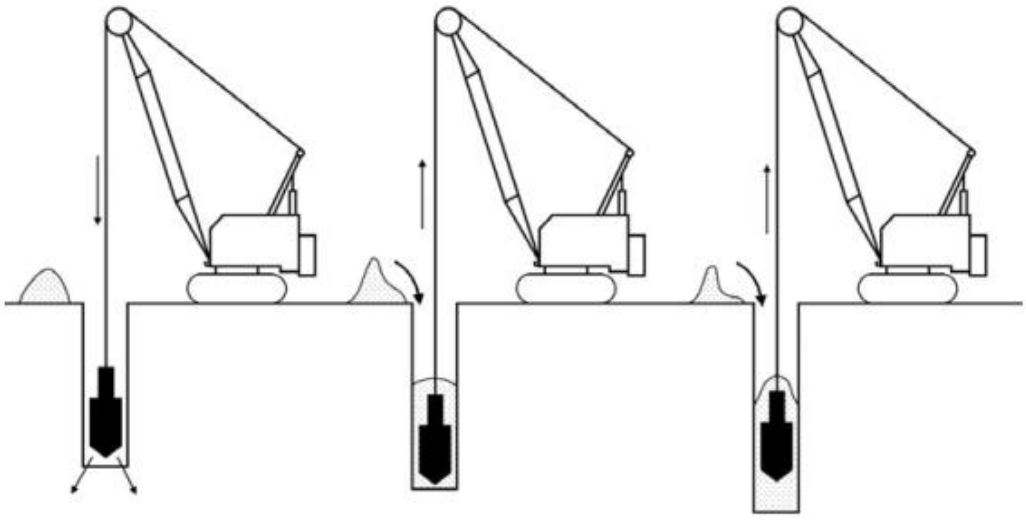

Figure 1.15. Top feed Vibro-replacement installation (Schaefer et al., 2017b)

b. Vibro-displacement

Vibro-displacement refers to the dry, top or bottom feed process. Almost no in situ soil appears at the surface but is displaced by the backfill material. The main difference between vibro-displacement and Vibro-replacement is the absence of jetting water during the initial formation of the hole in the Vibro-displacement method. Figure 1.16 shows the bottom-feed Vibro-displacement method.

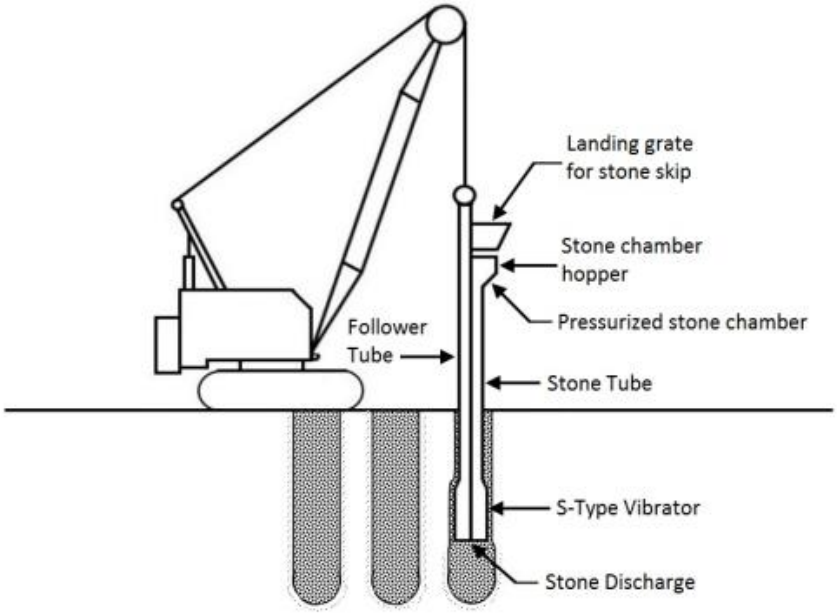

Figure 1.16. Bottom feed Vibro-displacement method (Schaefer et al., 2017b)

1.3.3.2. Allowable bearing capacity

According to (Bowles, 1997), there is no theoretical procedure for predicting the combined improvement obtained by stone columns and soil, so it is usually assumed the foundation loads are carried only by the several stone columns with no contribution from the intermediate ground. Stone columns are usually placed 1-3m apart. (Bowles, 1997) gives an approximate formula for the allowable bearing capacity of stone columns as represented in equation 1.28.

$$q_a = \frac{K_P}{F_s}(4c + \sigma_r') \tag{1.28}$$

where:

$K_p = \tan^2(45 + \frac{\emptyset'}{2})$

$\emptyset'$ =drain angle of friction of stone

c = drained cohesion (or c_u for the undrained cohesion)

σ_r' = effective radial stress measured by pressure meter

F_s = safety factor

The total load allowable for a stone column of cross-sectional area A_c is:

$$Q_a = q_a A_c \tag{1.29}$$

1.3.3.3. Consolidation reduction using stone columns

The area replacement factor, which indicates the area of soft soil replaced or displaced by the stone columns, is the most critical element in a stone column treatment. The analytical method used to design our stone columns is that proposed by De BeerVan Impe in 1983. The analysis done is the unit cell analysis. This method consists in verifying the stresses and settlements in the column and surrounding soil. The following relation (equations 1.30 to 1.35) when computed give the settlement and stresses present in the column and surrounding soils.

- Constant column volume

$$d_f H = \left(d_f + 2S_h\right)(H - S_v) \tag{1.30}$$

- Elastic strain in the plane-strain condition of the soil:

$$S_v = \frac{H}{2E_t}(1 - v_t^2)\left(\sigma_{ht}' - \frac{v_t}{1-v_t}\sigma_{vt}'\right) \tag{1.31}$$

Where:

$$E_t = \frac{(1+v_t)(1-2v_t)}{1-v_t} E_{eod,t} \quad (1.32)$$

- Active plastic state for the column

$$\sigma'_{hc} = k_{ac}\sigma'_{vc} = \sigma_{ht} \quad (1.33)$$

$$\sigma' - ht = k_{at}\sigma'_{vt} \quad (1.34)$$

iv) External load considerations

$$P_o b = \left(d_f + 2S_h\right)\sigma'_{vc} + (L - 2S_h)\sigma'_{vc} \text{ c} \quad (1.35)$$

Where:

s_v and s_h are the vertical and horizontal settlement of the soil respectively,

p_0 is the load at the base of the embankment.

1.3.4. Deep Mixing Method (DMM)

From an engineering point of view, deep mixing is a ground improvement technique in which the soil is mixed in situ with cementitious (such as cement, lime, and fly ash), chemical or even biological reagents in the form of slurry or powder to improve the engineering properties (strength, consistency, permeability of soil and deformability characteristic) of soft ground (Porbaha, 1998)(Ahmad et al., 2017). It works on the principle of replacement, densification, consolidation/dewatering, filling the void admixture stabilisation, thermal treatment and reinforcement (Terashi, 2004). After mixing, a chemical reaction occurs between the stabilising agent and the clay, producing a cemented composite material. The reaction increases the strength of the soil and thus enhances the bearing resistance and settlement performance (Chew et al., 2004).

1.3.4.1.Classification of Deep Mixing Methods

(Bruce, 2000) developed a classification system based on construction parameters including binder type, mixing mechanics, and location of the mixing tool. The parameters are based on the following fundamental characteristics; The method of introducing the “binder” into the soil, the method used to penetrate the soil and/or mix the agent, the location, or the vertical distance over which mixing occurs in the soil. Most authors in recent times have used the classification system based on the method of introducing the binder into the soil. This classification system could be divided into the wet deep mixing method and the dry deep mixing method.

a. Wet Deep Mixing Method

Wet deep mixing methods are single, or multi-shaft wet mixing processes that use primarily cement-based slurries to create isolated elements, continuous walls, or blocks. Shallower mixing may also be conducted to stabilise masses of soil. The wet method can be implemented in coarse-grained, fine-grained, and organic soils and peat. Their equipment comprises a batch plant to supply slurry and a mixing machine to inject and mix the slurry into the ground. Wet mixing methods are used for both offshore and on-land projects. Figure 1.17 shows a picture of deep mixing by wet method with the double axis mixing tool equipment at the top left-hand corner of the figure.

Figure 1.17. Deep mixing by the wet method; insert shows double axis mixing tool(Schaefer et al., 2017a)

b. Dry Deep Mixing method

Dry mixing methods are typically single-auger techniques that primarily use lime, cement, or slag mixtures to create isolated columns, walls, or blocks for soil stabilisation and reinforcement. The method involves the use of dry binders injected into the soil and thoroughly mixed with moist soil as sing in figure 1.18. The soil is premixed using specialised tools during

downward penetration until it reaches the desired depth. During withdrawal of the mixing tool, the dry binder is then injected and mixed with premixed soil leaving behind a moist soil mix column (Makusa, 2012). The dry method can be implemented in soft fine-grained soils and organic soils and peat(Mary et al., 2013). Dry mixing equipment comprises a binder mixing and preparation system and a mixing machine.

Figure 1.18. Deep mixing by the dry method; insert shows blades of mixing tool, with a port for binder delivery on the shaft (Schaefer et al., 2017a)

1.3.4.2. Deep Mixing installation patterns

In the application of the deep soil mixing method for the improvement of problematic soils, the soil columns could be installed in blocks, single columns, panels or stabilised grids depending on the purpose of improvement represented in figure 1.19 (Abbey et al., 2015). In the group column type improvement, treated soil columns or elements are installed in rows with either rectangular or triangular arrangements in the ground. In the wall type improvement, the long walls of treated soil with or without short walls oriented perpendicular to the centreline of superstructures are produced by overlapping adjacent columns. The grid-type improvement is an intermediate type between the block type improvement and the wall type improvement. The stabilised soil columns are installed by overlapping execution so that grid-shaped improved

masses are produced in the ground. In block type improvement, a huge improved soil mass is formed in a field by overlapping all the stabilised soil (Pourakbar, 2015).

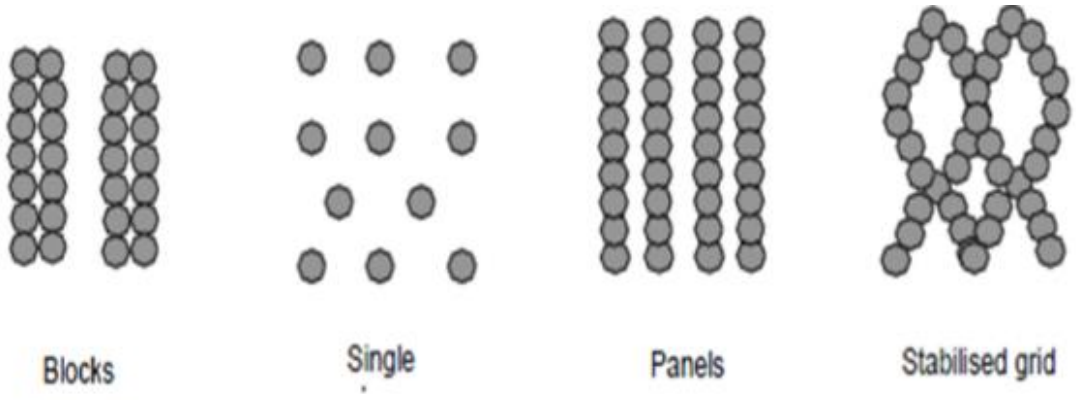

Figure 1.19. Different types of deep mixing installation patterns (Abbey et al., 2015)

1.3.4.3. Phase relationship in soil on the addition of a binder

When binders like cement, lime, and slag cement are mixed with soil, the result is a multiphase material, as shown in figure 1.20 (right) for dry mixing and (left) for wet mixing. Dry mixing is generally used in soft, saturated, or nearly saturated soil. Wet mixing can be applied to soils with any degree of saturation. For wet mixing whether the base soil is saturated or unsaturated, the resulting mixture is generally saturated or nearly saturated.

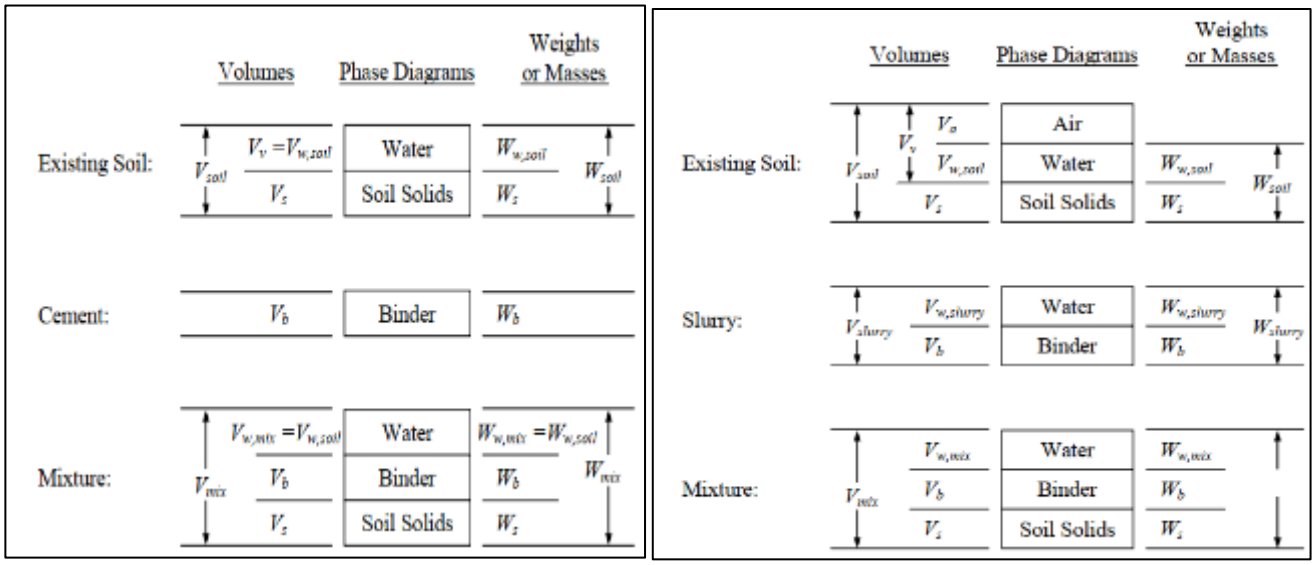

Figure 1.20. Illustration. Phase diagrams for dry mixing (left). Phase diagrams for dry mixing (right)(Mary et al., 2013).

1.3.4.4. Application of deep mixing method

Significant improvement in the physical and mechanical properties of soft soils has been achieved through the mixing of these soils with cement, lime, fly ash and other hydraulic binders to produce a soil-binder column. The resulting soil material possesses higher strength, lower compressibility and lower hydraulic conductivity. Typical applications of the deep mixing method in soil improvement include the following;

- Embankment stability
- Embankment settlement reduction
- Foundations of structures
- Braced excavation
- Bridge abutment
- Mitigation of liquefaction potential
- Cut slope stability
- Impact on nearby structures

1.3.5. Applicability Limits for soil stabilisation techniques

All ground modification technologies have limits on their applicability. Limitations may be defined as soil type applicability, depth of treatment and availability and installation of stabilisation material. (Schaefer et al., 2017b) the proposed general applicability of this technology (see appendix 3).

1.4. Abutment Walls

An abutment is a structure located at the end of a bridge that provides the basic functions of Supporting the end of the first or last span and retaining earth underneath and adjacent to the approach roadway. As a component of a bridge, the abutment provides vertical support to the bridge superstructure at bridge ends, connects the bridge with the approach roadway, and retains the roadway base materials from the bridge spans(Chen & Duan, 2014)(Demetrios & Jim, 1995).

1.4.1.Types of abutment

According to (Chen & Duan, 2014) abutments can be classified into open-end abutments and closed-end abutments based on the relationship between the bridge abutment and roadway or channel that the bridge over crosses and Monolithic and Seat-Type Abutments based on the connection type between the abutment stem and bridge superstructure. This is represented in figure 1.21. A generic figure of a bridge abutment showing its basic functions is represented in figure 1.22.

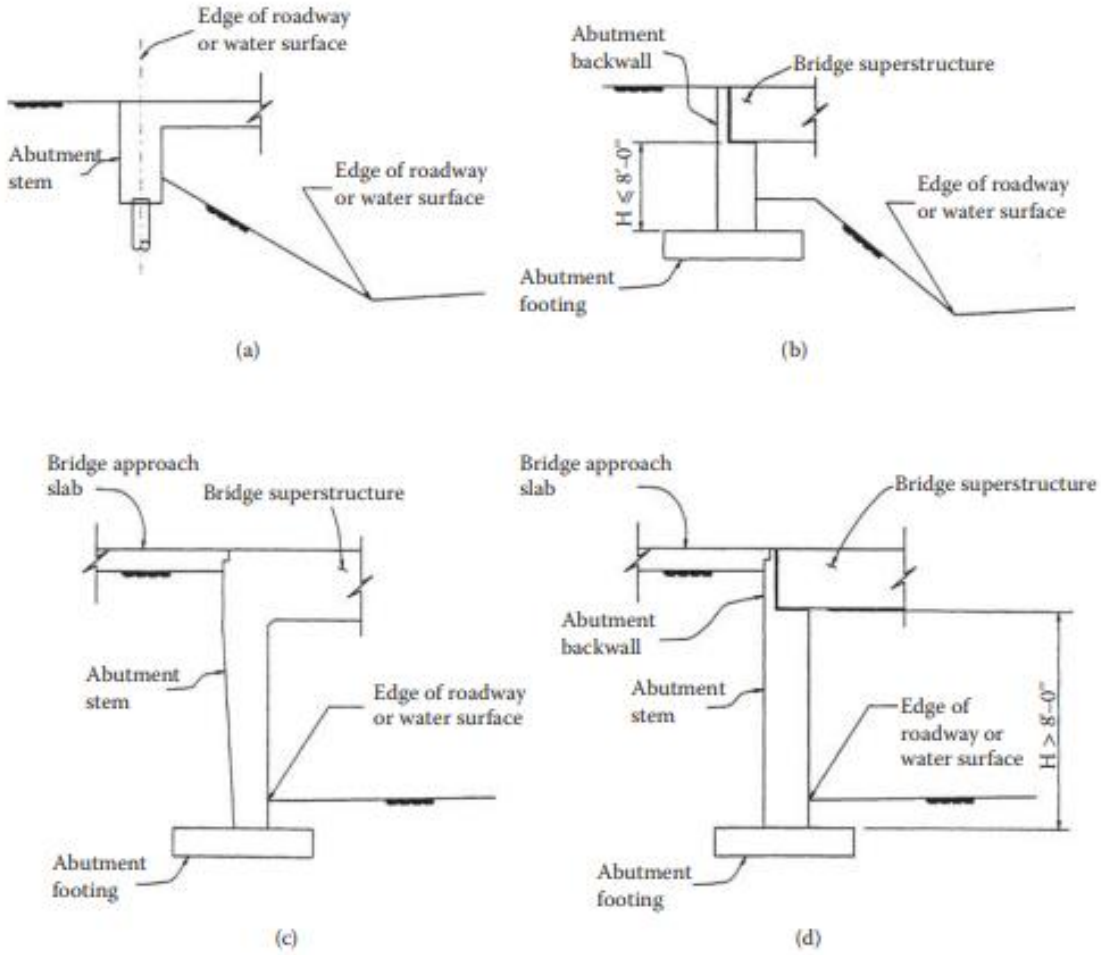

Figure 1.21. Typical abutment types. (a) Open-end, monolithic type, (b) Open-end short stem type, (c) Closed-end, monolithic type, (d) Closed-end, short stem type(Chen & Duan, 2014)

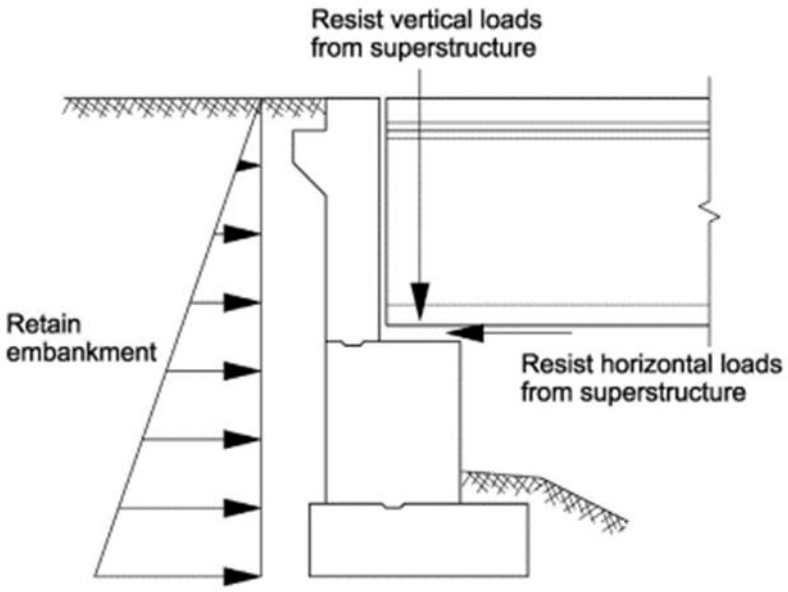

Figure 1.22. The primary function of a typical abutment

1.4.2. Criteria for abutment selection

The selection of an abutment type needs to consider all available information and bridge design requirements. These may include bridge geometry, roadway and riverbank requirements, geotechnical conditions, right-of-way restrictions, architect requirements, and economic considerations.

Conclusion

Soft soils are problematic due to their poor condition, according to the literature review's summary. To enhance the state of these problematic soils, several stabilisation procedures could be applied. They include the use of surcharged preloading material, prefabricated vertical drains, stone columns, deep and mass mixing, and, in some situations, partial or entire excavation of soft soils and replacement with soils of better properties. All of these methods aim to improve the effective stress, soil stiffness, and soil deformation when a superstructure is built on them. The proceeding chapter will present the methodology of both the analytical and numerical modelling and analysis in the case study.

CHAPTER 2. METHODOLOGY

Introduction

The previous chapter introduced the concept of soft soil, the generalities of soft soil classification, parameters affecting soft soil and soft soil reinforcement techniques. This chapter will have as its main objective to describe the methodology of the work. The methodology is the branch of knowledge that deals with the method and its application in a particular field of study (David et al., 2014). It is the part of the study that establishes the research procedure after the problem has been defined, therefore achieving the desired objectives. The methodology will be divided into four sections, the first being the site recognition. This chapter will also focus on the description of the design procedure and the governing equations used in the numerical modelling of stabilised soil. It shall focus on the methods used in the stabilisation of soft soil using preloading, prefabricated vertical drains and the use of stone columns.

2.1. Site recognition

Using Google Maps and Google Earth, the correct geographical position of the site was determined. Documentary research will also be used to identify the location. This is aimed at supplying the project area's geographical position and then showing it on a map, as well as its topography and climatic conditions, which include the area's temperatures and precipitation, all of which are variables impacting soil quality.

2.2. Site visit

The physical description and observation of the research area are the main components of the site visit. With the abutment in place, accessible project reports, as well as recorded or academic studies relevant to the research area, will be examined for more information.

2.3. Data collection

For this study, two types of data will be required: geometrical data and geotechnical data.

2.3.1. Geometrical data

The project's geometric data will mostly consist of 2D plan drawings, which will include information such as cross-sections (longitudinal profile and transversal profile), and abutment width and length. The stratigraphy would be constructed based on borings carried over different

cross-sections of the soil. The soil geometrical data will be got from GEOS Ingénieurs Conseil (report missionG3 phase étude au sens de la norme NF P-94-5000 de novembre 2013) report.

2.3.2.Geotechnical parameters

There exists a wide variety of tests that can be performed on soil to obtain its geotechnical parameters. These tests can be classified according to the place of realisation as either, in-situ tests or laboratory tests. This study will cover data got from the project report (Rapport de mission G3- Franchissement du second pont sur le Wouri, 2015) which will include data got from both in-situ site investigations and laboratory investigations.

2.4. Method of analysis.

To obtain findings, the study will employ both analytical and numerical methods. The analytical method will use author-proposed stimulations, while the numerical analysis employs the finite element method, which will be implemented using the PLAXIS 2D V20.02 software.

2.4.1. Analytical Method

The analytical method will include modelling of consolidation settlement without reinforcement, the analysis of consolidation settlement of a soil sample reinforces using prefabricated vertical drains, and the analysis of consolidation settlement of a soil sample with the use of stone column reinforcement.

2.4.1.1. Analytical modelling of settlement without reinforcement

Settlement in any soil structure occurs in three phases which are immediate settlement, primary consolidation settlement and secondary consolidation. The sum of these phases of settlement gives the total settlement the soil can undergo, as seen in equation 2.1.

$$S = S_i + S_c + S_\alpha \tag{2.1}$$

a. Immediate settlement

The immediate settlement will be computed using the Elastic method proposed by Christian and Carter. They proposed that undrained settlement can be computed using an equation represented in equation 2.2 with its parameters read from a graph. A correction factor will be applied to the fine soil layer to get the layer's undrained settlement (See appendix 4). The total immediate settlement will be calculated by adding all settlements of the different layers. Details are presented in section 1.2.1.1.

$$S_e = \mu_0 \mu_1 \frac{q_0 B}{E_u} \tag{2.2}$$

b. Primary consolidation settlement

The consolidation settlement is calculated assuming that the fine soil layer is a normally consolidated soil clay, since the value of the pre-consolidation stress $\Delta\sigma_p$ is unknown. The computation equation is represented in equation 2.3.

$$s_{eod} = \frac{H_o}{1+e_0} C_c \frac{\sigma'_{zo}+\Delta\sigma'_z}{\sigma'_{zo}} \quad (2.3)$$

To calculate the primary consolidation settlement, the stress increment $\Delta\sigma'_z$ is first calculated using the Osterberg's formula represented in equation 1.6. (see section 1.2.1.1 b). The correction factor proposed by (Skempton & Bjerrum, 1984) will be used to correct the primary consolidation settlement represented in equation 2.4. β depends on the type of soil, the foundation geometry and the H/B ratio which can be got from specific tables (See appendix 4).

$$S_c = \beta S_{eod} \quad (2.4)$$

c. Secondary consolidation

Secondary consolidation begins theoretically at the end of the primary consolidation settlement, but in reality, it begins at about the time when 95% of the primary consolidation has been done. To calculate this, the secondary consolidation equation represented in equation 2.5, can be used.

$$s_\alpha = \frac{H_0}{1+e_o} c_\alpha \ log \frac{t}{t_P} \quad (2.5)$$

2.4.1.2. Analytical modelling of settlement with the use of Prefabricated Vertical drains

(Hansbo et al., 1974)and (Hansbo, 1987) proposed a solution used for the analysis of horizontal consolidation settlement of soil reinforced with prefabricated vertical drains. His equation is represented in equation 2.6. Vertical consolidation settlement is considered negligible for soils with low permeability, and the consolidation settlement can be considered due to horizontal consolidation only. The equations (1.19) (1.20) (1.21), and (1.22) in section 1.3.2.2. gives a thorough walk through the computation of the horizontal consolidation.

$$u_h = 1 - exp\left(-\frac{8T_h}{u_s}\right) \quad (2.6)$$

To know the drainage distance between two PVDs, a time frame of 18 months is set, for which 95% of the settlement is required to have occurred. The equation of the computation of time required for soil settlement under PVD reinforcement is represented in equation 2.7.

$$t = \frac{D_e^2}{8c_h}\left(In(n) - \frac{3}{4}\right) In\left(\frac{1}{1-u_h}\right) \quad (2.7)$$

2.4.1.3. Analytical modelling of settlement with the use of stone columns

The analytical method used to design stone columns is that proposed by De BeerVan Impe in 1983 as described in section 1.3.3. of the literature review. The analysis done is the unit cell analysis. Assuming a rectangular layout of the columns, an area equivalence to obtain a plane strain model in which each column line is turned into a wall with a thickness d_f is obtained, represented in equation 2.8

$$\alpha = \frac{\pi D^2}{4ab} = \frac{d_f}{b} \quad (2.8)$$

Where D is the column diameter and a and b are the longitudinal and transverse interspaces. For this analysis, the following are considered:

- The Self-weight of soil and the Shear stress in the lateral side of the column (horizontal and vertical stresses are principal) are neglected.
- Column strains are assumed to be at constant volume.
- Installation method is done by displacement.
- The soil parameters are E_t and v_t.

By computing the simultaneous equations (1.30) (1.31) (1.32) (1.33), and (1.34) in section 1.3.3. proposed by (De Beer, 1985) the horizontal settlement, the vertical settlement and stresses around the stone columns can be goth.

2.4.2. Numerical modelling - Finite Element Analysis- PLAXIS 2D

Finite element analysis (FEA) is the process of predicting and understanding how an item will respond to various physical situations by using calculations, models, and simulations. FEA employs the finite element method (FEM), a numerical methodology that divides an object's structure into many sections, or elements, and then joins the elements at nodes. Furthermore, FEA is an excellent alternative procedure for laboratory research studies, particularly in the case of big physical models, which saves time and money involved with physical model development(Azhani & Ramli, 2018). Advanced numerical approaches, such as the FEM, enable users to do complicated analyses that aid in the description of soil behaviour and structure, but also their interactions. When constructing a finite element model for a geotechnical project, the most significant aspects to consider are the constitutive model and the corresponding set of model parameters. (seyedmohsen, 2020)

PLAXIS 2D is a two-dimensional finite element program that can be used to analyse deformation, stability, and flow in a variety of geotechnical applications. A plane strain or an axisymmetric model can be used to simulate real-world situations. The software has a convenient graphical user interface that allows users to quickly create a geometry model and finite element mesh based on a representative vertical cross-section of the problem. Moreover, because the soil is a multi-phase material, special procedures for dealing with hydrostatic and non-hydrostatic pore pressure in soil are required. Soil layers, structures, loads, and boundary conditions are entered using simple drawing procedures using computer aided designs (CAD), allowing for detailed, accurate modelling of real-world situations. A finite geometry model can be derived from this geometry model (R. Brinkgreve, 2006)(PLAXIS, 2021).

2.4.2.1.Model

Plane strain or axisymmetric models can be used in two-dimensional finite element analysis. For geometries with uniform cross-sections and related stress states and loads across a specific length perpendicular to the cross-section, a plane strain model is utilised. For circular constructions with a homogeneous radial cross-section and stresses around the central axis, however, axisymmetric models are utilised. Both approaches provide a two-dimensional finite element model with two degrees of freedom in translation along the x- and y-axes. Plane strain analysis is utilised in numerical model calibration and model analysis.

2.4.2.2. Interface Element type

A 15-node or 6-node triangular element can be used to model soil layers and other groupings. The variable field (displacements) is interpolated in fourth order using a 15-node element, and the numerical integration uses twelve Gauss points, also known as stress points. To simulate the soil layers and other volume elements in the current version of PLAXIS, the user can choose between 6-node and 15-node triangular elements. The position of nodes and stress points in soil elements for both 6-node and 15-node triangle elements is depicted in Figure 2.1. The main difference between these two types of soil elements is that the 15-node triangle uses fourth-order interpolation for displacements and uses twelve Gauss points (stress points) for numerical integration, whereas the 6-node triangle uses second-order interpolation for displacements and uses three Gauss points for numerical integration. When compared to a 6-node triangle, the utilisation of a 15-node triangle requires more memory and results in a slower calculation.

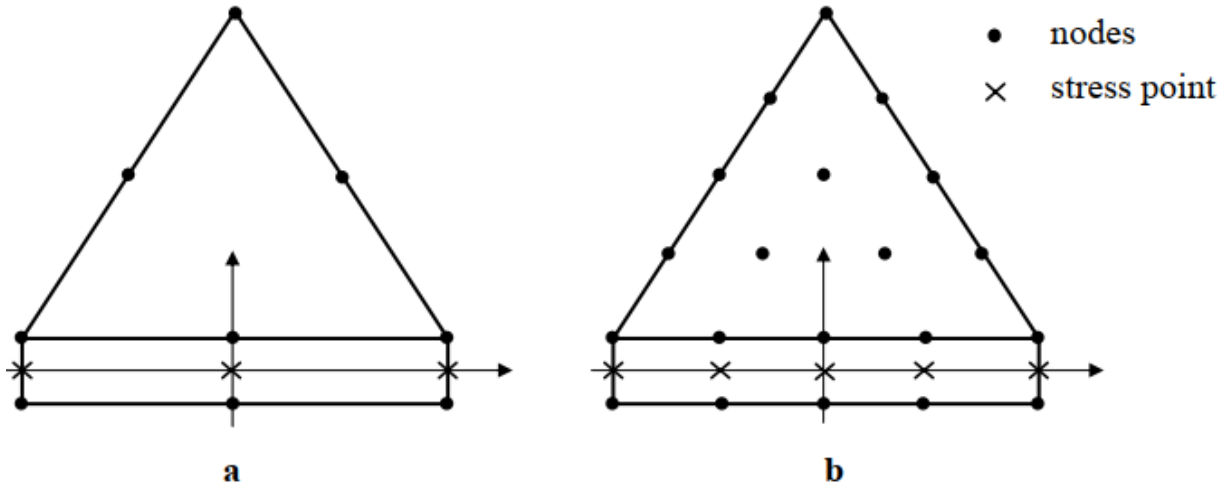

Figure 2.1. Distribution of nodes and stress points in interface elements and their connection to soil elements (R. Brinkgreve, 2006)

2.4.2.3. PLAXIS Input program

The input program is a pre-processor that comes with all of the tools you'll need to create and modify a geometry model, generate a finite element mesh, and define calculation phases. Soils, structures, mesh, flow conditions, and stage construction are the five progressive modes that make up the input program. The geometry modes are the first two in the series, while the calculation modes are the last three. The initial condition is generated in a separate mode of the input program (initial condition mode). Here you'll find the title bar, menu bar, explorers (selection, model, and phase explorers), side toolbar, command line, drawing area, and status bar.

2.4.2.4. Geometry

A geometry model is a two-dimensional representation of a three-dimensional object that is made up of three elements: points, lines, and clusters. A geometry model should include a representation of subsoil layers, structural objects, construction stages, and loadings.

2.4.2.5. Modelling Soil Behaviour

PLAXIS is software that presents various soil models that can be used to evaluate soil deformation. Among these is the linear elastic perfectly plastic model or Mohr-Coulomb Model (MC), the Hardening Soil Model (HS), and the Soft Soil Creep Model (SSC) (PLAXIS, 2021)

which will be used in the numerical model of this project. Three sorts of behaviour have been facilitated in the software to incorporate pore pressure effects: drained behaviour, undrained behaviour, and non-porous behaviour. When no excess pore pressure is formed in dry soils, a drained behaviour is applied, with full drainage due to high permeability and/or low rate of loading. This is an excellent alternative for simulating long-term soil conditions. To generate excess pore pressure, undrained behaviour is chosen. Non-porous behaviour is employed in the model to ignore both initial and excess pore pressure. PLAXIS V20.02, uses two methods of analysis, one with effective stress parameters and the other with total stress parameters. It is possible to specify undrained behaviour using an effective model if the effective stress parameters are known.

a. Linear elastic perfectly plastic model or Mohr-Coulomb Model (MC)

The first-order approximation of true soil behaviour is the Mohr-coulomb model. This elastic completely plastic model is a first-order model that only comprises a small number of properties that are observed in real-world soil behaviour. The Mohr-Coulomb model requires a total of five parameters, all of which are well known to most geotechnical engineers and can be determined using simple soil tests. Table 2.1. lists these parameters along with their standard units(R. Brinkgreve, 2002)

Table 2.1. Mohr-Coulomb's model Parameters (R. Brinkgreve, 2002)

Symbol	Name	Unit
E	Young's modulus	$[kN/m^2]$
v	Poisson's ratio	$[-]$
φ	Friction angle	$[°]$
c	cohesion	$[kN/m^2]$
ψ	Dilatancy angle	$[°]$

i. Young's modulus (E)

In both the elastic and Mohr-Coulomb models, PLAXIS uses Young's modulus as the basic stiffness modulus. The shear modulus (G) is the ratio of shearing stress to shearing strain, and it is strongly linked to the Young's modulus (E) and Poisson's ratio (v). this is represented in equation 2.9

$$G = \frac{E}{2(1+v)} \tag{2.9}$$

The unloading modulus, E_{ur} and the first loading modulus, E_{50} Both tend to rise with confining pressure in soils. As a result, deep soil layers are stiffer than shallow soil layers. Furthermore, the measured stiffness is dependent on the stress path taken.

ii. Poisson's ratio (v)

When the Mohr-Coulomb model is employed for gravity loading, choosing a Poisson's ratio (v) is particularly simple. PLAXIS should produce accurate at rest pressure (k_o) ratios for this type of loading, as shown in equation 2.10. It is simple to choose a Poisson's ratio for one-dimensional compression that produces a realistic value of k_o as shown in equation 2.11. In most situations, v values will fall between 0.3 and 0.4. Such values can be used for loading circumstances other than one-dimensional compression in most cases. However, values in the range of 0.15 to 0.25 are more commonly used for unloading circumstances.

$$K_0 = \frac{\sigma_h}{\sigma_v} \tag{2.10}$$

$$\frac{\sigma_h}{\sigma_v} = \frac{\nu}{1-\nu} \tag{2.11}$$

iii. Cohesion (c)

PLAXIS operate with both cohesive and cohesionless soils. A small value of cohesiveness is highly recommended in a non-linear analysis (c between 0.2kPa-1kPa). The software has an additional parameter option that allows users to simulate the rise in shear strength or cohesion with depth.

iv. Frictional angle (φ)

The friction angle φ (phi) is entered in degrees. High friction angles, such as those seen in dense sands, significantly increase the plastic computational effort. With increasing friction angle, computing time grows more or less exponentially. As a result, while making preliminary calculations for a project, large friction angles should be avoided. The shear strength is substantially determined by the friction angle, as shown in Figure 2.2. by Mohr's stress circles.

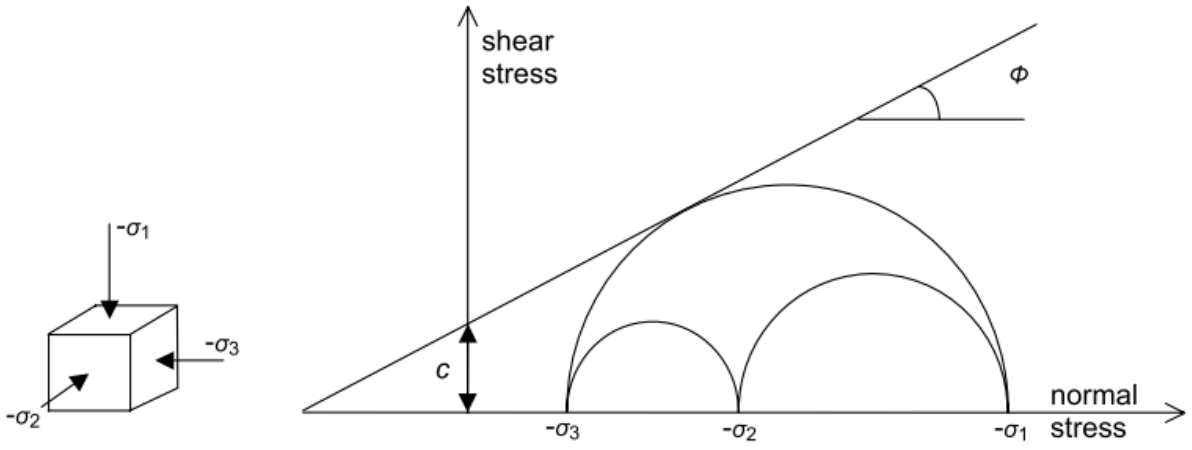

Figure 2.2. Stress circles at yield; one touches Coulomb's envelope (Brinkgreve, 2002)

v. Dilantancy angle (ψ)

The dilatancy angle is measured in degrees. Clay soils, except for heavily overconsolidated strata, have negligible dilatancy ($\psi \approx 0$). Sand dilatancy is determined by the density as well as the friction angle. The order of magnitude for quartz sands is $\psi \approx \phi - 30°$. The angle of dilatancy is essentially zero for values less than 30°. Only exceptionally loose sands can justify a tiny negative value (Bolton, 1986).

b. Soft soil creep model

The creep and stress relaxation are not taken into account in the Hardening Soil model. All soils exhibit some creep, and primary compression is followed by secondary compression to some extent.

Soft soils, such as normally consolidated clay, silt, and peat, have a high degree of compressibility and creep compression. Data from oedometer tests best illustrates this. As a result, PLAXS created the Soft Soil Creep model, which may be used to solve foundation or embankment settlement problems where soft soil behaviour is predominant. When employing the Soft Soil Creep model, it's critical to have the right initial soil conditions. It also contains information on pre-consolidation stress to account for the effects of over-consolidation. The Soft Soil Creep model has the following essential characteristics:

- Stress-dependent stiffness (logarithmic compression behaviour).
- Distinction between primary loading and unloading-reloading.
- Secondary (time-dependent) compression.

- Memory of pre-consolidation criteria.
- Failure behaviour according to Mohr-Coulomb's criterion.

The essential parameters for the Soft Soil Creep model are as follows:

- Failure parameters as in the Mohr-Coulomb model; Cohesion(c), Friction angle(φ), Dilatancy angle (ψ).
- Parameters of the Soft Soil Creep model; Modified compression index *(λ^*),* Modified swelling index *(κ^*)*, Modified secondary compression index *(μ^*).*

An isotropic compression test and an oedometer test can both be used to acquire these characteristics.

i. Modified swelling index and modified compression index

These parameters can be obtained from an isotropic compression test including isotropic unloading. When plotting the logarithm of the mean stress as a function of the volumetric strain for clay-type materials, the plot can be approximated by two straight lines.

ii. Cohesion

The dimension of stress exists in cohesiveness. A tiny effective cohesion, including zero, may be used. When cohesion is entered, an elastic region that's partly in the 'tension' zone is got. The undrained shear strength cannot be specified with strong cohesion and a friction angle of zero. Model input parameters should always be based on effective values. It is possible to use the PLAXIS to model undrained behaviour using effective parameters. It is good to note that the resulting effective stress path may be inaccurate, resulting in unrealistic undrained shear strength. As a result, when Undrained is used as the drainage type, the resulting stress state must be compared to a known undrained shear strength profile.

iii. Friction angle

The effective angle of internal friction represents the increase of shear strength with an effective stress level. It has a degree scale attached to it. It is not permissible to have a zero-friction angle. However, while using high friction angles, caution should be exercised. Rather than using a higher number based on tiny strains, the critical state friction angle is frequently advocated. Furthermore, choosing a high friction angle will increase the computing requirements significantly.

iv. Dilatancy angle

The dilatancy of materials that may be characterised by the Soft Soil model can be ignored in most cases. In the Soft Soil model's default settings, a dilatancy angle of zero degrees is taken into account.

v. Poisson's ratio

In the Soft Soil model, Poisson's ratio ν is the well-known pure elastic constant rather than the pseudo-elasticity constant as used in the linear elastic perfectly plastic model (PLAXIS, 2021). Its value will often be in the range of 0.1 to 0.2. If the usual Soft Soil model parameter setting is chosen, $v_{ur} = 0.15$ is used automatically. Poisson's ratio plays a minimal effect in loading typically consolidated materials, but it becomes crucial in unloading problems. As a result, Poisson's ratio should be based on the ratio of the horizontal stress increment to the vertical stress increment in oedometer unloading and reloading rather than the normally consolidated K_0^{nc} value.

c. Hardening soil Model

A hardening plasticity model's yield surface is not fixed in principal stress space, unlike an elastic perfectly plastic model, but it can expand due to plastic straining. Shear hardening and compression hardening are the two basic types of hardening that can be distinguished. Modelling irreversible strains due to primary deviatoric loading is done using shear hardening. In oedometer loading and isotropic loading, compression hardening is used to mimic irreversible plastic stresses owing to initial compression (PLAXIS, 2021). The Hardening Soil model is a sophisticated model for predicting the behaviour of many soil types, including soft and stiff soils. When soil is subjected to primary deviatoric loading, its stiffness decreases and irreversible plastic strains form. The observed relationship between the axial strain and the deviatoric stress can be well approximated by a hyperbola in the unique situation of a drained triaxial test. The stress dependence of soil stiffness is a key aspect of the current Hardening Soil model. Some basic characteristics of the model are:

- Stress-dependent stiffness according to a power-law Input parameter m
- Plastic straining due to primary deviatoric loading Input parameter E_{50}^{ref}
- Plastic straining due to primary compression Input parameter E_{oed}^{ref}
- Elastic unloading / reloading Input parameters E_{ur}^{ref} , νu

Some of the parameters in the current hardening model are similar to those in the Mohr-Coulomb non-hardening models. The failure parameters are $c, \varphi,$ and $\emptyset$.

2.4.2.6. Material behaviour

In principle, all model parameters in PLAXIS are meant to represent the effective soil response. An important component that affects soil behaviour is the presence of pore water. It significantly affects the behaviour of soil. PLAXIS provides a variety of drainage options to incorporate the water-skeleton interaction into the soil response (PLAXIS, 2012):

- Drained behaviour: Excess pore pressures are not formed when this setting is used, which is the case for dry soils and adequate drainage. This technique can also be used to model long-term soil behaviour without having to know the precise history of undrained loading and consolidation.
- Undrained behaviour: This setting is used for saturated soils in cases where pore water cannot freely flow through the soil skeleton. The flow of pore water can sometimes be neglected due to low permeability and/or a high rate of loading. The distinction is made between three different methods of modelling undrained soil behaviour; Method A (Undrained A) Method B (Undrained B), and Method C (Undrained C).
- Non-porous behaviour: Using this setting neither initial nor excess pore pressure will be taken into account in clusters of this type.

2.4.2.7. Model generation

The reinforced soft soil with PVDs and stone columns will be modelled using three types of material models. In the overall embankment modelling, soil elements will be used to simulate the PVD and stone column material. The surrounding soft soil and the blanket layer shall be modelled using the soft soil creep model (in undrained, consolidation, and drained conditions). The Mohr-Coulomb model will be used to simulate the blanket layer and embankment fill in drained conditions. And the Hardening soil model will be used in the modelling of the compact and stiff clay layers in the soil geometry.

2.4.2.8. Geometry, loading and boundary conditions

The model will be divided into 13 clusters when the geometry is set up. The first seven and eighth clusters, respectively, represent the foundation soil and the stone column or PVD for the different models. The remaining clusters represent the blanket fill layer and the embankment, respectively. However, the three final clusters were subdivided to represent the

stages of embankment construction. The geometry of each model will be determined by the following conditions; Loading the entire area of the PVD and stone columns, as well as the surrounding soft soil, at intervals by applying embankment loads. The entire case study is modelled, and standard fixities are assigned to the boundary conditions in PLAXIS. A model width of 80 m is chosen and fixed boundary conditions are applied to both left and right vertical ends while partially fixed boundary condition is applied to lower horizontal boundary condition. The top horizontal boundary condition is left free so it can deform.

2.4.2.9. Mesh creation

PLAXIS 2D employ unstructured mesh, which is generated automatically and has global and local mesh refinement options. PLAXIS 2D offers five mesh density options ranging from very coarse mesh to very fine mesh. Finer mesh models give more accurate results, but they put more strain on processors, potentially causing the software to crash. The coarse mesh model gives results that are less dependable but less taxing on the machine's performance. The fine-mesh model is designed to create a balance between functionality and accuracy therefore used in this case study. In regions where high loads and strains are expected, the mesh was refined.

a. Elements

During the generation of the mesh, clusters are divided into triangular elements. A choice can be made between 15-node elements and 6-node elements. The powerful 15-node element provides an accurate calculation of stresses and failure loads. In addition, 6-node triangles are available for a quick calculation of serviceability states. Considering the same element distribution, the meshes composed of 15-node elements are much finer and much more flexible than meshes composed of 6-node elements, but calculations are also more time-consuming. In addition to the triangular elements, which are generally used to model the soil, compatible plate elements, geogrid elements and interface elements may be generated to model structural behaviour and soil-structure interaction.

b. Nodes

A 15-node element consists of 15 nodes and a 6-node triangle is defined by 6 nodes. Adjacent elements are connected through their common nodes. During a finite element calculation, displacements (u_x and u_y) are calculated at the nodes. Nodes may be pre-selected for the generation of load-displacement curves.

c. Stress points

In contrast to displacements, stresses and strains are calculated at individual Gaussian integration points (or stress points) rather than at the nodes. A 15-node triangular element contains 12 stress points while a 6-node triangular element contains 3 stress points may be pre-selected for the generation of stress paths or stress-strain diagrams.

d. Initial conditions

The initial situation must be specified after the geometry of the model has been created and the finite element mesh has been generated. PLAXIS allows you to specify the initial conditions. This option has two modes: one for generating the initial water pressure and another for specifying the initial geometry configuration and generating the initial effective stresses.

e. Calculation Software

The calculation can be performed after generating a finite element model, and the calculation type must be specified in this step.

2.4.2.10. Calculation types

The Calculation programme allows choosing between various methods of analysing the actual problem. There are three basic types of calculations: plastic calculations, consolidation analyses, and phi-c reductions (safety analysis).

- The plastic calculation should be used to perform an elastic-plastic deformation analysis without having to account for excessive pore pressures over time. Except when the Soft Soil model is used, the plastic calculation does not account for the time effect.
- When analysing the development or dissipation of excess pore pressures in water-saturated clay-type soils as a function of time, consolidation analysis should be used. True elastic-plastic consolidation analyses are possible with Plaxis. After an undrained plastic calculation, a consolidation analysis without additional loading is usually performed. Loads can also be applied during a consolidation analysis. By selecting consolidation and then entering the desired number of days, different periods can be considered. If you want a complete consolidation analysis, choose Minimum Pore Pressure, which reduces all excess pore pressure. In this research, plastic calculation and consolidation analyses were used.
- Shear parameters can be reduced to performing phi-c reduction (safety analysis). To calculate the safety factor, a safety analysis can be performed after each calculation phase and thus for each construction stage. The phi-c reduction, on the other hand, cannot be used

as a starting condition for another calculation phase because it fails. All of the above analyses will be used in the current research.

2.4.2.11. Loading types

The loading must be specified after the calculation type has been specified. The following loading options are available:

Staged construction is the most prevalent method of loading. The load type feature allows you to change the geometry and load configuration by deactivating or reactivating loads, volume clusters, and structural elements produced in the geometry input. Using staged construction, different loading, and excavation processes can be correctly and realistically recreated. You must first generate a geometry model that contains all of the objects that will be used in the calculation before you can perform a stage construction calculation. In stage construction, either a plastic calculation or a consolidation analysis can be employed, and both have been applied in the current work. When the abutment wall is built, a surcharge load will be introduced to the embankment construction to reduce final consolidation.

2.4.2.12. Output

When the calculations are completed, the results can be viewed in the Output program. A large amount of data can be obtained from a finite element calculation such as stresses, pore pressures and displacements for soils, and displacement.

2.4.2.13. Curves

There is an option to preselect points of interest in the model in the Calculation program. If such a point is preselected, the displacement, stress, or pore pressure of the point can be viewed in the Curves subprogram for each iteration, step, or time. The results can be viewed as a table or a graph.

2.5. Cost analysis

A cost analysis will be conducted to ensure that the ground improvement technology presented in this work is financially viable. The cost will be calculated by multiplying the required quantities by the unit prices obtained from a market study of prices. The formula used to calculate the volume of material required by the column or vertical drains is presented in equation 2.12

$$V = \pi \left(\frac{D}{2}\right)^2 * H * N \qquad (2.12)$$

Where D, H, and N are the diameter, height, and the number of columns, respectively. By multiplying the surface area of the section by the thickness of the Pozzolana layer as represented in equation 2.13, the volume of the Pozzolana (drainage blanket) may also be calculated.

$$V = A * T \tag{2.13}$$

Where:

A is the area of the Pozzolana Layer,

T is the thickness of the layer.

Conclusion

This chapter presented the methodology of the work. It began with documentary research for the recognition of the site. The investigations made provided the monitoring data which gave the cross-section and geotechnical parameters of the soil prior to the abutment construction. Geometrical data provided soil surface conditions together with cross-sectional data of the project while geotechnical data presented the soil stratigraphy and physical characteristics of the soil. The numerical analysis was conducted in this chapter using the PLAXIS Version 20.02 2D finite element tool. It outlined the various processes required for applying preloading in conjunction with prefabricated vertical drains and stone columns to reinforce soft soil. In the end, a cost estimation for the comparative analysis of the different reinforcement methods used was discussed. The results from the documentary research, site visit, the data obtained, and the implementation of an analytical and numerical procedure to evaluate the settlement of soil are discussed in the following chapter.

CHAPTER 3. RESULTS AND INTERPRETATIONS

Introduction

The goal of this chapter is to present and analyse the settlement of soft soils using different reinforcement methods. The results obtained from the methodology used in the previous chapter will be presented as well. This section will focus on the overall presentation of the site, with particular attention paid to its geographic position, climate, relief, vegetation, and geology. To test the consolidation behaviour of the soft soil model under different reinforcement conditions, the PLAXIS v20.02 FEM package was used to model the soil to give a realistic behaviour of all of the necessary data obtained. The modelling of the soils using PVD and stone column reinforcements, as well as a discussion of the parametric study's findings, are presented in the following sections.

3.1. General Site Presentation

The presentation of the study area shall be done through the geographical location, geology, climate, relief, hydrology and hydrogeology to know the different factors influencing the use of soil inclusions in the stabilisation of the abutment.

3.1.1. Geographical Location

Douala is situated on the south-eastern shore of the Wouri River estuary, on the Atlantic Ocean coast. As Cameroon's largest city, it is located in Cameroon's Littoral region, home to Central Africa's largest seaport and airport, as well as the country's economic capital. It is located at latitude 4.061536 (4° 3' 41.5296"N), and longitude 9.786072 (9° 47' 9.8592" E). The city is an important industrial and transportation centre, with, a number of roads and railway stations linking many other parts of the country. Figure 3.1 presents the map of Douala showing its major road, airport, settlement location and major river distributions.

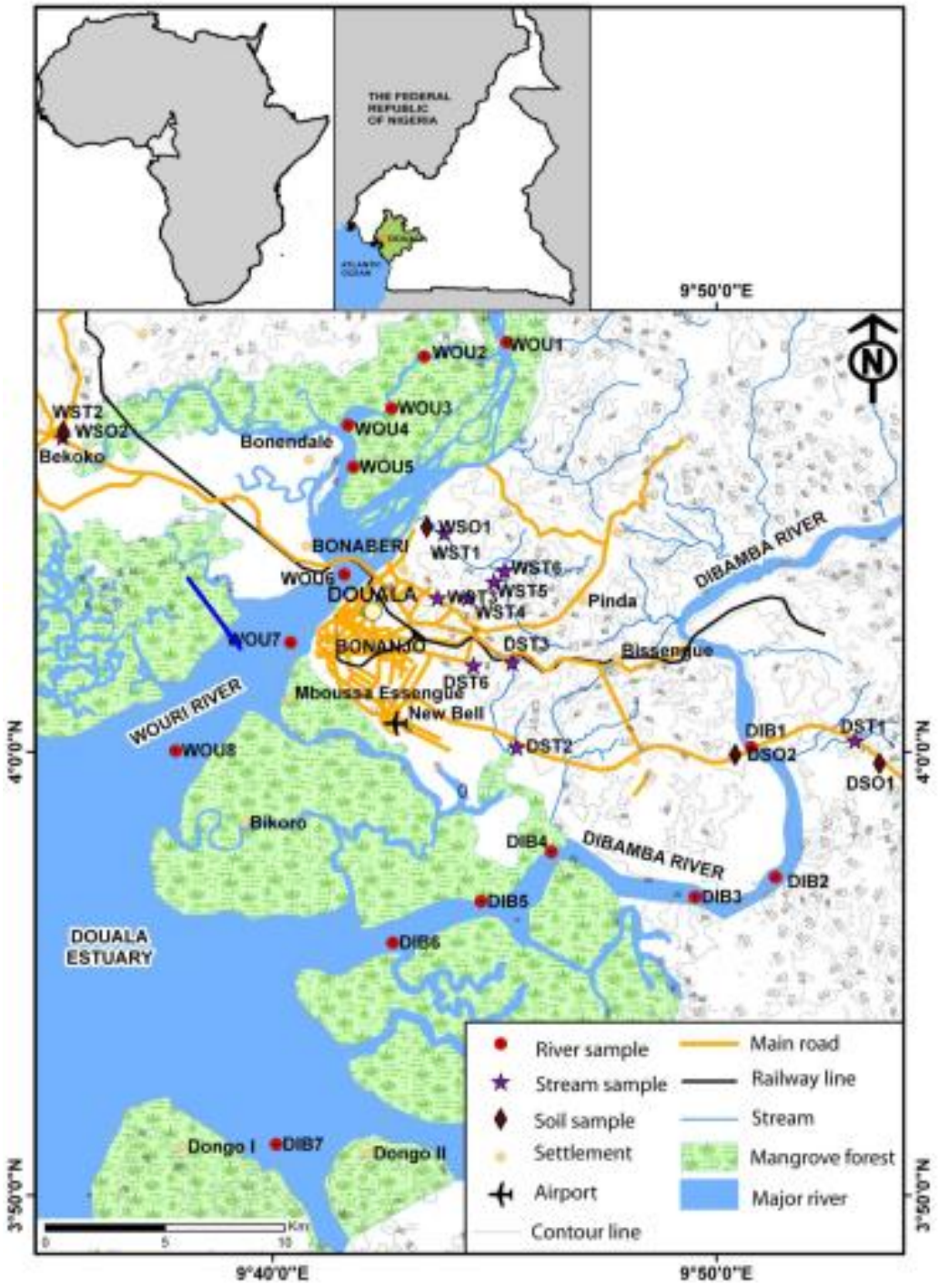

Figure 3.1. Map of Douala metropolis (Tening et al., 2013)

3.1.2. Climate

Douala's location allows for an existent tropical monsoon climate with relatively steady temperatures throughout the year. It has a brief dry season and a heavy monsoon for the rest of the year. Douala is located in or near the subtropical wet forest biome, according to the Holdridge life zones system of bioclimatic classification. Its weather is normally warm and

humid, with a mean annual temperature of 26,7°C that fluctuates by 3.2°C and average humidity of 83 %. It receives on average, 3854.3 mm of rain per year (standard deviation = 464.4 mm) (Bertil, 2019). It is driest in December, with an average of 28 mm of precipitation, and wettest in August, with an average of 700 mm of rain. Figure 3.2 presents an overview of the average monthly precipitation and temperature variation of Douala.

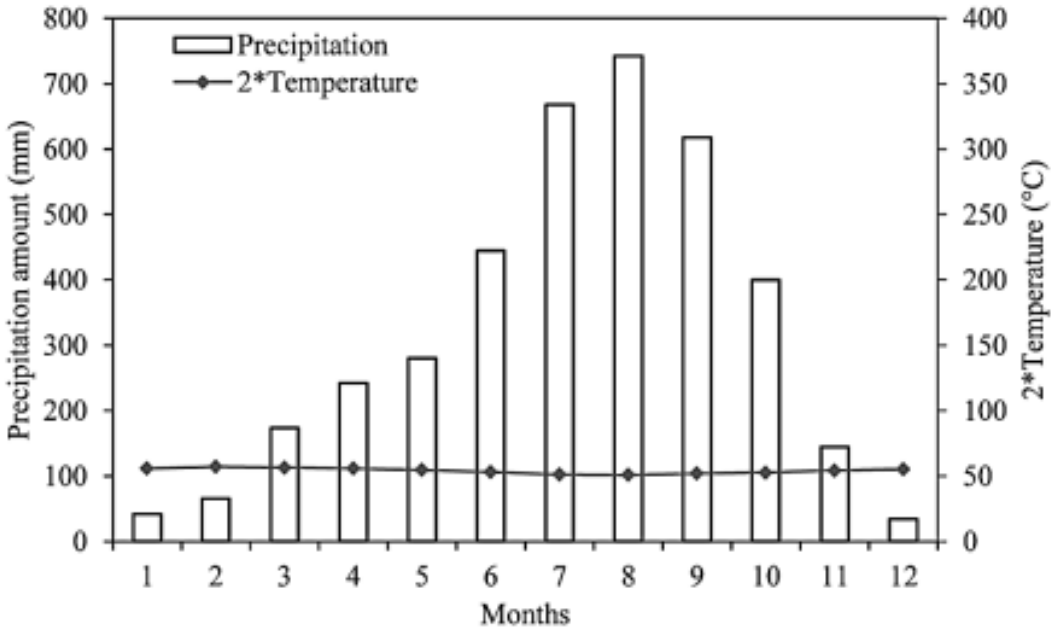

Figure 3.2. Ombrothermal diagram of the region of Douala. (Bertil, 2019)

3.1.3. Geology

The Douala's coastal basin is composed mainly of Cretaceous marine sandstone and limestone which are from ranges 1000m to 2000m thick. These are overlain by a series of Plio-Quaternary marine sand and estuarine clay and silt. Figure 3.3 presents a geological plan view of the south-eastern Wouri estuary while figure 3.4 shows the cross-sectional geology of the soil line linking points A to B.

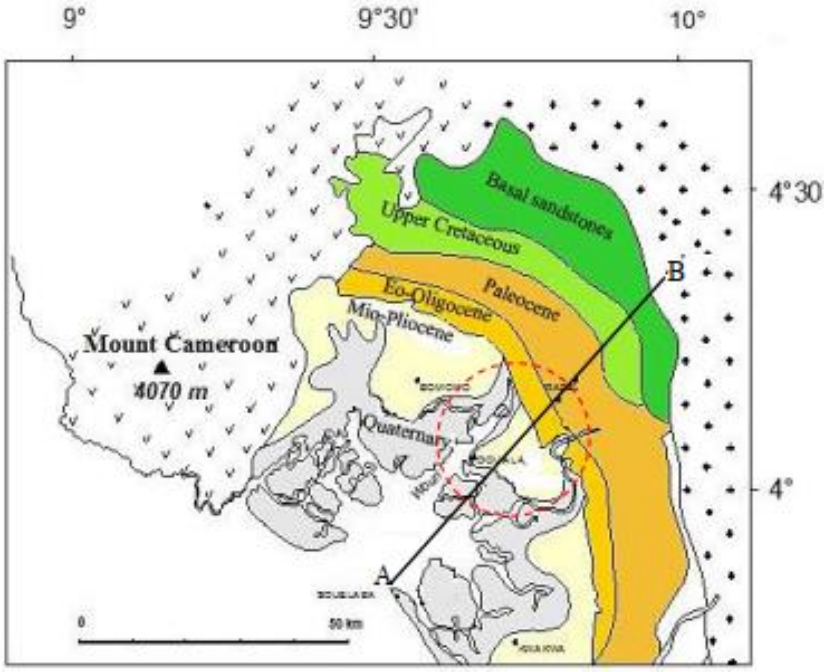

Figure 3.3. Geological plan view through the Douala sedimentary basin (Bertil, 2019)

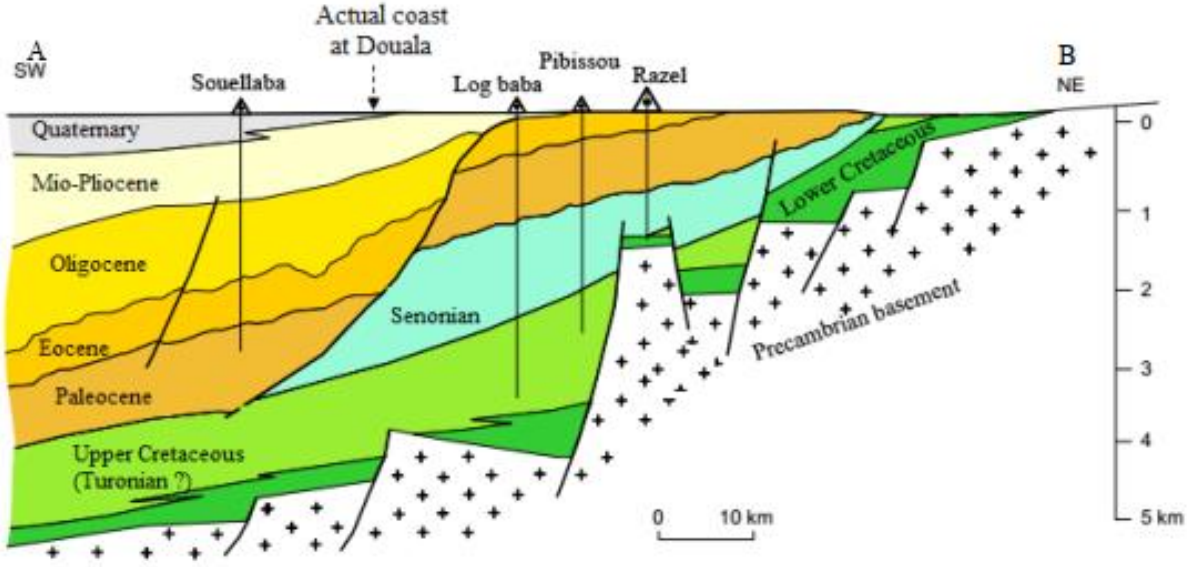

Figure 3.4. Geological cross-section through the Douala sedimentary basin (Bertil, 2019)

3.1.4. Hydrology and hydrogeology

Due to the long rainy seasons, which supply the groundwater and streams, the city of Douala experiences unusually high humidity, which is followed by strong evaporation during the short dry season. Douala's hydrological system is quite dense, with its main rivers being the Wouri within Senegal, Dibamaba, Moungo, and Nyong. Bonnes-courses, Epolo, Mbanya, Mbopi, Bologo, Ngoua, Lonmayagui, Kambo, TongoBassa, and Beseke are among the city's

many watersheds. The groundwater regime is determined by regional hydrology, which is impacted by the type of soil present (Bertil, 2019).

3.1.5.Relief

The city of Douala is located on a sandy plateau. Its elevation ranges from 0 m to about 22 m above mean sea level (MSL) and on average could be 13 m above MSL. It has a morphology whose terrain increasingly evolves from coasts to the interior of the territory and becomes more and more rugged as we move away from the short. This relief consists of a set of valleys mostly flat bottomed. The coastal region is characterised by a short maritime façade in the arc and formed by a succession of sedimentary plains, rivers and streams that flow into the Atlantic Ocean.

3.1.6. Demography

The town of Douala is Cameroon's most populous and largest city. It covers an area of 210km2 and has a population of about 3.536 million people (UN Habitat, 2019), giving it a population density of about 16838 people per km^2. According to these statistics, the population growth rate in 2019 was 3.63%, which is lower than the record of the previous years, indicating that population growth is slowing.

3.1.7. Economic activities

Douala is a city with modest oil resources in Africa, but it is in good agricultural condition, therefore it has one of the best economies in Africa. However, it also faces some problems like other developing countries such as a high dependence on civil service, floods and storms that affect business development. As the economic capital of Cameroon, it hosts about 50% of Cameroon's major companies making it a site of attraction for both internal and foreign investors. Unlike the rural populations of Cameroon that grow their food, inhabitants of Douala are mostly dependent on foodstuff imported from neighbouring villages

3.2. Physical presentation of the site

The project involves the construction of a second bridge over the Wouri River. It includes the construction of a bridge supporting a road deck and a railway deck. The study area is located at the Wouri River estuary. On the left bank (Deïdo side), land has been reclaimed from the river (embankments). According to the geological map of Cameroon and the available data, the bedrock present is the argillites and siltstones of the Mio-Pliocene. The overlying land is made up of embankments and alluvium (sandy embankments) more or less clayey sands, containing pockets of clayey (soft clay) and/or organic (silt, peat, etc.) soil. The already-existing bridge

and abutment at the side were constructed on deep foundation soil. The site project and already existing abutment are represented in figures 3.5 and 3.6.

Figure 3.5. Aerial view of the Wouri estuary from Google earth (Google, 2022)

Figure 3.6. Lateral view of the abutment wall of the second bridge over the river Wouri.

3.3. Data presentation

The main technical data used in this study are geometrical and geotechnical.

3.3.1. Geometrical data

The C8 abutment is located at PK 1+455 of the project on the left bank of the Wouri. It is founded on five piles with a diameter of Ø 1800 lowered to the Mio-Pliocene bedrock. The PC7 pier, located about 12 m downstream from C8, is also founded on two rows of 5 piles with a diameter of Ø 1800 (piles already made to date). To date, the land, initially located at level 2 NGC at about 2.5 NGC, was backfilled up to about 4 NGC to the right of C8. The technical block of the C8 abutment is planned up to level 10.2 NGC, i.e. an embankment 6.2 m high to be put in place. Figures 3.7and 3.8 show the transverse and longitudinal stratigraphy of the soil.

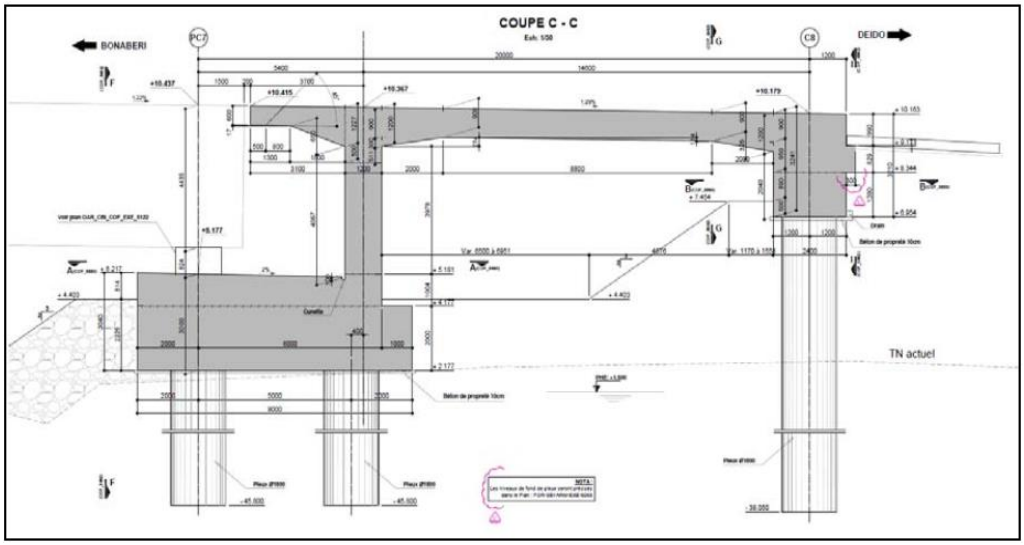

Figure 3.7. Typical transverse profile at PK 1+455

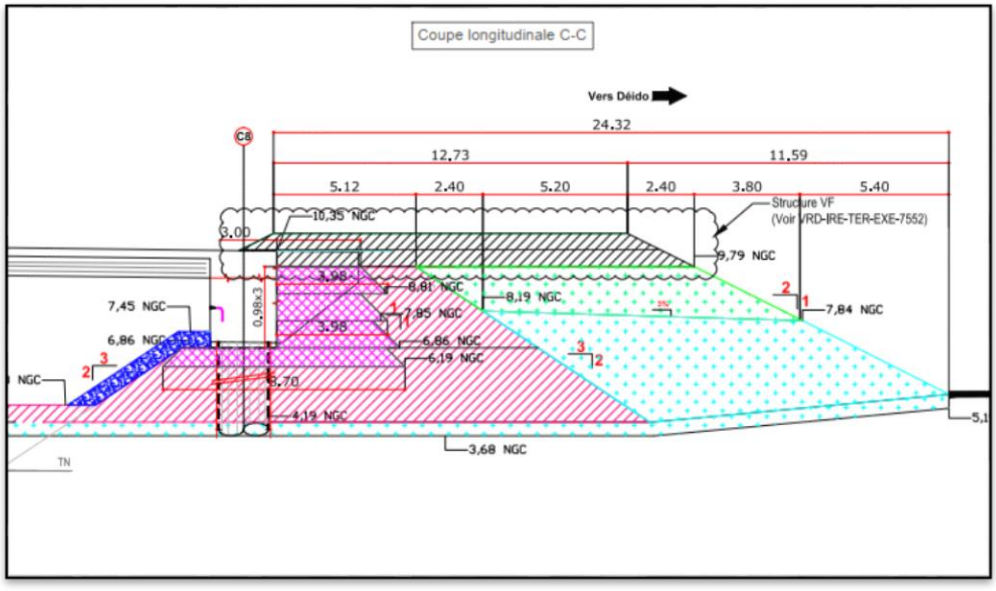

Figure 3.8. Typical longitudinal profile at PK 1+455 (Raport-Sagea Satom, 2015)

3.3.2. Geotechnical data

The PK 1+455 profile was chosen for the analysis because it corresponds to the area under the abutment. In the following sections, geotechnical data for the embankment soil and foundation soil obtained from in situ and laboratory tests are presented.

3.3.2.1. Foundation soil geotechnical data

The foundation soil in this case study is a mix of different soil types. In situ tests such as pressuremeter sounding to about 80 m, SPT corer down to 40.43 m depth, static penetration test CPT0, descended to 24.3 m depth, static penetration test CPT1, descended to 26.8 m depth, and CPT2 static penetration test descended to 20.5 m depth were used to define the soil stratigraphy and resistance, while laboratory tests such as Direct shear test, Atterberg limit tests, Oedometer test, and Permeability were carried out for confirmation. The stratigraphic profile of the soil obtained from the test is shown in the table 3.1. and table 3.2

Table 3.1. Retained geological section

Soil type	Top of soil layer [NGC]	Thickness [m]
Clayey sand	4.0	2
Fine sand	2.0	3
Micaceous slime	-1.0	3.5
Fine to coarse loose sand	-4.5	20.5
Medium to coarse sand gravelly compact	-25.0	6
Compact clay	-31.0	5
Stiff clay	-36.0	/

Table 3.2. Geotechnical parameters retained from the project site

Soil Type	γ $[kN/m^3]$	q_{c} (−)	E_{eod} $[MPa]$	P_i^* [-]	α [-]	E_m $[MPa]$	C' [KPa]	φ' [°]	c_u $[kN/m^2]$	λ_{cu} [-]	c_c [-]	c_α [-]	c_v $[m/s]$
Pozzolana	17	-					0	35					
Clayey Sand	20	-	15	1.0	0.33	45	5	29					
Fine Sand	19	5	8	1.0	0.33	24	0	32					
Micaceous Slime	13	1	5	0.5	1.00	5	-	-	67	15	0.4	0.012	10^{-6}
Fine to coarse loose Sand	19	2.5	7	0.6	0.33	21	0	28					
Medium to coarse sand gravelly compact	19	-	15	2.0	0.33	45	-	-					
Compact Clay	20	-	20	2.5	1.00	20	-	-					
Stiff Clay	20	-	80	6.0	1.00	80	-	-					

3.3.2.2. PVD geotechnical data

Colbond drain prefabricated vertical drains were used in this project. Table 3.3 below lists the features of the Colbond drain.

Table 3.3. Drain properties from Colbond drain® CX1000 product information(Colbond, 2008)

Properties of Colbond Drain	Unit	Mean Value	Test Method
Characteristics of composite/unit per strip			
Weight	g/lm	80	EN ISO 9864
Width	m	0.1	
Thickness	mm	4	EN ISO 9863-1
Mechanical characteristics			
Tensile strength	kN	2.5	EN ISO 10319
Elongation at 1 kN	%	3	EN ISO 10319
Hydraulic Properties			
Discharge capacity	m^3/s	$140*10^{-6}$	EN ISO 12958
Opening size	μm	75	EN ISO 12956
Permeability	mm/s	70	EN ISO 11058

3.3.2.3. Stone column geotechnical data

The proposed parameters for the stone columns in our case study will be derived from Dipty and Girish's literature.

Table 3.4. Properties of gravel material for stone column (Dipty and Girish, 2009)

parameter	E $[MP_a]$	v $[-]$	c' $[KP_a]$	ψ' [°]	$\emptyset$ [°]	k_h $\left[\frac{m}{day}\right]$	k_v $\left[\frac{m}{day}\right]$	γ $\left[\frac{kN}{M^3}\right]$
value	45000	0.3	0	0	50	6	6	19.4

3.3.2.4. Groundwater condition

The groundwater levels at the site of the project were found to range between 0.5NGC and 1NGC around the abutment wall.

3.3.2.5. Embankment geotechnical data

The embankment soil is composed of Pozzolana and strong reddish clay with the parameters presented in Table 3.5

Table 3.5. Embankment soil Parameters-Reddish clay (Project Documents)

Soil type	γ_d[kN/m^3]	γ_{opt}[kN/m^3]	E[kPa]	Φ'[°]	C'[kPa]	N [-]
Pozzolana	14,5	16,5	70000	40	0	0.25
Clayed Sand	17	20	50000	29	5	0.3

3.4. Presentation of design results

The different reinforcement methods prescribed in the previous chapter were carried out using both analytical and numerical computations and the results are presented in the following sections.

3.4.1. Analytical designs result

The soil below the abutment wall was analysed without reinforcement to see its total settlement after which the soil model was reinforced with PVD and stone columns, and analysed. The results got are presented in the sections below.

3.4.1.1. Results from the Analytical computation of soil settlement without reinforcement

Settlement analysis was divided into immediate settlement, primary consolidation and secondary consolidation. The sum of the different processes gave the total analytical settlement got from the study

a. Immediate settlement

After computations were carried out as proposed by Christian and Carter, the total immediate settlement was got by summing the immediate settlement of the different layers. the embankment loads applied to the soil sample and the immediate settlement results are represented in table 3.6, and table 3.7 respectively.

Table 3.6. Embankment load and dimension data input parameters

q_0	160	[KN]
B	30	[m]
L	-	[m]
D	0	[m]

Table 3.7. Immediate settlement from analytical design

Soil layer	Thickness $[m]$	Layer height $[m]$		$\frac{H}{B}$	$\frac{L}{B}$	μ_0	μ_1	E_u $\left[\frac{KN}{m^2}\right]$	s_i' $[m]$	$s_i = s_{i_b}' - s_{i_t}'$ $[m]$
Clayey Sand (CS)	2	T	0	0	1	1	0	45000	0	0.0051
		B	2	0.0667	1	1	0.05	45000	0.01	
Fine Sand (FS)	3	T	2	0.0667	1	1	0.05	24000	0.01	0.0133
		B	5	0.1667	1	1	0.12	24000	0.02	
Micaceous Slime (MS)	3.5	T	5	0.1667	1	1	0.12	5000	0.11	0.0073
		B	8.5	0.2833	1	1	0.2	5000	0.18	
F-C Loose Sand (FC - S)	20.5	T	8.5	0.2833	1	1	0.2	21000	0.04	0.0456
		B	29	0.9667	1	1	0.41	21000	0.09	
M-C Sand compact (G)	6	T	29	0.9667	1	1	0.41	45000	0.04	0.0041
		B	35	1.1667	1	1	0.45	45000	0.05	
compact clay (CC)	5	T	35	1.1667	1	1	0.45	20000	0.1	0.0045
		B	40	1.3333	1	1	0.47	20000	0.11	
stiff clay (SC)	-	T	40	1.3333	1	1	0.47	80000	0.03	0.0017
		B	45	1.5000	1	1	0.5	80000	0.03	

$$\text{Total immediate settlement } (s_i) = 0.0815 \text{ m}$$

b. Primary consolidation settlement

Primary consolidation settlement computation was carried out on the layer of fine soil and the results are represented in the tables 3.8. table 3.9 and table 3.10

Table 3.8. Embankment geometry parameters and load

B_1	5	[m]
B_2	10	[m]
q_0	152	[KN]

Table 3.9. Computation of $\Delta\sigma_z'$

Layers	Thickness $[m]$	depth $[m]$	α_1 [-]	α_2 [-]	I [-]	$\Delta\sigma_z'$ [MPa]
Clayey Sand (CS)	2	0				
		2	0.2	1.19029	1	431
Fine Sand (FS)	3	5	0.5	0.7854	0.80	122
Micaceous Slime (MS)	3.5	7	0.5	0.62025	0.46	70.4
		8.5	0.5	0.53172	0.33	49.7
F-C Loose Sand (FC -S)	20.5	10	0.5	0.46365	0.24	36.1
		14	0.5	0.34302	0.11	16.4
		18	0.4	0.27095	0.05	7.42
		22	0.4	0.22348	0.02	2.76
		24	0.4	0.2054	0.01	1.28
		28	0.3	0.17671	0.00	-0.7
M-C Sand compact (G)	6	32	0.3	0.155	0.00	-1.8
		35	0.3	0.1419	0.00	-2.4
Compact clay(CC)	5	40	0.2	0.12435	-0.00	-2.9
Stiff clay (SC)	5	45	0.2	0.11066	-0.00	-3.2

Table 3.10. Primary consolidation settlement results from analytical design

Layers Name	Layer [m]	Depth [m]	γ $\left[\frac{kN}{m^3}\right]$	γ_w $\left[\frac{kN}{m^3}\right]$	γ' $\left[\frac{kN}{m^3}\right]$	σ'_z [MPa]	$\Delta\sigma'_z$ [MPa]	C_c [-]	e_0 [m]	S_{eod} [m]
Clayey Sand (CS)	2	0	20	10	10	0	0			
		2	20	10	10	20	431			
Fine Sand (FS)	3	5	19	10	9	47	122			
Micaceous Slime (MS)	3.5	7	13	10	3	53	70.4	0.4	2	0.5511
		8.5	13	10	3	57.5	49.7	0.4	2	0.3328
F-C Loose Sand (FC -S)	20.5	10	19	10	9	71	36.1			
		14	19	10	9	107	16.4			
		18	19	10	9	143	7.42			
		22	19	10	9	179	2.76			
		24	19	10	9	215	1.28			
		28	19	10	9	251	-0.68			
M-C Sand compact (G)	6	32	19	10	9	287	-1.84			
		35	19	10	9	314	-2.39			
compact clay	5	40	20	10	10	364	-2.94			
Stiff clay (SC)	5	45	20	10	10	414	-3.22			

$$\boldsymbol{S_{eod} = 0.89415\ m}$$

Symptom and Bjerum correction factor $\beta = 0.85$.

$$\textbf{Primary consolidation settlement } (\mathbf{s_c}) = \mathbf{0.760307\ m}$$

c. Secondary consolidation

The computation of secondary settlement was computed following the method described in the methodology and the result is presented in Table 3.11

Table 3.11. Analytical computation of secondary consolidation

C_α	0.012	-
t	10	years
U	0.95	%
$\boldsymbol{T_v}$	1.2	–
H	3.5	m
$\boldsymbol{C_v}$	0.000001	$\frac{m^2}{s}$
$\boldsymbol{C_v}$	31.536	$\frac{m^2}{year}$
$\boldsymbol{t_{95}}$	0.1107068	years
t_{95}	40.407986	days

secondary consolidation $s_\alpha = 0.02738156$ m

The total settlement is the sum of the immediate settlement, primary and secondary consolidation as stated in the methodology. The results of the total settlement after analytical computations are:

$$\mathbf{S = S\_i + S\_c + S\_\alpha\ (10\ years) = 0.081586 + 0.76707 + 0.02738156}$$
$$\mathbf{= 0.8693m}$$

3.4.1.2. Results from Analytical computation of abutment reinforcement with PVD

Using the solution proposed by (Hansbo, 1987) as stated in the methodology, the results for the drainage spacing to reduce consolidation time were computed and the results are represented in table 3.12.

Table 3.12. input parameters for the Hansbo solution

U_h	$C_h\left(\frac{m^2}{day}\right)$	d_s $[m]$	$k_h\left(\frac{m}{day}\right)$	$k_s\left(\frac{m}{day}\right)$	$q_w\left(\frac{m^3}{day}\right)$	t $[day]$	l $[m]$
0.95	1.976	0.199	0.00094	0.00023	0.00014	35	11

Drain spacing $= 2.54$ m

3.4.1.3. Results from the analytical computation of stone columns

The analytical design used in this work is that proposed by De Beer-Van Impe in 1983. The design's goal was to determine the stresses and vertical settlement in the column and

surrounding soil and limit this settlement below the project specification. The following are input data used in the analytical computation;

$P_o = 160k$ $E_t = 3714.2kPa$

$v_t = 0.3$ $k_{ac} = 0.33$

$k_{at} = 0.51$ $a = b = 4\ m$

$H = 11\ m$ $D = 1.2\ m$

Considering a rectangular arrangement of the columns, an area equivalence of the stone column was found to get a plane strain model in which every column line is transformed into a wall with a thickness.

$d_f = 0.126$

The equations (1.30) (1.31) (1.32) (1.33) (1.34), and (1.35), were computed using Microsoft Excel, and the six equations were solved simultaneously to find the settlements and stresses. The following results were obtained from the calculations:

$\boldsymbol{S_v = 0.01705m}$ $\boldsymbol{S_h = 2.147\ x10^{-5}m}$ $\boldsymbol{\sigma'_{vt} = 171\frac{KN}{m}}$

$\boldsymbol{\sigma'_{ht} = \sigma'_{hc} = 87.21\frac{KN}{m}}$ $\boldsymbol{\sigma'_{vc} = 264.27\frac{KN}{m}}$

3.4.2. Numerical analysis results

The program PLAXIS 2D V20.02 was used to numerically model a realistic case study, as stated in the methodology. The model was first run without any reinforcement to check for the consolidation time and settlement degree, after which PVD and stone columns were used to reinforce the soil and the models ran conservatively. The soil parameters used in the test came from GEOS Ingénieurs Conseil (report missionG3 phase étude au sens de la norme NF P-94-5000 de novembre 2013) report, while the stone column parameters came from the adopted stone column parameters proposed by (Dipty and Girish 2009). Table 3.1, Table 3.2, table 3.3 table 3.4 and table 3.5 present the input soil parameters, PVD parameters and stone properties. The Mohr Coulomb model was used to model the soil embankment while varying soil models dependent on the properties of the soil were used in modelling the other soil layer. Table 3.13 represents the summary material used and their material model.

Table 3.13. Summary of material used and the material model

Material	Material model	Loading condition
Clayey Sand	Mohr Column	Drained
Fine Sand	Mohr Column	Drained
Micaceous slime	Soft soil creep	Undrained A
Medium to coarse gravelly compact	Mohr Column	Drained
Compact clay	Hardening soil	Undrained B
Stiff clay	Hardening soil	Undrained B
Pozzolana	Mohr Column	Drained
Embankment sand	Mohr Column	Drained

3.4.2.1. Results from the modelling of soft soil without reinforcement

Based on the parameters in Table 3.1 and Table 3.2, the soft soil layers were defined geometrically and qualitatively. The standard fixity boundary conditions were used, which allowed no horizontal displacement but only vertical displacement on the lateral sides. The soil was subjected to an embankment load, which represents the abutment load, traffic loads, as well as a surcharge load to limit settlement after the construction phase. The water table at the base of the embankment was then determined using geotechnical reports. The embankment was modelled in three stages using staged construction. After each stage of construction, the model was allowed to undergo a consolidation period of 20 days. The final consolidation stage was set to stop at a minimum poor pressure dissipation of between 0-2kPa. Figure3.9 shows the finite element model used to simulate the behaviour of the embankment in initial conditions, while figures 3.10 and 3.11 shows the meshing system and calculation steps for the soil initial conditions, respectively.

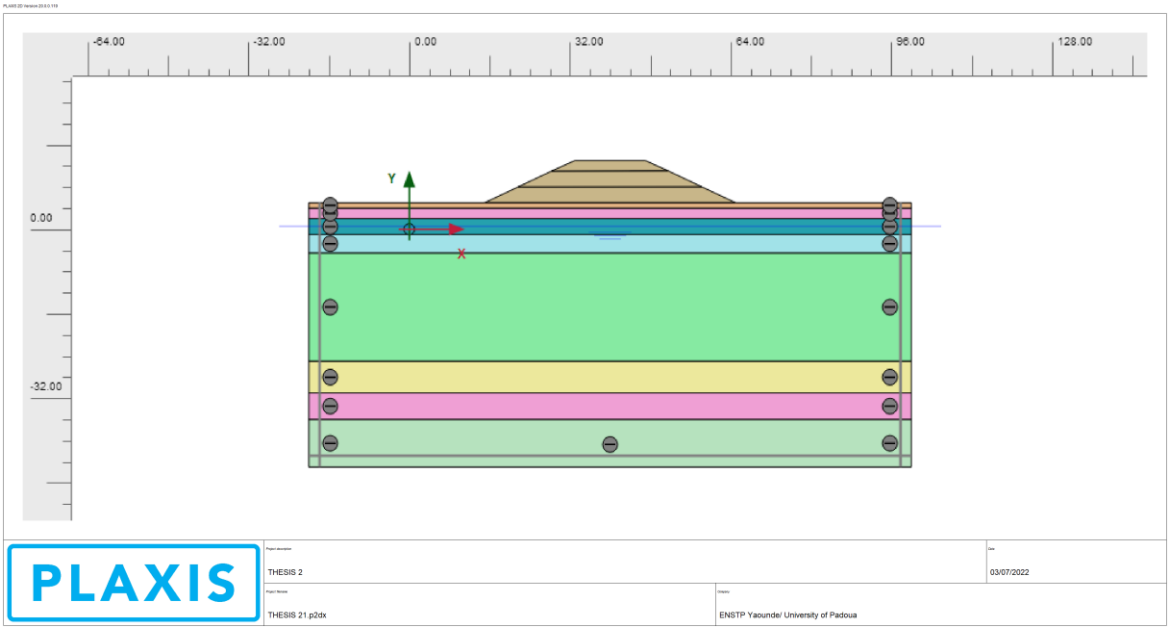

Figure 3.9. Model of embankment load on soft soil without reinforcement

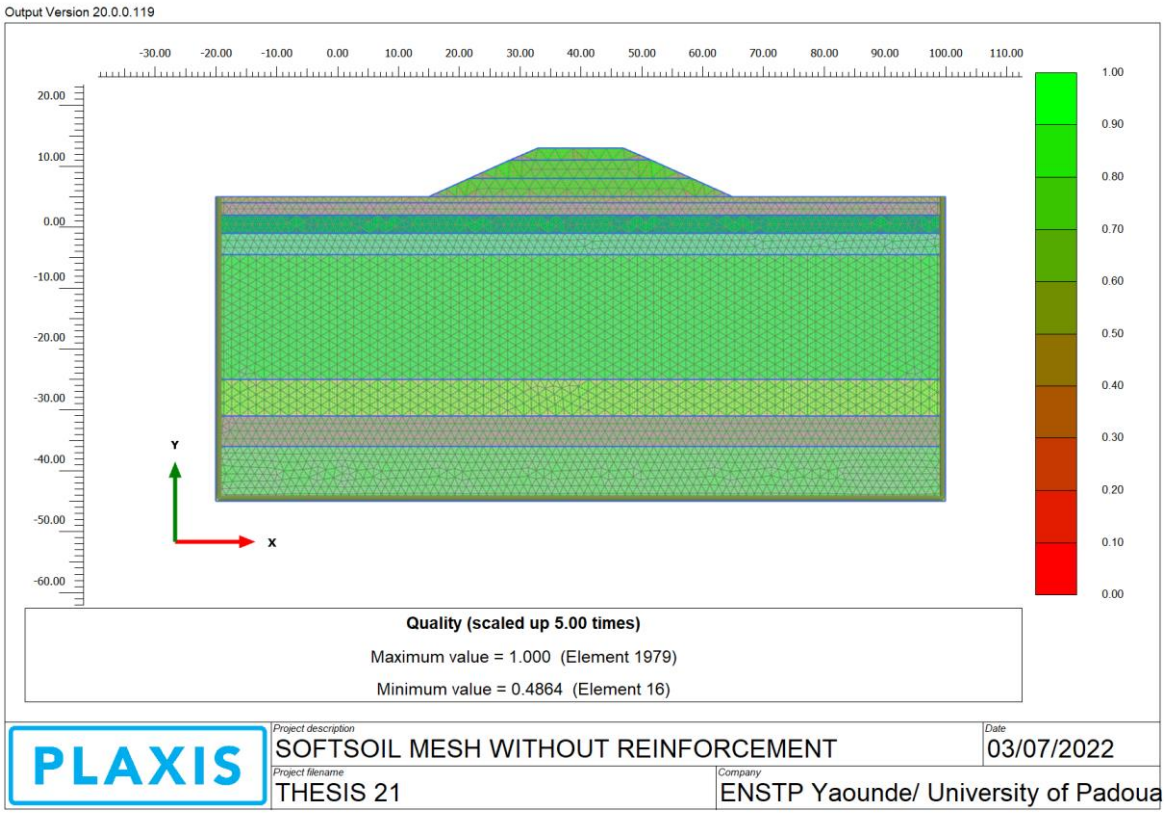

Figure 3.10. Meshing system of embankment load on soft soil without reinforcement.

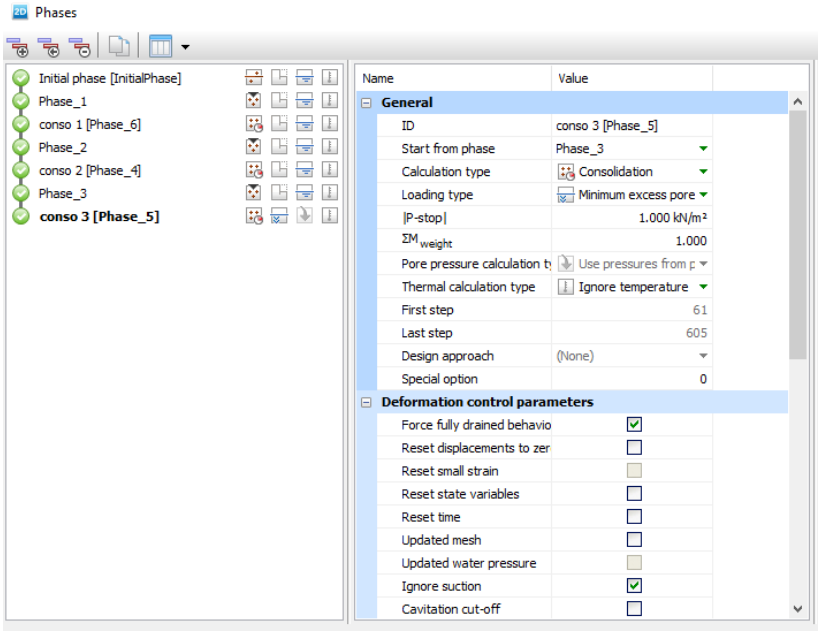

Figure 3.11. Calculation steps of the soft soil without reinforcement.

PLAXIS' FEM model estimates a variety of model parameters, including settlements, excess pore water pressures, and consolidation end time. Different points on the model were chosen for numerical study to assess settlements and excess pore water pressures. The expected deformation obtained from the analytical result was used to consider the points chosen. One point came from the micaceous clay layer's centre, whereas the other came from the fine sand layer and the surface of the model. Embankment deformation was not considered in the model. The points chosen for the analysis are shown in figure 3.12.

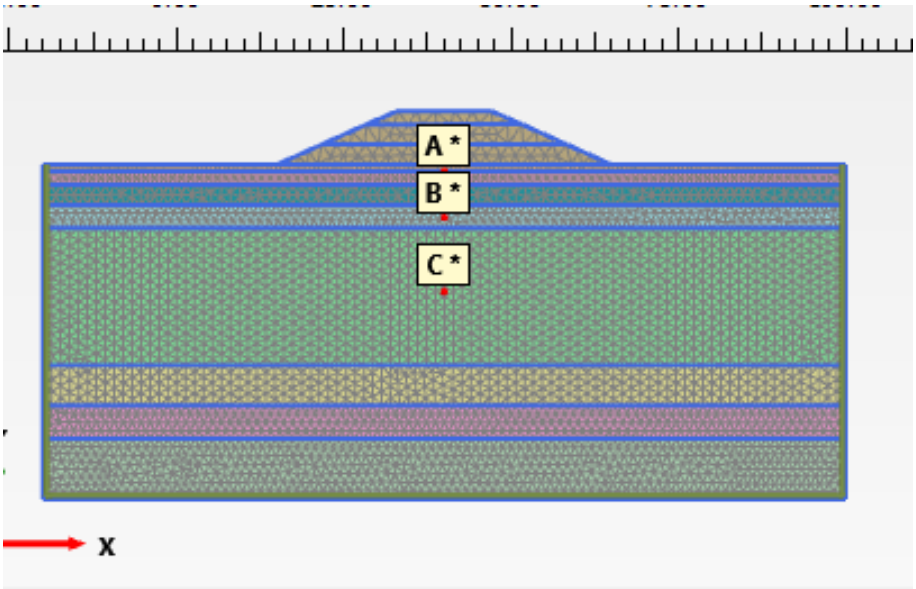

Figure 3.12. Critical analysis points for unreinforced soil samples

a. Settlement of soil model without reinforcement

In three steps, embankment loads were applied to the soil model. For the first step, embankment sand was applied to a depth of 3 m and left to settle for 20 days. This was done gradually throughout all stages, with the final stage of consolidation allowing the soil to deform until a minimal pore pressure was reached. A maximum deformation of 0.891m was obtained after a consolidation period of 2051 days (5 years 7 months) represented in figure 3.13. Three points A, B and C, were picked from the top soil layer (A), the centre of the micaceous clay layer (B), and the middle of the Fine to coarse loose sand layer (C), respectively, to study the displacement of the different layers over time. It was noted that the deformation of the soil due to the embankment loads decreased with an increase in depth. In figure 3.14, it is seen that the settlement of different soil layers continues gradually until the minimum pore pressure is arrived at. The rate of settlement then drops gradually on the minimum pore pressure of between 0-2kPa is arrived at. Data of soil deformation at points A, B and C at the end of each construction stage is represented in table 3.14.

Table 3.14. Settlement of soil without reinforcement verse time at points A, B, and C

Stage	**Stage 1**	**1ST Con**	**Stage 2**	**2ND Con**	**Stage 3**	**3RD Cond**
Time (days)	**5**	**15**	**35**	**45**	**50**	**2051**
Settlement at A (m)	0.068	0.115	0.180	0.239	0.278	0.891
Settlement at B (m)	0.058	0.078	0.126	0.142	0.155	0.418
Settlement at C (m)	0.035	0.033	0.060	0.058	0.069	0.079

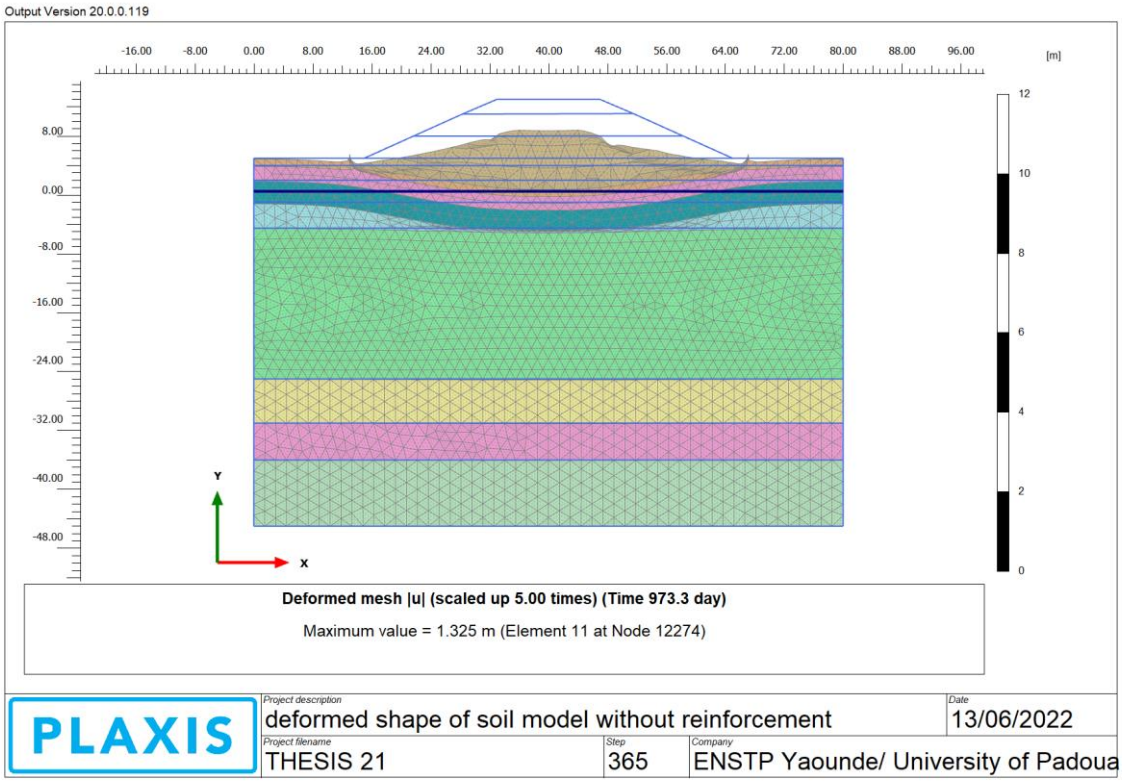

Figure 3.13. Deformation of the soft soil model without reinforcement.

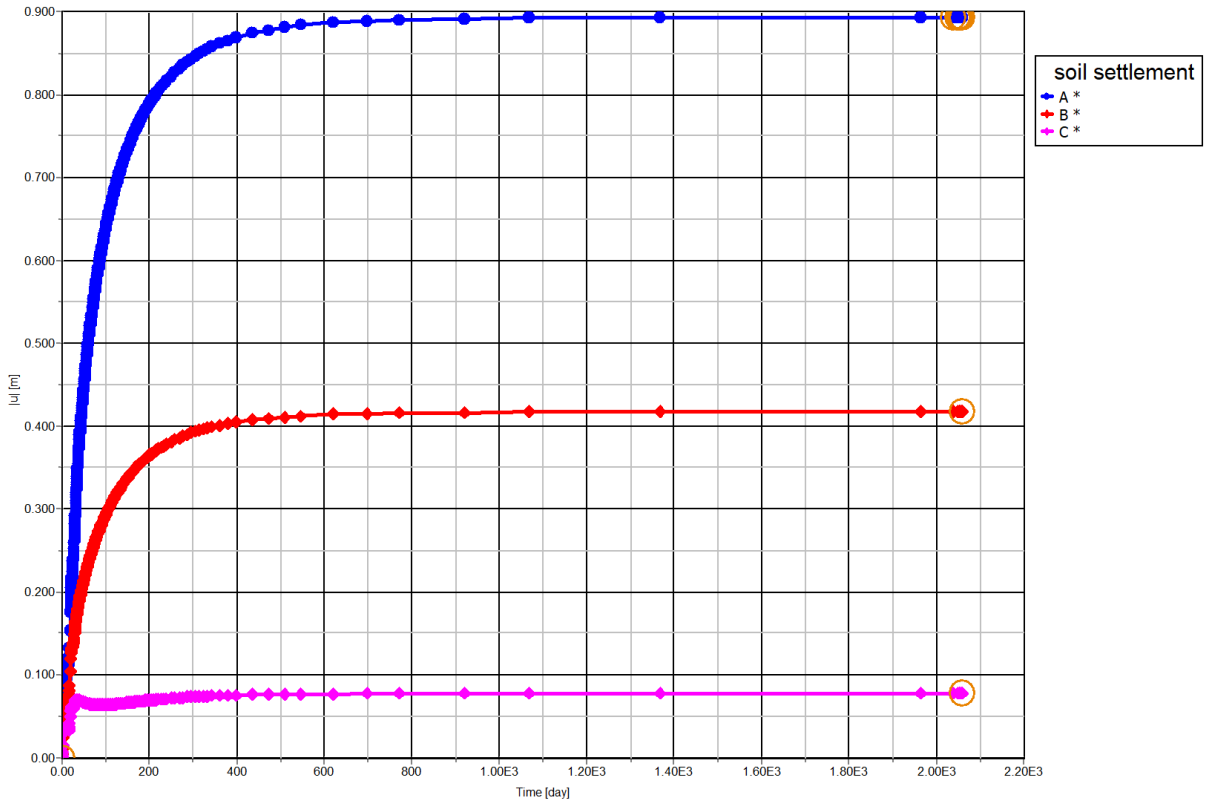

Figure 3.14. Deformation of points A, B, and C, with time on the reinforced soft soil model.

b. Variation of the excess pore with time for soil model without reinforcement

To analyse excess poor pressure variation over time, the Same 3 points from A, B, and C, used to analyse the computation of settlement were maintained. As illustrated in figure 3.15, excess pore water pressures reached their maximum values following the construction stages of each embankment fill phase. During the short consolidation phase, it progressively declined for each step but continued to diminish with time once the last stage was completed until it approached zero when the consolidation was complete. The maximum excess pore pressure value was observed at point B with a value of $118.365\frac{kN}{m^2}$. while points A and C recorded excess pore pressure values of $89.126\frac{kN}{m^2}$ and $45.98\frac{kN}{m^2}$ respectively. Table 3.15 gives numerical values of the excess pore pressure at the end of each stage of the construction process for points A, B and C.

Table 3.15. Excess pore pressure values for unreinforced soil sample at the end of each stage construction process of points C, D and E

Stage	**Stage 1**	**1ST Con**	**Stage 2**	**2ND Con**	**Stage 3**	**3RD Cond**
Time (days)	**5**	**25**	**35**	**45**	**550**	**2051**
EPP at A $\frac{kN}{m^2}$	42.359	41.256	74.448	72.063	89.126	0
EPP at B $\frac{kN}{m^2}$	62.511	52.779	108.770	95.625	118.365	0
EPP at C $\frac{kN}{m^2}$	0.035	0.033	0.060	0.058	45.98	0

Where: EPP=excess pore pressure

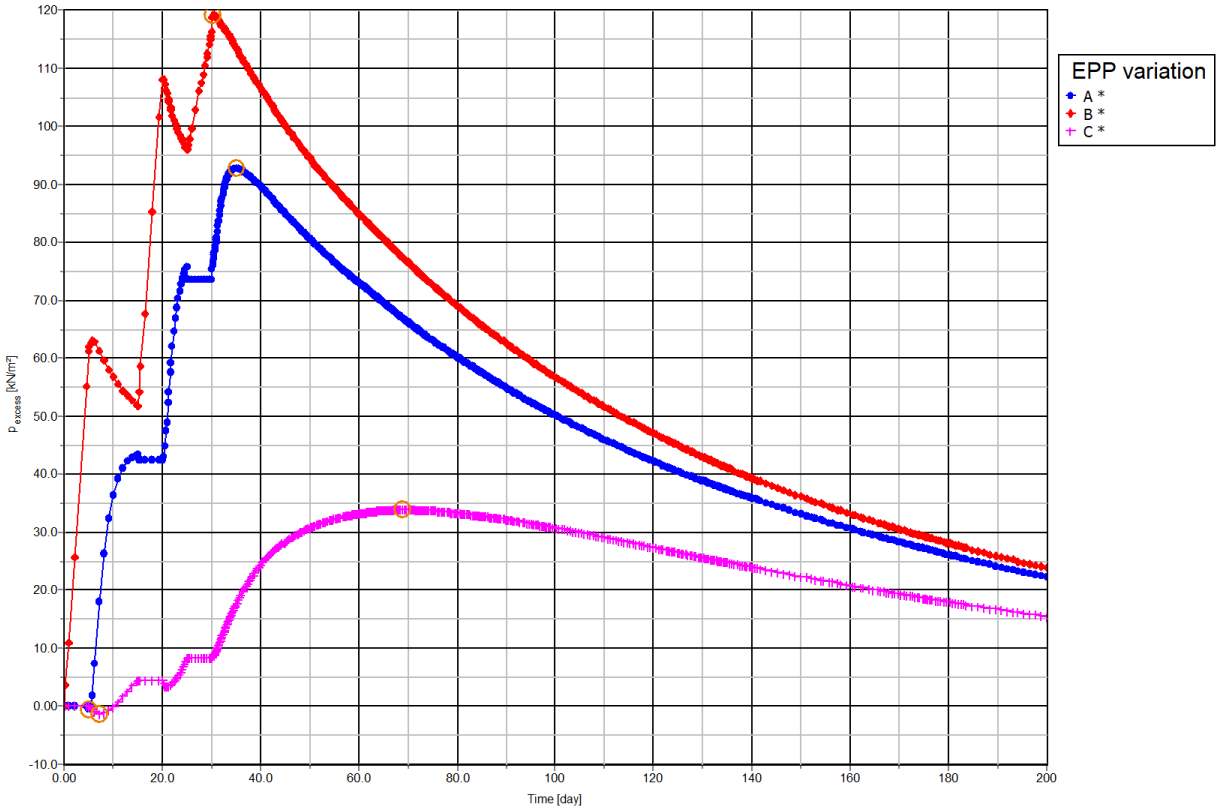

Figure 3.15. Excess Pore pressure variation over time at points A, B, and C for unreinforced soil sample

3.4.2.2. Results from the modelling of soft soil reinforced PVD

This case study was modelled using the same parameters as the soil model without reinforcement, with the addition that prefabricated vertical drains (PVD) of 10 m were inserted every two and a half metres of the soil samples to aid drainage. On top of the soil, a 1m thick Pozzolana layer was built to act as a drainage mechanism for the extra pore pressure. Table 3.3 lists the features of the Colbond drain that was employed. The finite element model used to predict the behaviour of soft soil in the reinforced setting is shown in Figure 3.16, while the meshing system and calculation processes in reinforced conditions are shown in figures 3.17 and 3.18, respectively.

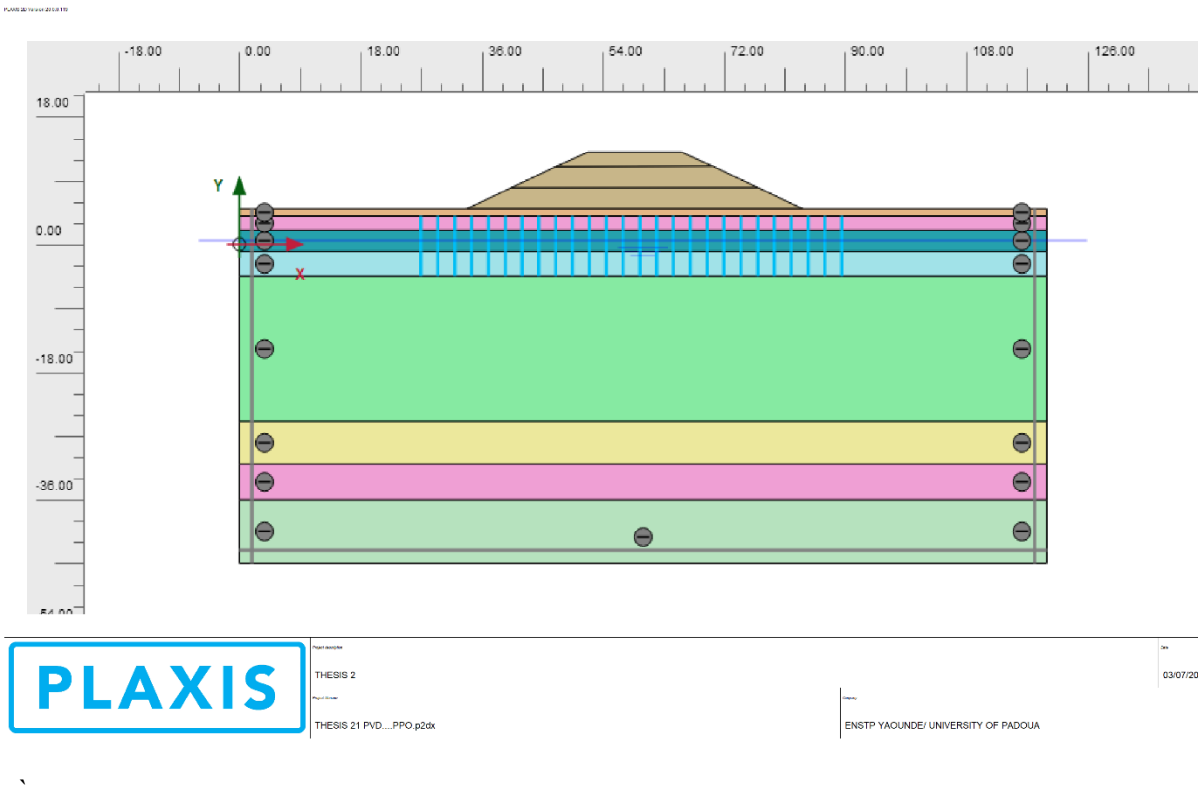

Figure 3.16. Model of embankment load on soft soil reinforced with PVD

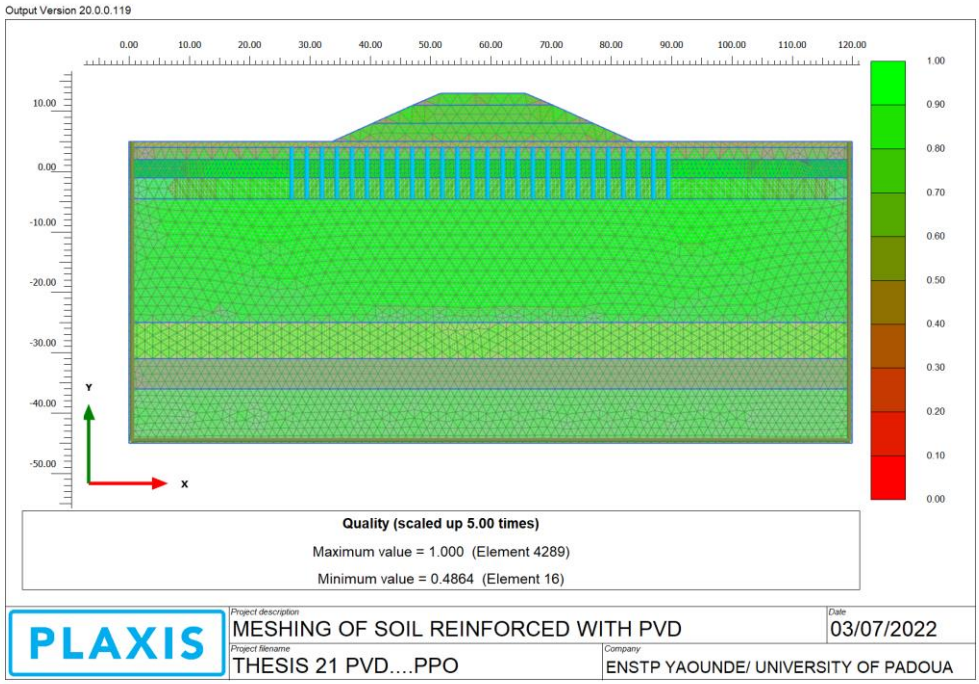

Figure 3.17. Meshing system of embankment load on soft soil with prefabricated vertical drain as reinforcement

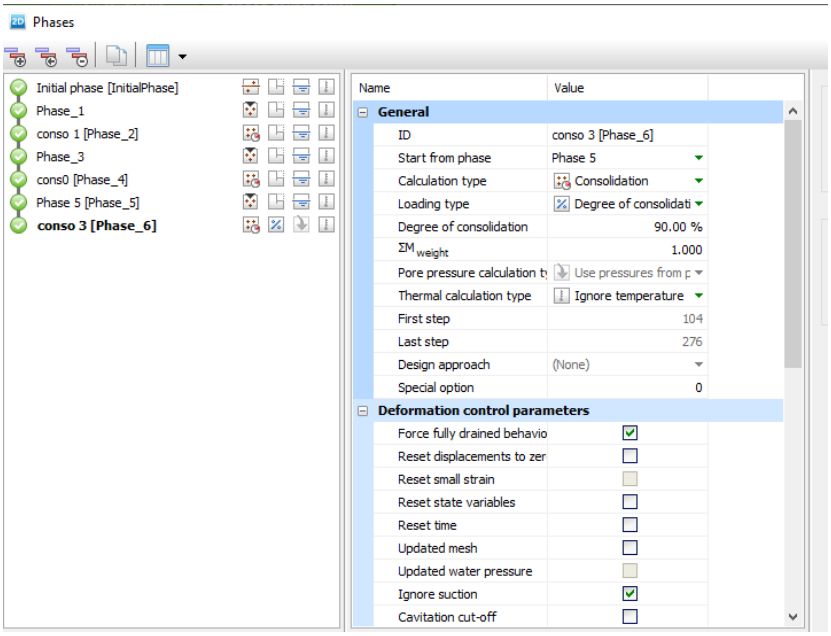

Figure 3.18. Calculation steps of the soft soil with PVD as reinforcement

The same computations as that of soil without reinforcement were carried out to see the evolution of deformation with time as well as the variation of pore pressure. Different sites were chosen for numerical study to assess settlements and excess pore water pressures. The expected deformation obtained from the analytical result was used to consider the points chosen. One point came from the micaceous clay layer's centre (B), whereas the other came from the fine sand layer(C) and the surface of the model (A). Embankment deformation was not considered in the model since it was modelled to be a structural element. The points chosen for the analysis are seen in figure 3.19.

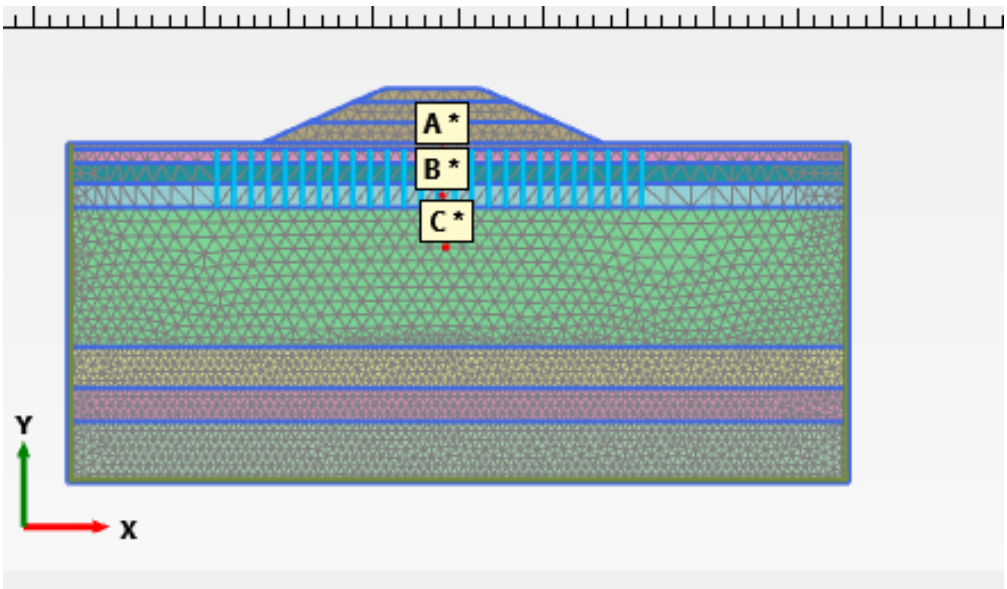

Figure 3.19. Critical analysis points of soil reinforced with PVD

a. Settlement of soil model reinforced with PVD

The structure was subjected to a series of loads in stages. For the first stage, embankment sand was applied to a depth of 3 m and left to settle for 20 days. This was done gradually throughout all the stages, with the final stage of consolidation allowing the soil to deform until a minimal pore pressure was reached. A maximum deformation of 0.856 m was obtained after the consolidation period which lasted 427 days was over. Figure 3.20 gives a picture of the soil deformation at the end of the consolidation period. To monitor the deformation of the soil at various layers, 3 points A, B, and C were chosen from the Soil surface, micaceous slime and the Fine to Coarse Loose sand layers respectively seen in figure 3.19. The deformation was observed to decrease with an increase in depth. Point A recorded the highest deformation of 0.856m While Point B and C recorded lower deformations of 0.457m and 0.08 m respectively, all represented in the figure 3.21. from the deformation curve, it is observed that most of the deformation occurs between days 0-40 for all points. Records of deformation values at the end of every construction stage for all three points are recorded in table 3.16.

Table 3.16. Settlement of soil reinforced with PVD verse time at points A, B, and C

Stage	**Stage 1**	**1ST Con**	**Stage 2**	**2ND Con**	**Stage 3**	**3RD Cond**
Time (days)	**5**	**25**	**35**	**45**	**50**	**427**
Settlement at C (m)	0.062	0.397	0.450	0.991	1.018	0.856
Settlement at B (m)	0.260	0.399	0.475	0.536	0.550	0.457
Settlement at E (m)	0.039	0.038	0.068	0.069	0.080	0.080

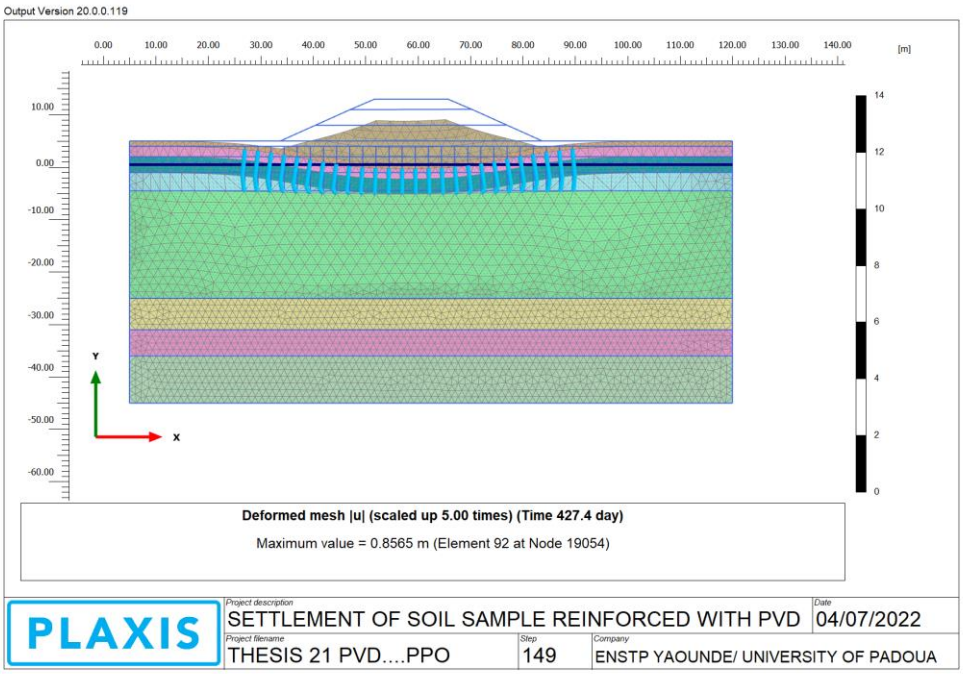

Figure 3.20 Deformation of soil reinforced with PVD

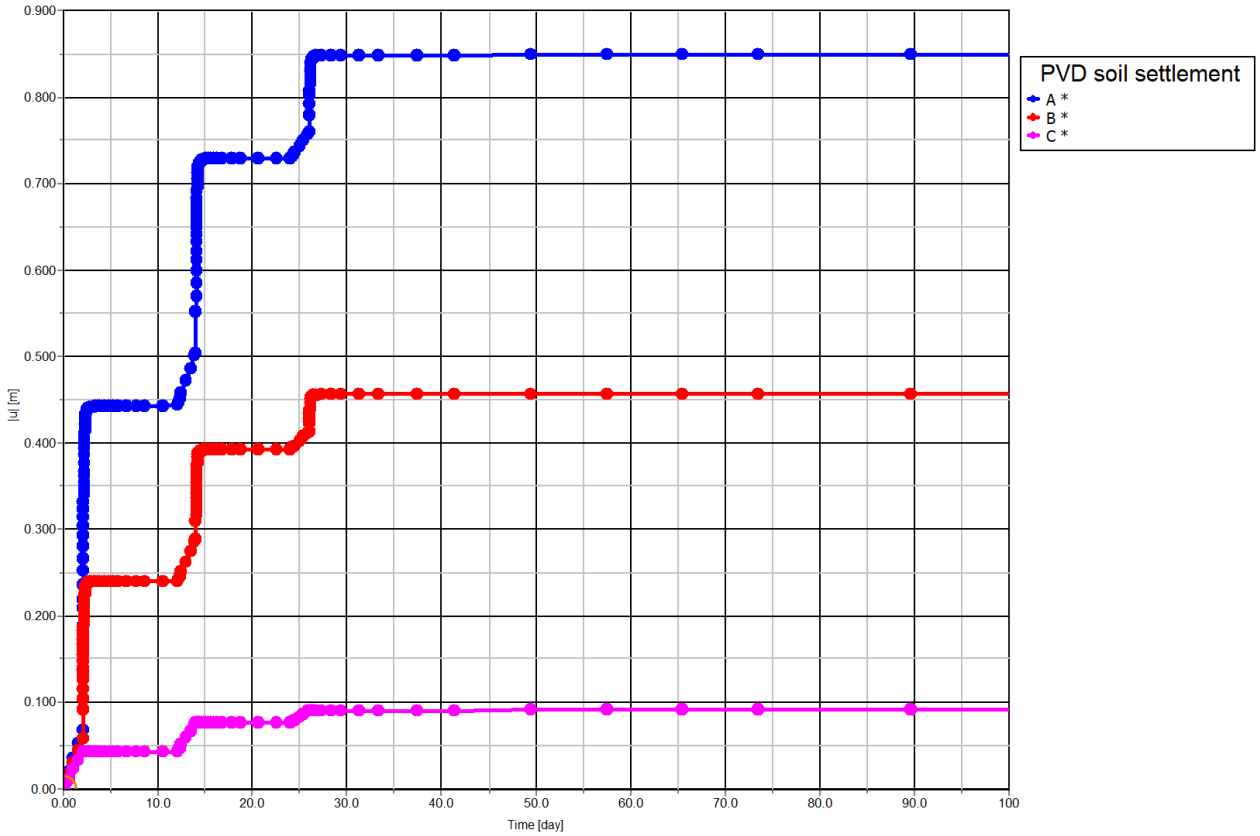

Figure 3.21. Comparative settlement of points C, D, and E with time of soils reinforced with PVD

b. Variation of the excess pore with time for soil model reinforced with PVD

Excess pore pressure is an important factor when it comes to consolidation analysis because it affects the effective stress of the soil thereby affecting the rate of consolidation. To visualise the behaviour of excess pore water pressure over time, three points A, B, and C were chosen from the fine sand layer, micaceous slime layer and loose sand layer respectively. The maximum effective pressure recorded was found at point B with a value of 71.78 $\frac{kN}{m^2}$. The pore pressure of the two other layers recorded very low values. Point A recorded a pore pressure1.8 2 $\frac{kN}{m^2}$ while point C recorded 0.47 $\frac{kN}{m^2}$. Figure 3.22 presents the variation of pore water pressure at points A, B and C with time. The results at the end of the stage construction values for each of the points with time are represented in table 3.17

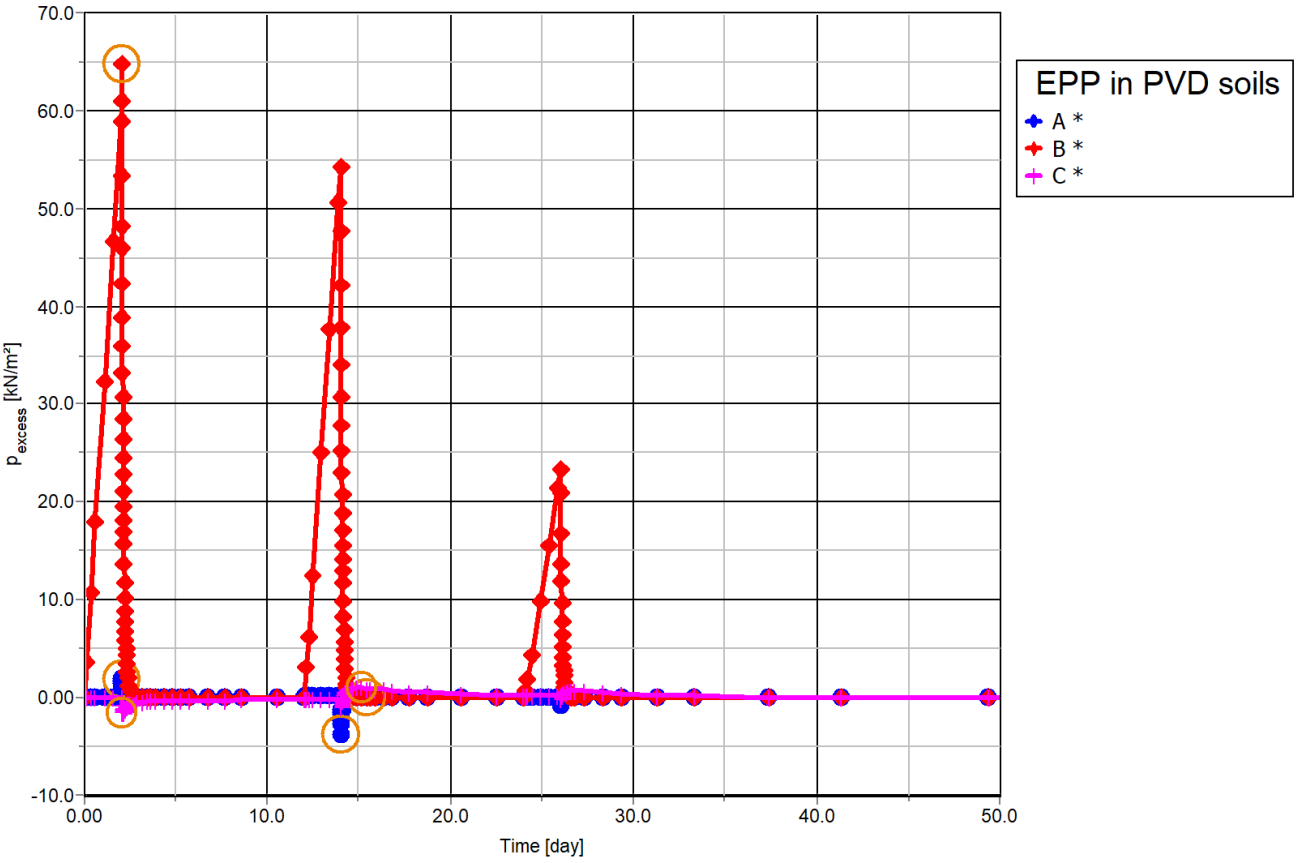

Figure 3.22. Excess Pore pressure variation over time at points A, B, and C for soil reinforced with PVD

Table 3.17. Excess pore pressure values of soft soil sample reinforced with PVD at the end of each stage construction process of points A, B and C

Stage	**Stage 1**	**1ST Con**	**Stage 2**	**2ND Con**	**Stage 3**	**3RD Cond**
Time (days)	**5**	**25**	**35**	**45**	**50**	**427**
EPP at A $\frac{kN}{m^2}$	0.82	-0.45	0.228	0	0	0
EPP at B $\frac{kN}{m^2}$	96.39	0.25	73.57	0.206	48.85	0
EPP at C $\frac{kN}{m^2}$	1.47	0.05	1.45	-0.05	0.069	0

3.4.2.3. Modelling of soft soil reinforced with Stone column

The stone columns were designed to meet project criteria, of a 10-year settlement limit of less than 5 cm. The PLAXIS 2D V20.02 stone column model was regarded to be the Vibro replacement model for stone column installation, in which a portion of the soil was removed and sent to the surface so that the column could be placed. The axisymmetric property was chosen for the project to equilibrate the horizontal deformation in both directions. The micaceous slime layer was modelled using the hardening soil model with the adjustment parameters provided by (Brinkgreve, 2010). Stone columns with a diameter of 1.5 m and a length of 20 m were drilled 3 m apart in the earth. Table 3.4 shows the properties of the stone column. To drain the excess water, a layer of 1m thick Pozzolana was modelled using the Mohr Column model, while all other layers were modelled with the same properties as the design without reinforcement. Figure 3.23 displays the finite element model used to simulate the behaviour of soft soil creep in reinforced settings, while figures 3.24 and 3.25 illustrate the embankment meshing system and calculation procedures in reinforced conditions, respectively.

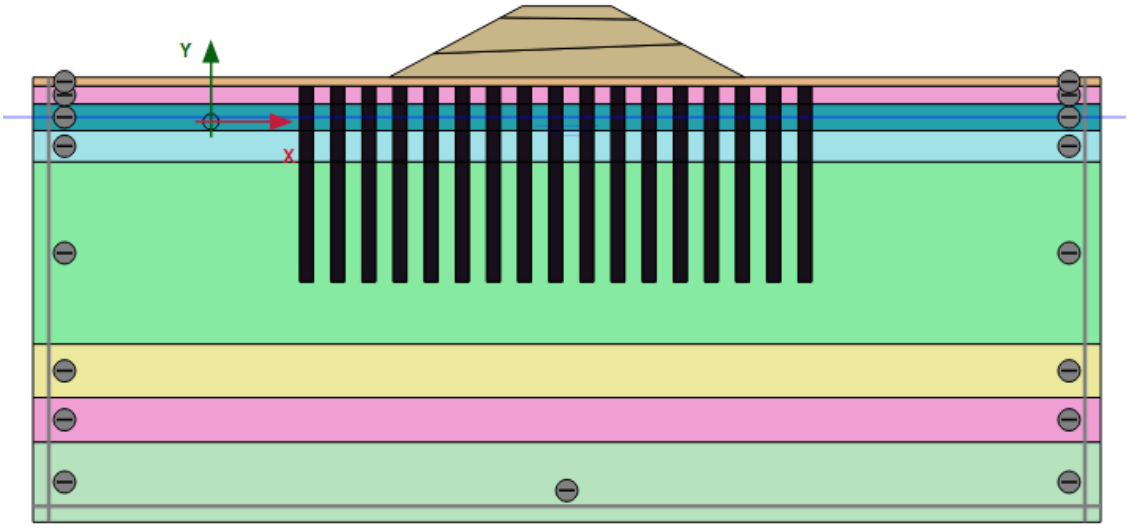

Figure 3.23. Model of embankment load on soft soil reinforced with Stone Column

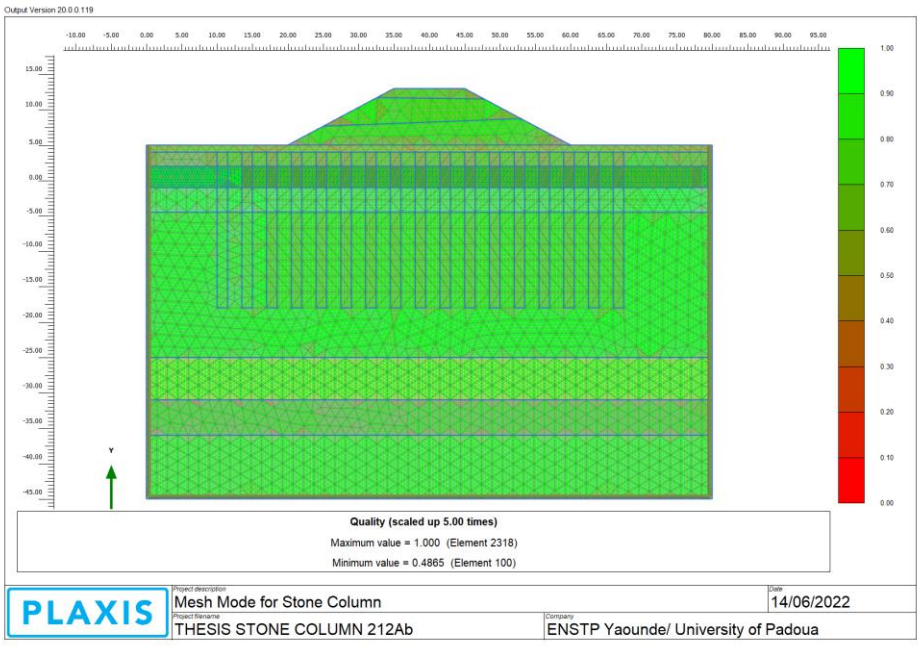

Figure 3.24. Meshing system of embankment load on soft soil reinforced with stone columns

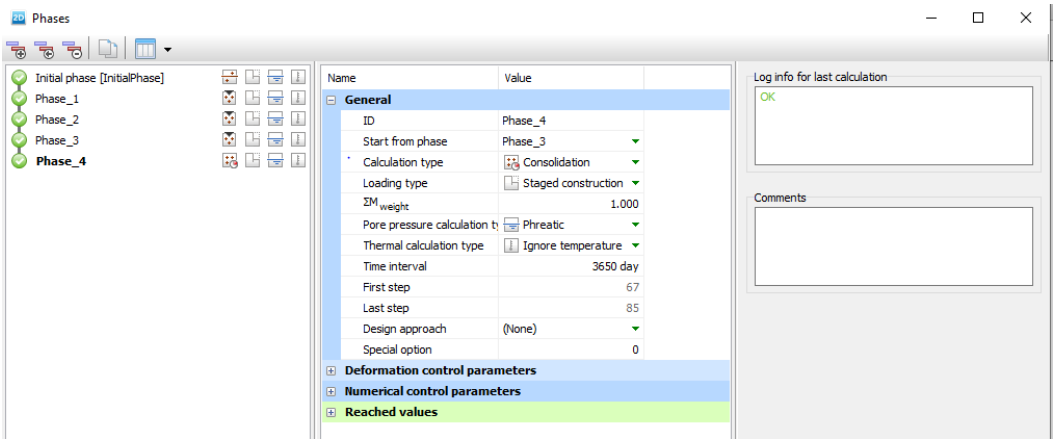

Figure 3.25. Calculation steps of the soft soil with stone columns as reinforcement

The same computations as that of soil without reinforcement were carried out to see the evolution of deformation with time as well as the variation of pore pressure. Three points below the middle of the embankment were chosen for numerical study to assess settlements and excess pore water pressures. The expected deformation obtained from the analytical result was used to consider the points chosen. One of the points came from the micaceous clay layer's centre, whereas the other came from the fine sand layer and the surface of the model illustrated in figure 3.26. Embankment deformation was not considered in the model since it was modelled to be a structural element.

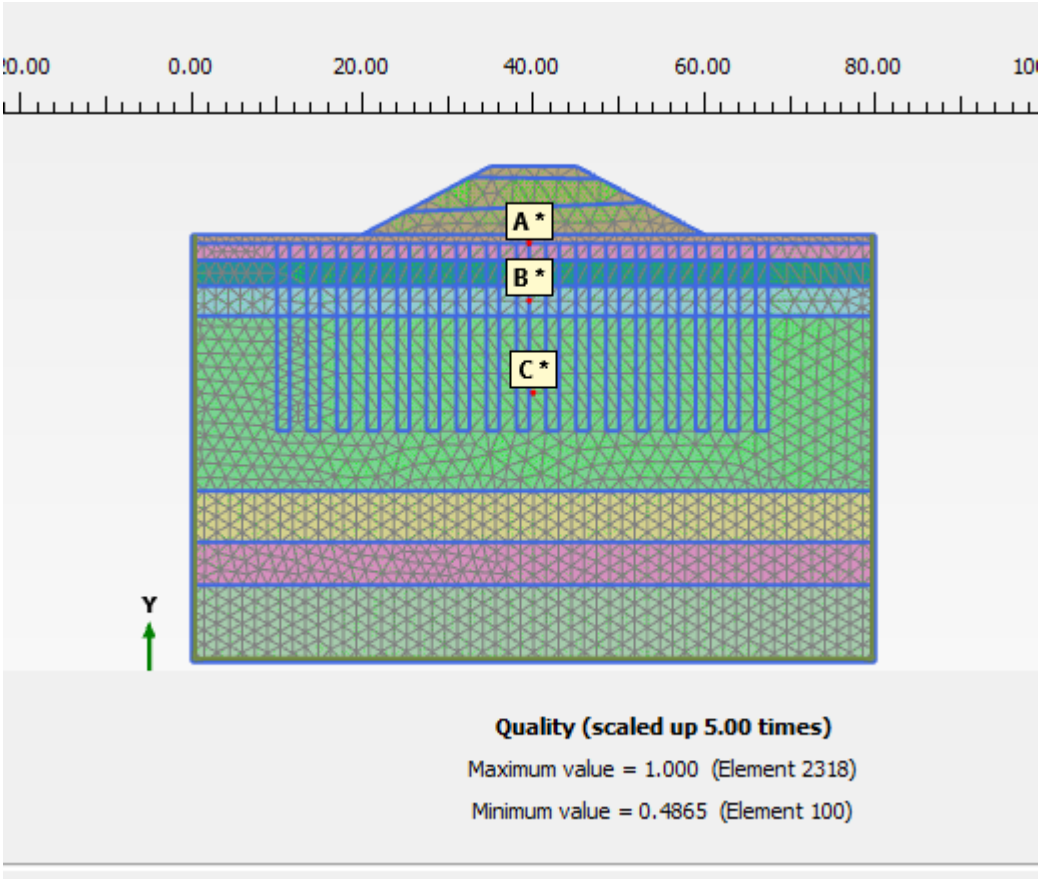

Figure 3.26. Critical analysis points of soil reinforced with Stone Column

a. Settlement of soil model reinforced with stone columns

After ten years of consolidation computation, the maximum deformation observed was 0.045 m seen in figure 3.27. Three points A, B and C, were picked from the top soil layer (A), the centre of the micaceous clay layer (B), and the middle of the Fine to coarse loose sand layer (C), respectively, to study the displacement of the different layers over time. All points along the stone column under the midpoint of the embankment were seen to deform almost the same with an average maximum settlement of 0.045 m as shown in figure 3.28. the results of stage deformation at the end of each stage is presented in table 3.18.

Table 3.18. Settlement of soil reinforced with Stone Column verse time at points A, B, and C

Stage	Stage 1	1ST Con	Stage 2	2ND Con	Stage 3	3RD Cond
Time (days)	2	12	14	24	26	3660
Settlement at C (m)	0.060	0.063	0.109	0.117	0.130	0.130
Settlement at D (m)	0.055	0.055	0.096	0.097	0.107	0.107
Settlement at E (m)	0.032	0.032	0.056	0.056	0.062	0.062

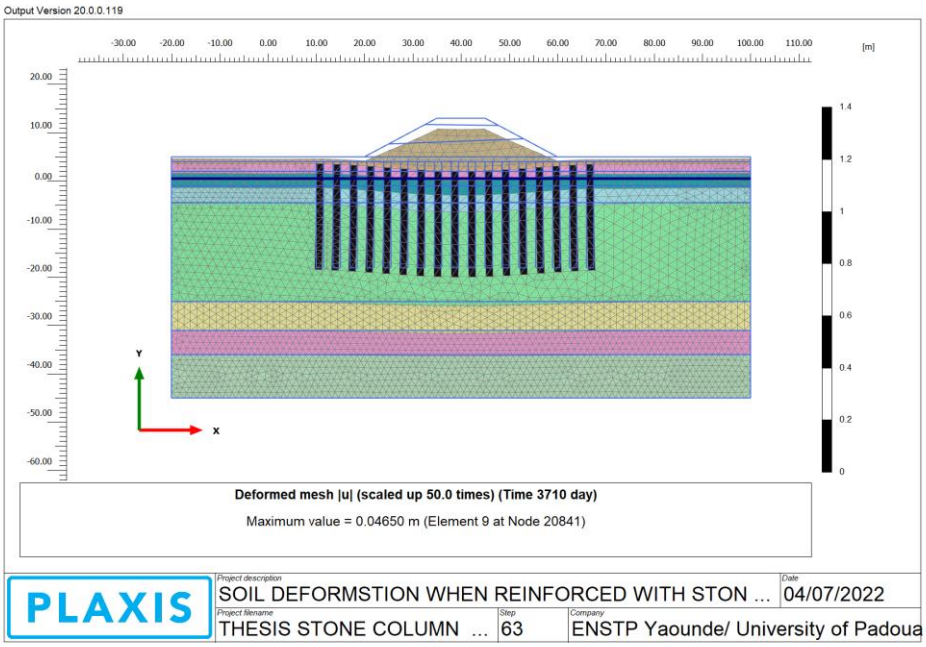

Figure 3.27. Deformation of soil reinforced with stone columns

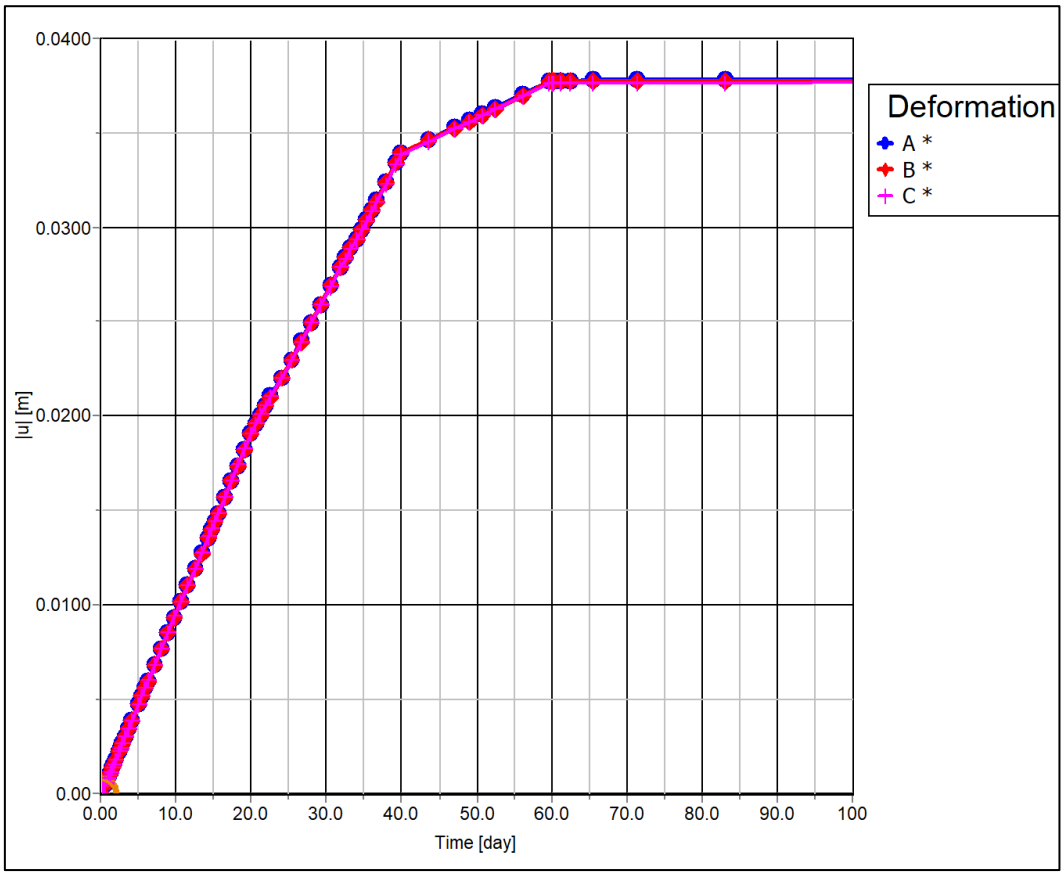

Figure 3.28. Comparative settlement of points A, B, and C of soils reinforced with Stone Columns

b. Variation of the excess pore with time for soil model reinforced with stone columns

When it comes to consolidation analysis, excessive pore pressure is essential because it affects the effective stress of the soil, which impacts the rate of consolidation. The same three points used to evaluate the settlement with time were the same points used to evaluate the pore pressure variation. All the points, A, B, and C had the same pressure variation with a maximum pore water pressure of 0.09 $\frac{kN}{m^2}$ shown in figure 3.29. from the analysis, pore pressure variation with time was minimal and values remained almost constant for all points of analysis indicating that all the embankment load applied was carried by the stone column.

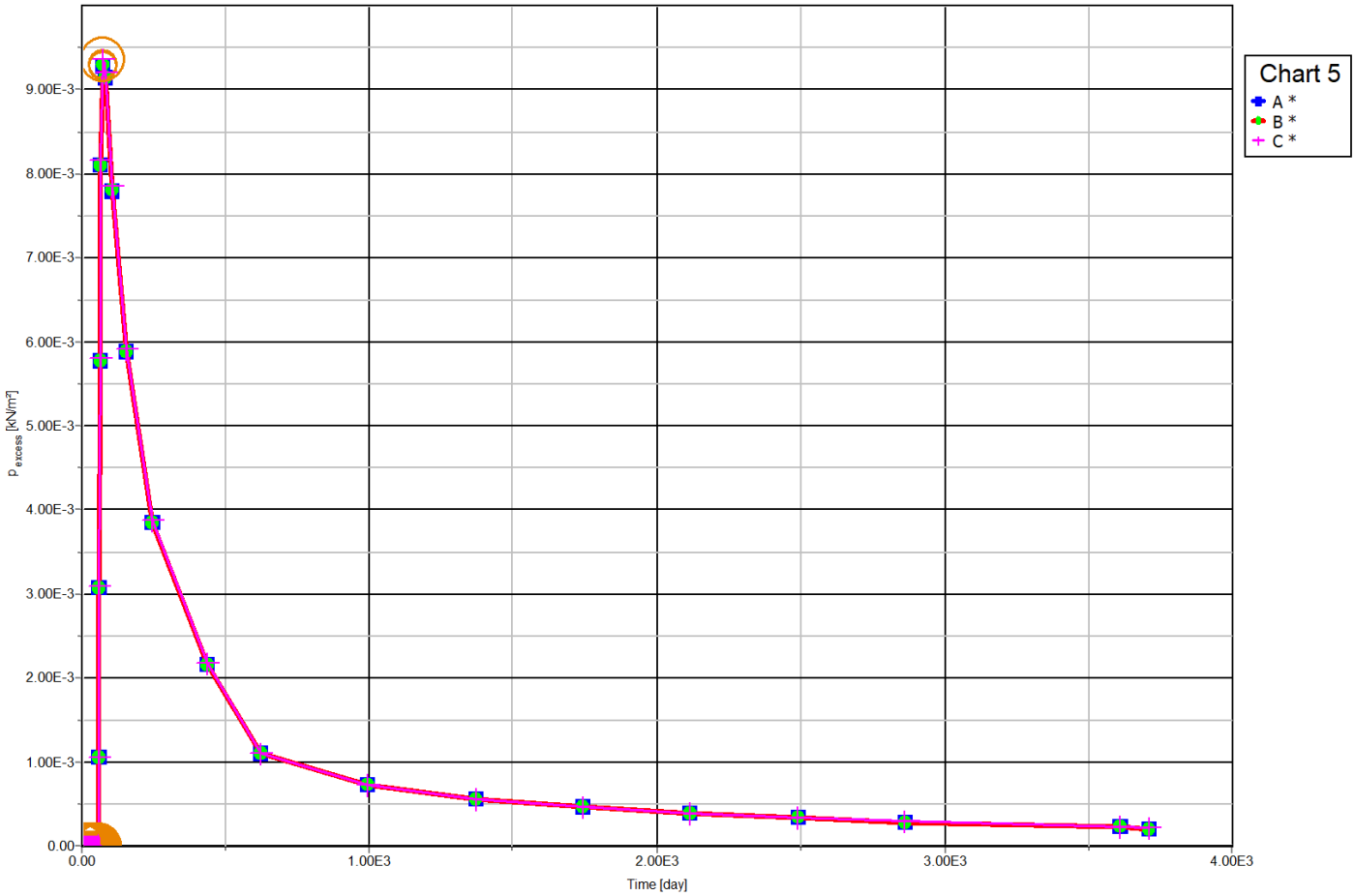

Figure 3.29. Excess Pore pressure variation over time at points A, B, and C for soil reinforced with stone columns.

3.4.3. Result interpretation

In the preceding paragraphs, a comparison of the consolidation time, pore pressure variation, and settling between the different approaches will be shown to discover which method is most suited for this particular scenario.

3.4.3.1. Effects of soil reinforcement with PVDs

An examination of the embankment settlement and excess pore pressures can provide the typical degree of consolidation during embankment construction. When comparing the settlement of the case without reinforcement and an embankment load of 9 m above the soil to the case reinforced with PVDs, it is seen that the use of PVDs reduces vertical shear deformation near the crest, heave at the toe, and horizontal deformation. Comparing points, A of both models (soil model without reinforcement, and soil model reinforced with PVD) it is seen that the settlement time is reduced by 79,2% (from 2050 days without reinforcement to 427 days when reinforced with PVD) which reduces the construction time to less than 1/4 of the initial construction time when dealing with soils without reinforcement. The average increase in undrained shear strength is somewhat constant throughout the thickness of the deposit due to the presence of PVDs. Figure 3.30 illustrates the calculated vertical displacements at ground level (point A) with and without PVD reinforcing at the end of construction.

Considering the effective pore water variation at point B (about midway through the soft soil layer under the embankment). There is a significant drop in the maximum pore pressure variation when the PVD is introduced. The maximum pressure variation drops from an initial value of 118 kN/m^2 to less than 19 kN/m^2. The rate of dissipation of the excess pore pressure experiences an 80.03 % reduction in dissipation time due to the presence of radial consolidation which facilitates this reduction. Figure 3.31 shows the variation of excess pore pressure at point B (soft soil layer) for both PVD-reinforced and unreinforced soils. The usage of prefabricated vertical drains has the advantage of speeding up the consolidation process by shortening the drainage path and taking advantage of the foundation soil's naturally higher horizontal hydraulic conductivity. PVDs are clearly capable of significantly improving foundation stability.

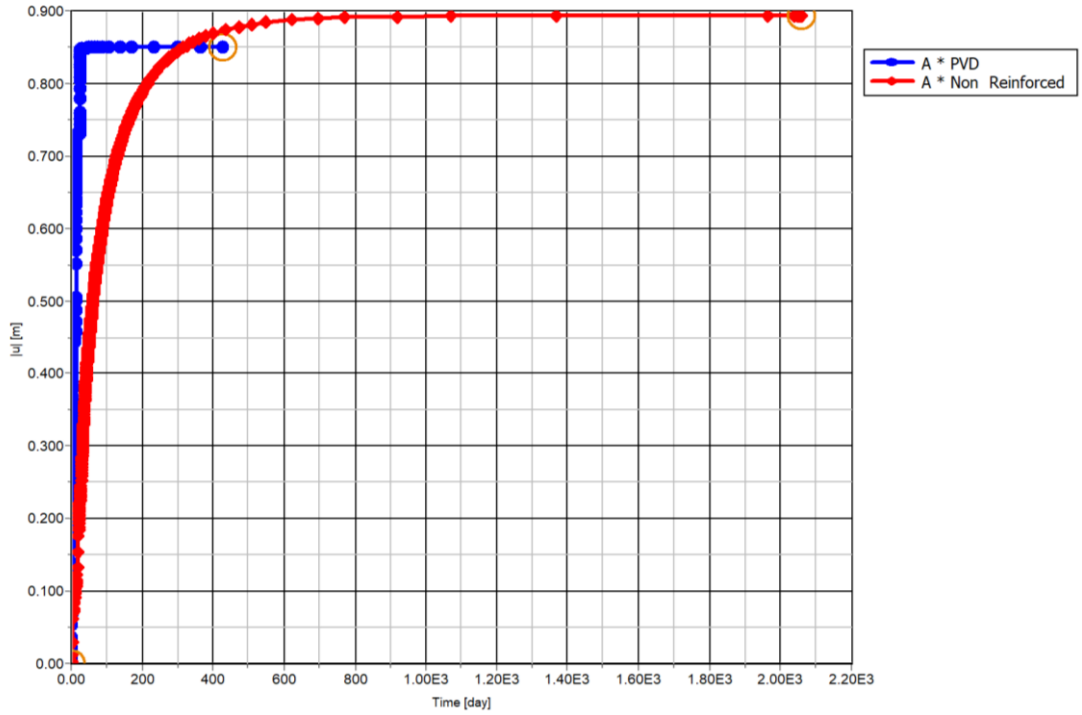

Figure 3.30. Comparative settlement of Point A reinforced with PVD (red) and point A with no soil reinforcement (blue)

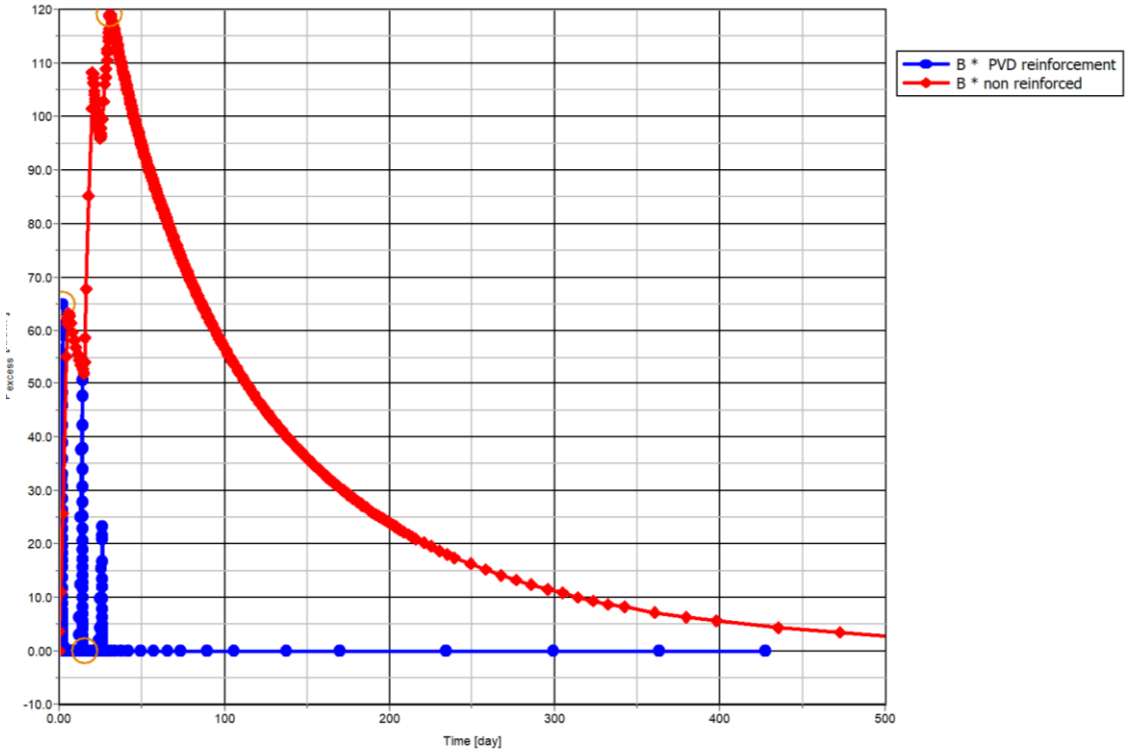

Figure 3.31. Comparative excess pore pressure variation of Point A reinforced with PVD (red) and point A with no soil reinforcement (blue)

3.4.3.2. Effects of soil reinforcement with stone columns

Stone columns also behave as vertical drains and because of the drained property of their constitutive material it accelerates the process of consolidation. Using identical parameters for analysis, the soil model without reinforcement during construction and within the project construction specified duration anticipated higher values for settlements. As expected, the settlement shrunk by a 96% reduction. Stone columns have an important function in reducing settlement in the structures on which they are built. Reinforcing the soils with stone columns transfers most of the load of the embankment to the stone columns reducing the excess pore pressure produced as a result of the embankment loading in the local soils that surrounds the stone column. Figure 3.32 represents the reduction of deformation of the soil caused by the installation of stone columns.

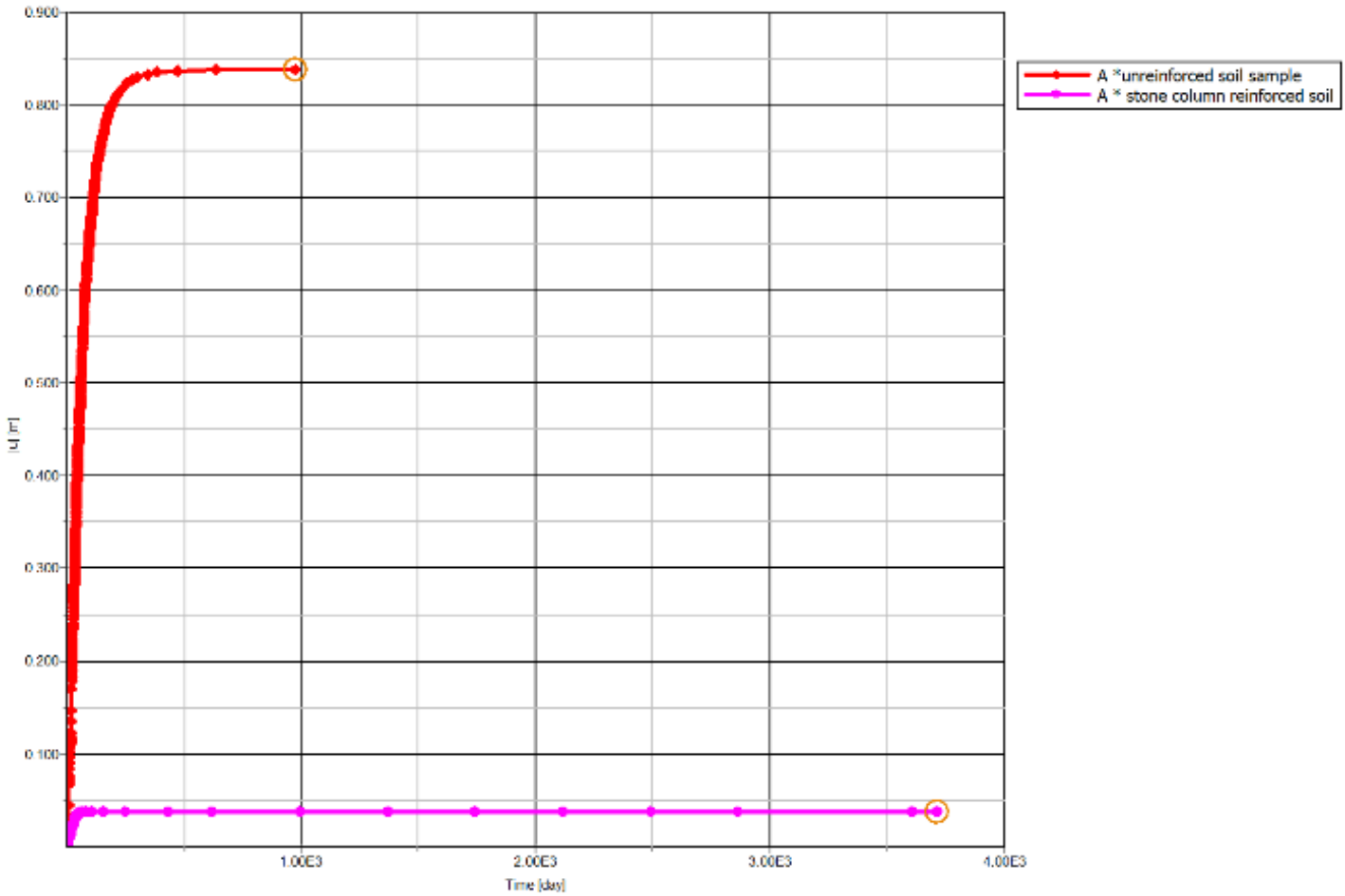

Figure 3.32. Comparative settlement of Point A reinforced with stone columns (purple) and point A with soil reinforcement (Red).

3.4.3.3. Comparative analysis of soils reinforced with PVD and soils reinforced with stone columns

The goal of civil engineering practice is to discover a solution to a specific problem, but identifying answers is rarely enough to bring a project to a successful conclusion. Optimisation is the process of continually seeking the optimum solution to a problem. For cost optimisation, cost values will be taken using the current prices of materials in Cameroon.

a. Economic evaluation of soil improvement by PVD associated with embankment for preloading

Three materials were used in the suggested solution: 25/63 Pozzolana, PVD, and embankment sand. Figure 3.19 can be used to calculate the amount of PVD required to calculate the section's cost. Table 3.19 illustrates the PVD installation quantity, material unit price, and overall cost, as well as embankment installation and removal. The cost of constructing a single section of reinforcement is reflected in this price (Details are available in Appendix 5).

Table 3.19. Cost of execution of a soil section reinforced with PVD

Material	Unit	Total Quantity	Cost Per Unit(FCFA)	Total Cost for a Section Installation (FCFA)
PVD	m	286	15000	4290000
cost of installation	m	286	25000	14,300,000
Embankment sand (installation/ removal)	m	225	14000	3150000
Pozzolana	m^3	40	21000	840000
Total				22,580,000

b. Economic evaluation of soil improvement by Stone Column

This proposed solution primarily consists of two materials: 25/63 Pozzolana, and gravel. The volume (cylinder) will be estimated using the equations in section 2.5 (equations 2.15 and 2.16) and the stone column quantity will be determined by starting from Figure 3.27 to determine the number of columns required. The quantity, the unit price of the material and the total cost required for stone column construction is represented in table 3.20 This cost represents the cost of construction for a single section of the reinforcement (detail results in appendix 6).

Table 3.20. Cost of execution of a soil section reinforced with stone column

Material	Unit	Total Quantity (m^3)	Cost Per Unit (FCFA)	Total Cost for a Section Installation (FCFA)
Stone Column (Gravel 25/63)	m^3	159.04313	93,000	19,085,175.37
Pozzolana	m^3	40	21,000	840,000
Cost of installation	m^3	159.04313	30,000	4,771,293.843
Total				**39,010,350.74**

c. Multi-criteria Analysis

The cost of a solution for soil reinforcement by PVD with a preloading embankment of a soil section is anticipated to be around 22,580,000FCFA, which includes the costs of preloading and unloading embankments as well as the PVD. The cost of installing a Colbond drain linear metre is 25000FCFA. The cost of the second option, stone column reinforcement, is estimated to be around 39,010,350.74 FCFA. 30000FCFA is the cost of installing a meter cube stone column. Tables 3.19 and 3.20 show that the PVD reinforcing approach reduces the cost of the abutment foundation by approximately 42.1 %. When compared to the use of PVD, which includes a consolidation time, similar projects using stone column reinforcement demonstrate that construction duration is on average 7 months, time beneficial. PVD enhancement takes longer to construct than stone column reinforcement because it comprises preloading and unloading processes during embankment construction. The benefits of each specification of both soil reinforcement techniques that might be employed to stabilise the foundation of the abutment of the second bridge over the river Wouri are summarised in Table 3.21.

Table 3.21. Multi-criteria analysis of studied improvement

Techniques	Reinforcement by PVD	Stone Column reinforcement
Qualification of local entrepreneurs	Good	Good
Duration of execution	16 months	7 months
Environmental impact	insignificant	insignificant
Cost	Less Costly (42.1% less)	More costly

Conclusion

This chapter's main goal was to report and evaluate the results of the soil reinforcement beneath the abutment wall of the second bridge across the Wouri River. To do this, a comprehensive overview of the site was offered, focusing on its geographic location, relief, geology, economic activity, climate, and hydrology. The findings of the various reinforcement procedures (stone columns and PVD) were presented after a brief discussion of the project data. A cost analysis was used to start a multi-dimensional comparison of the numerous soil reinforcing techniques that were explored during this study. Finally, the appropriateness of the various approaches to the local environment was assessed.

GENERAL CONCLUSION

The study was conducted to determine possible cost-effective methods for strengthening the soft soil bed beneath the abutment wall of the second bridge over the Wouri River. A review of the fundamental principles of soft soils and their property were conducted. Following that, various reinforcement approaches were examined in depth to determine which ones were most suited to the case study in general. An analytical simulation was performed as a control for the numerical simulation. Two soil improvement techniques were investigated: the first was PVD drilling to a depth of 10 m, followed by the step-by-step construction of a preloading embankment; the second was stone column reinforcement to a depth of 20 m. 2D finite element studies were performed using the finite element computer program PLAXIS V20.02. The numerical simulations detailed in this study were the outcome of two-dimensional finite element analysis. A series of comprehensive parametric studies were conducted to investigate the impact of variations in the values of various design methods (preloading, PVD coupled with preloading, or stone column soil reinforcement) on the performance of bearing on a compressible soil layer and the ability to be accepted in project terms.

The findings of 2D finite element assessments of the soil when reinforced with various materials revealed the benefits of different reinforcement methods when different project parameters were considered. In the analysis, time, cost, and the availability of an experienced labour force were all taken into account. As a result of these investigations, the following conclusions were reached:

- The response to reinforcement is influenced by the mechanical qualities of the soft soil layer beneath a soil bed.
- PVD proved to be a practical method for achieving a high degree of primary consolidation when used in conjunction with preloading embankments. As a result, a large portion of the settlement will be released during the period when access embankments are being built. The effectiveness of PVD soil improvement is mostly determined by the drain spacing used. Using PVD for soil reinforcement turns out to reduce the cost of construction by 42% less than soil reinforced with stone columns.
- Stone columns Reinforcement used to reach a settlement limit of less than 5 cm from project specifications results in a reduction in project execution time. This

reinforcement approach guarantees a large improvement in bearing capacity, a reduction in the consolidation settlement, and quicker consolidation.

- In terms of time savings, using stone column reinforcement rather than PVD would be preferable. The use of stone column reinforcement can cut the time it takes to build a foundation in half (50% reduction in time). As a result, this strategy is appropriate for projects with a short life cycle and tight deadlines.
- In a multi-criteria comparison of the two improvement strategies, the PVD was found to be more advantageous from an economic standpoint. Both stabilisation approaches have experienced workers from nearby companies who have worked on similar projects and have a lower environmental impact on the soils.

Further research could include the use of geogrids or geosynthetics as an encasement to increase confinement and thus the capacity of stone columns; the impact of cementing the upper half of the column on its capacity; as well as a cost comparison of the two methods to determine which is the most cost-effective.

BIBLIOGRAPHY

Abbey, S. J., Ngambi, S. & Ngekpe, B. E. (2015). Understanding the Performance of Deep Mixed Column Improved Soils – A Review. *International Journal of Civil Engineering and Technology (IJCIET)*, *6*(3), 97–117.

Ahmad, S. A. R., Aliff, R. B., & Khairun, N. M. S. (2017). *The Deep Mixing Method: Bearing Capacity Studies*. Springer International Publishing Switzerland. https://doi.org/DOI 10P1007/s10706-107-0196-x

ASTM. (2017). Standard Practice for Classification of Soils for Engineering Purposes (Unified Soil Classification System). *Engineering Village*, *v*, 2021. https://doi.org/10.1520/D2487-17

Azhani, Z. & Ramli, N. (2018). Numerical modelling techniques of soft soil improvement via stone columns: A brief review. *Research Gate*, *April*. https://doi.org/10.1088/1757-899X/342/1/012002

Balasubramaniam, A. S., & Brenner, R. P. (1981). Consolidation and settlement of soft clay. In *Developments in Geotechnical Engineering* (Vol. 20, Issue C, pp. 479–566). Elsevier Scientific Publishing Company, Amsterdam. https://doi.org/10.1016/B978-0-444-41784-8.50010-1

Barksdale, R. D. & Bachus, R. C. (1983). Design and Construction of stone Column Vol. 1 – FHWA Report No. FHWA-RD-83/026. *Geotechnical Engineering Circular*, *December 1983*.

Bell, F, G. (1993). *Engineering Treatment of Soils*. E and FN Spon, Taylor & Francis group.

Bergado, D. T., Alfaro, M. C., & Balasubramaniam, A. S. (1993). Improvement of soft Bangkok clay using vertical drains. *Geotextiles and Geomembranes*, *12*(7), 615–663. https://doi.org/10.1016/0266-1144(93)90032-J

Bertil, N. (2019). Hydrological processes in a hyper-humid coastal area with strong anthropogenic influences (Douala, Cameroon): A geochemical study of water dynamic from the atmosphere to the subsurface. *Hdrology, Université Bourgogne Franche-Comté; Université de Douala*.

Bilal, M. & Talib, A. (2016). A study on advances in ground improvement techniques. *Research*

Gate, *April*. https://doi.org/10.13140/RG.2.1.4865.4965

Bolton, M. D. (1986). The strength and dilatancy of sands. *Géotechnique*, *Vol. 36 No*(I), 55–78.

Bowles, J. E. (1997). *Foundation Analysis and Designs Fifth Edition* (Fifth Edit). The McGraw-Hill Companies, Inc.

Brinkgreve, R. (2002). PLAXIS Version 8 Material Models Manual. In *Plaxis*.

Brinkgreve, R. (2006). PLAXIS Version 8 Reference Manual. *PLAXIS Version 8 Reference Manual STATIK*, *33*(June).

Brinkgreve, R. B. J., & Engin, E. (2010). Validation of empirical formulas to derive model parameters for sands. *Research Gate*, *January 2015*. https://doi.org/10.1201/b10551-25

Bruce, D. A. (2000). *An Introduction to the Deep Soil Mixing Methods as Used in Geotechnical Applications* (FHWA_RD-99). Federal Highway Administration.

Budhu, M. (2011). *SOIL MECHANICS AND FOUNDATIONS* (3rd Editio). John Wiley & Sons, Inc.

Chen, W. F. & Duan, L. (2014). Bridge engineering handbook, second edition: Substructure design. In C. Wai-Fah & D. Lian (Eds.), *Bridge Engineering Handbook, Second Edition: Substructure Design* (second edition). Taylor & Francis. https://doi.org/10.1201/b15621

Cheng-hou, Z. (Nanjing H. R. I., Greeuw, G., Jekel, J., & Rosenbrand, W. (1990). A new classification chart for soft soils using the piezocone test. *Engineering Geology*, *29*, 31–47.

Chew, S. H., Kamruzzaman, A. H. M. & Lee, F. H. (2004). Physicochemical and Engineering Behavior of Cement Treated Clays. *Journal of Geotechnical and Geoenvironmental Engineering*, *130*(7), 696–706. https://doi.org/10.1061/(ASCE)1090—0241(2004)130:7(696)

Christopher, B. R., Gill, S. A., Giroud, J.-P., Juran, I., Mitchell, J. K., Schlosser, F., & Dunnicliff, J. (1990). Reinforced Soil Structures Volume I. Design and Construction Guidelines. *FHWA Report No. FHWA-RD-89-043*, *I*, 326. https://rosap.ntl.bts.gov/view/dot/972

Chu, J., Indraratna, B., Yan, S., & Rujikiatkamjorn, C. (2014). Overview of preloading methods for soil improvement. *Proceedings of the Institution of Civil Engineers – Ground Improvement*, *167*(3), 173–185. https://doi.org/10.1680/grim.13.00022

Colbond. (2008). *Colbonddrain ® CX1000*. 1–2.

David, E., Paul, G. & Justin, Z. (2014). *How to Write a Better Thesis* (3rd Edition). Springer New York.

De Beer, E. E. (1985). Golden Jubilee of the ISSMFE, Belgian Soci&y o f ISSMFE. In *Proceedings XV International Conference on Soil Mechanics and Geotechnical*.

Demetrios, E. T., & Jim, J. Z. (1995). Bridge engineering: design, rehabilitation, and maintenance of modern highway bridges. In *Choice Reviews Online* (Second Edition, Vol. 32, Issue 09). McGraw-Hill. https://doi.org/10.5860/choice.32-5110

Gouw, T. L. (2020). Case Histories on the Application of Vacuum Preloading and Geosynthetic-Reinforced Soil Structures in Indonesia. *Indian Geotechnical Journal*, *50*(2), 213–237. https://doi.org/10.1007/s40098-019-00391-5

Han, J. (2015). *Principles of Ground Improvement* (1st ed.). John Wiley & Sons, Inc.

Hansbo, S. (1987). 9th-SEAC-Bangkok Thailand-7-11 December 1987. *Design Aspect of Vertical Drains and Lime Column Installation*, 398–409.

Hansbo, S., Jamiolokowski, M., & Koks, L. (1974). Consolidation by Vertical Drains. *Institute of Civil Engineers*, 45–66. https://doi.org/https://doi.org/10.1680/geot.1981.31.1.45

Hawlader, B. C., Imai, G., & Muhunthan, B. (2002). Numerical study of the factors affecting the consolidation of clay with vertical drains. *Geotextiles and Geomembranes*, *20*(4), 213–239. https://doi.org/10.1016/S0266-1144(02)00012-2

Hong, H. P., & Shang, J. Q. (1998). *Probabilistic analysis of consolidation with prefabricated vertical drains for soil improvement*. 666–677.

Hu, Y., Zhou, W., & Cai, Y. (2014). *Large-strain elastic viscoplastic consolidation analysis of very soft clay layers with vertical drains under preloading*. *157*(November 2013), 144–157.

Huat, B. B. K., Maail, S., & Mohamed, T. A. (2005). Effect of Chemical Admixtures on the

Engineering Properties of Tropical Peat Soils. *American Journal of Applied Sciences*, *2*(7), 1113–1120. https://doi.org/10.3844/ajassp.2005.1113.1120

Iskandar, R., Perwira, A., & Tarigan, M. (2018). *A Review on the Characteristics of the Smear Zone: Field Data Back Calculation Compared with Laboratory Testing A Review on the Characteristics of the Smear Zone: Field Data Back Calculation Compared with Laboratory Testing*. *November*. https://doi.org/10.2174/1874149501812010340

Kempfert, H.-G. (Universitat kassel), & Gebreselassie, B. kassel). (2006). *Excavations and Foundations in Soft Soils*. Springer Verag, Netherlands.

Kim, J., & Kim, D. (2018). Classification of inorganic natural fine-grained soils in Korea based on modified plasticity chart. *Marine Georesources and Geotechnology*, *36*(5), 579–588. https://doi.org/10.1080/1064119X.2017.1354101

Kim, P., Kim, T. C., Kim, Y. G., Myong, H. B., Jon, K. S., & Jon, S. H. (2021). Nonlinear consolidation analysis of soft soil with vertical drains considering well resistance and smear effect under cyclic loadings. *Geotextiles and Geomembranes*, *49*(5), 1440–1446. https://doi.org/10.1016/j.geotexmem.2021.05.012

Knapetts, J. A., & Criag, R. F. (2012). *Craig's Soil Mechanics* (8th edition). Spon Press.

Makusa, G. P. (2012). *Soil Stabilisation Methods and Materials in Engineering Practice*. *1*, 1–35.

Mary, E. C. B., Ryan, R. B., James, G. C., George, M. F., Terashi, M., & David, S. Y. (2013). *Federal Highway Administration Design Manual: Deep Mixing for Embankment and Foundation Support*. *FHWA_HRT_1*(October).

Mitchell, J. K. (1981). Soil improvement-State-of-the-Art Report. *INTERNATIONAL SOCIETY FOR SOIL MECHANICS AND GEOTECHNICAL ENGINEERING*.

Mitchell, J. K., & Soga, K. (2005). *Fundamentals of Soil Behavior* (3rd edition, Vol. 4, Issue 4). John Wiley & Sons, Inc. https://doi.org/10.1097/00010694-199407000-00009

Mohamad, F. A., Rahman, A. A. A., Abdul, K. N., Hettige, N. D., Rohasliney, H., Ashaari, Z. H. B., Maegala, N. M., Suhaila, Y. N., & Hasdianty, A. (2016). Challenges in Construction Over Soft Soil – Case Studies in Malaysia. *Materials Science and Engineering*, 0–8. https://doi.org/10.1088/1757-899X/136/1/012002

Moreno-Maroto, J. M., Alonso-Azcárate, J., & O'Kelly, B. C. (2021). Review and critical examination of fine-grained soil classification systems based on plasticity. *Applied Clay Science*, *200*(August 2020). https://doi.org/10.1016/j.clay.2020.105955

Murthy, V. N. S. (2003). *Geotechnical Engineering: Principles and Practices of Soil Mechanics and Foundation Engineering* (1st Edition). CRC Press. https://doi.org/https://doi.org/10.1201/9781482275858

Osterberg, J. O. (1957). Influence values for vertical stresses in a semi-infinite mass due to an embankment loading. *Proceedings of the 4th International Conference on Soil Mechanics and Foundation Engineering*, *1*, 393–394.

PLAXIS. (2012). *PLAXIS 2D Reference Manual 2012*.

PLAXIS. (2021). *Material Models Manual: PLAXIS CONNECT Edition V20.02*.

Porbaha, A. (1998). State of the art in deep mixing technology: part I. Basic concepts and overview. *Ground Improvement*, *2*(2), 81–92. https://doi.org/10.1680/gi.1998.020204

Pourakbar, S. (2015). Deep Mixing Columns. *Pertanika Journal of Scholarly Research Reviews*, *1*, 8–17.

Rixner, J, J, Kraemer, S, R., & Smith, A, D. (1986). *Prefabricated Vertical Drains Vol. I Engineering Guidelines* (first edition). Springfield Virginia.

Robertson, P. K. (1989). *Soil classification using the cone penetration test.* 151–158.

Sagea-Satom. (2015). *Geotechnique, Rapport de mission G3; justification du bloc technique PC7-C8*.

Schaefer, V. R, Berg, R. R., Collin, J. G., Christopher, B. R., DiMaggio, J. A., Filz, G. M., Bruce, D. A., & Ayala, D. (2017a). Ground Modification Methods – Reference Manual – Volume II. *Publication No. FHWA NHI-16-028 FHWA GEC 013*, *II*(132034), 542.

Schaefer, V. R, Berg, R. R., Collin, J. G., Christopher, B. R., DiMaggio, J. A., Filz, G. M., Bruce, D. A., & Ayala, D. (2017b). Ground Modification Methods Reference Manual – Volume I [FHWA-NHI-16-027]. *Geotechnical Engineering Circular No. 13*, *I*(132034), 386.

seyedmohsen, M. (2020). *Master Thesis: Tunnelling-induced deformation and damage on*

framed structures with masonry infills. *October*.

Sharma, J. S., & Xiao, D. (2000). Characterisation of a smear zone around vertical drains by large-scale laboratory tests. *Canadian Geotechnical Journal*, *37*(6), 1265–1271. https://doi.org/10.1139/t00-050

Skempton, A. W, & Bjerrum, L. (1984). A Contribution to the Settlement Analysis of Foundations on Clay. *Selected Papers on Soil Mechanics*, 74–84. https://doi.org/10.1680/sposm.02050.0012

Tening, A. S., Chuyong, G. B., Asongwe, G. A., Fonge, B. A., Lifongo, L. L., & Tandia, B. K. (2013). *Nitrate and ammonium levels of some water bodies and their interaction with some selected properties of soils in Douala metropolis, Cameroon*. *7*(July), 648–656. https://doi.org/10.5897/AJEST12.082

Terashi, M. (2004). The State of Practice in Deep Mixing Methods. *Grouting and Ground Treatment*.

Terzaghi, K. (1943). *Theoretical Soil Mechanics*. John Wiley & Sons, Inc.

Terzaghi, K., Peck, R. B., & Mesri, G. (1996). Soil Mechanics in Engineering Practice.pdf. In *John Wiley & sons* (p. 534).

Tsuruoka, T., & Yamakawa, M. (1996). Sand drain works for a large-scale man-made island. *Marine Georesources and Geotechnology*, *14*(3), 251–262. https://doi.org/10.1080/10641199609388315

Unizjersity, H. (1969). *On the effectiveness of sand drains*. *287*.

Wang, J.-H, Desai, C. S., & Zhang, L. (2019). Soft Soil and Related Geotechnical Engineering Practice. *International Journal of Geomechanics*, *19*(11), 02019001. https://doi.org/10.1061/(ASCE)gm.1943-5622.0001494

Wang, J., & Zhang, L. (2019). *Soft Soil and Related Geotechnical Engineering Practice*. *18*(10), 4018131. https://doi.org/10.1061/(ASCE)GM.1943-5622.0001494

Win, M. B. (senior V. P. senior P. G.-S. (2015). Marine Georesources & Geotechnology Step Loading Compression of Ultra-Soft Soil Under Radial Drainage Conditions. *Marine Georesources and Geotechnology*, *August*. https://doi.org/10.1080/1064119X.2015.1068895

Zhao, Z. (2018). Highway Construction of Soft Soil Foundation Processing Analysis. *Research Gate*, 31–33. https://doi.org/http://dx.doi.org/10.30564/frae.v1i1.10

Zhou, F, Xia, T., Yu, B., Xia, F., & Yu, F. (2021). *A Practical Design Method for Reducing Postconstruction Settlement of Highway Subgrade Induced by Soil Creep*. *2021*. https://doi.org/https://doi.org/10.1155/2021/4029439

APPENDICES

Appendix 1

Christian and Carter graphs for calculating the Coefficient function of D/B, μ_0 and Coefficient function of H/B and L/B μ_1

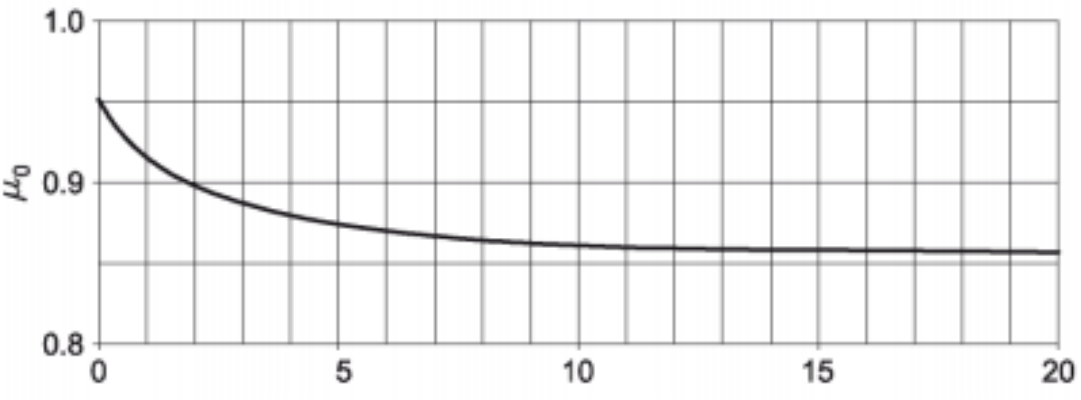

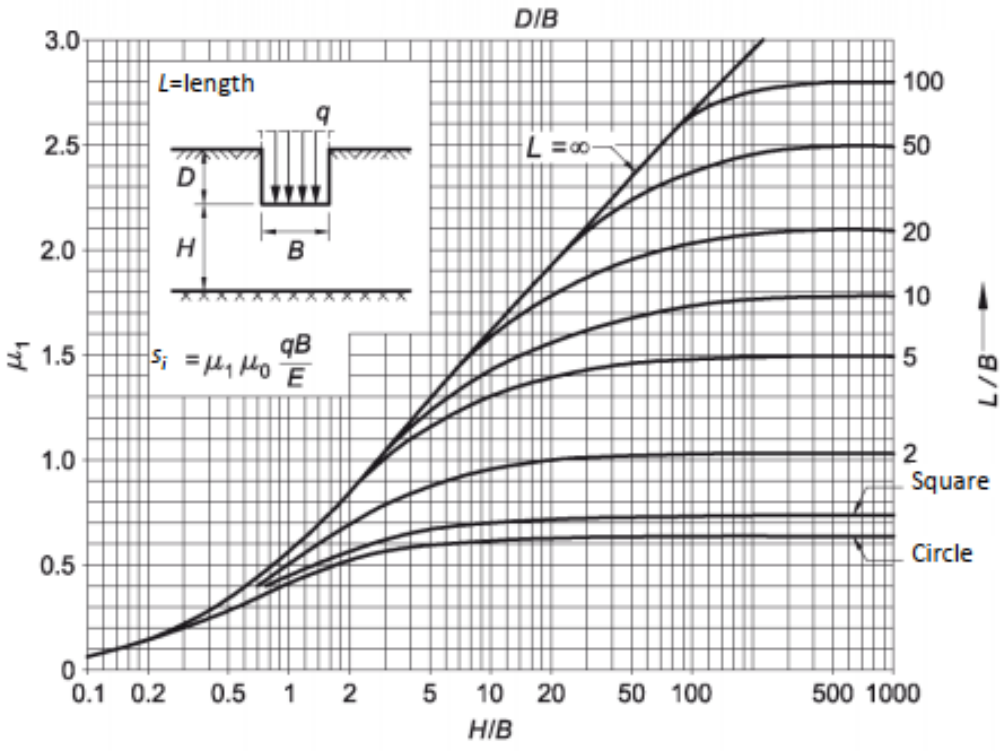

Appendix 2

Common types of vertical drains(Rixner et al., 1986)

General Type	Sub-Types	Remarks
SAND DRAINS	Closed end mandrel	Maximum displacement
	Screw type auger	Limited experience
	Continuous flight hollow stem auger	Limited displacement
	Internal jetting	Difficult to control
	Rotary jet	Can be non-displacement
	Dutch jet-bailer	Can be non-displacement
FABRIC ENCASED SAND DRAIN	Sandwick, Pack Drain, Fabridrain	Full displacement of relatively small volume
PREFABRICATED VERTICAL DRAIN	Cardboard drain	Full displacement of small volume
	Fabric covered plastic drain	Full displacement of small volume
	Plastic drain without jacket	Full displacement of small volume

Appendix 3

General Applicability of soil stabilisation Technologies(Schaefer et al., 2017b)

Category	Technologies	Applicability
Vertical Drains and Accelerated Consolidation	PVDs, with and without fill preloading	Compressible clays, saturated low strength clays
Lightweight Fills	Compressive Strength Fills: Geofoam; Foamed Concrete	Broad applicability; no geologic or geometric limitations
Lightweight Fills	Granular Fills: Wood Fiber; Blast Furnace Slag; Fly Ash; Boiler Slag; Expanded Shale, Clay, and Slate; Tire Shreds	Broad applicability; no geologic or geometric limitations
Deep Compaction	Deep Dynamic Compaction	Loose pervious and semi-pervious soils with fines contents less than 15%, materials containing large voids, spoils and waste areas
Deep Compaction	Vibro-Compaction	Cohesionless soils, clean sands with less than 15% silts and/or less than 2% clay
Aggregate Columns	Stone Columns	Clays, silts, loose silty sands, and uncompacted fill
Aggregate Columns	Rammed Aggregate Piers	Clays, silts, loose silty sands, uncompacted fill
Column Supported Embankments	Column Supported Embankments	Soft compressible clay, peats, and organic soils where settlement and global stability are concerns
Column Supported Embankments	Reinforced Soil Load Transfer Platform	Soft compressible clay, peats, and organic soils where settlement and global stability are concerns
Column Supported Embankments	Columns: Non-compressible	All soil types, in particular weak soils that cannot support surface loads
Column Supported Embankments	Columns: Compressible	All soil types except very soft soils low undrained shear strength
Soil Mixing	Deep Mixing	Suitable in large range of soils, ones that can be stabilized with cement, lime, slag, or other binders
Soil Mixing	Mass Mixing	Peat, soft clay, dredged soil, soft silt, sludges, contaminated soils
Grouting	Chemical (Permeation) Grouting	Wide range of soil types including weakly cemented rock-fill materials

Appendix 4

Skempton-Bjerrum graph for the calculation of the correction factor used in the conversion of the oedometric settlement to primary consolidation settlement.

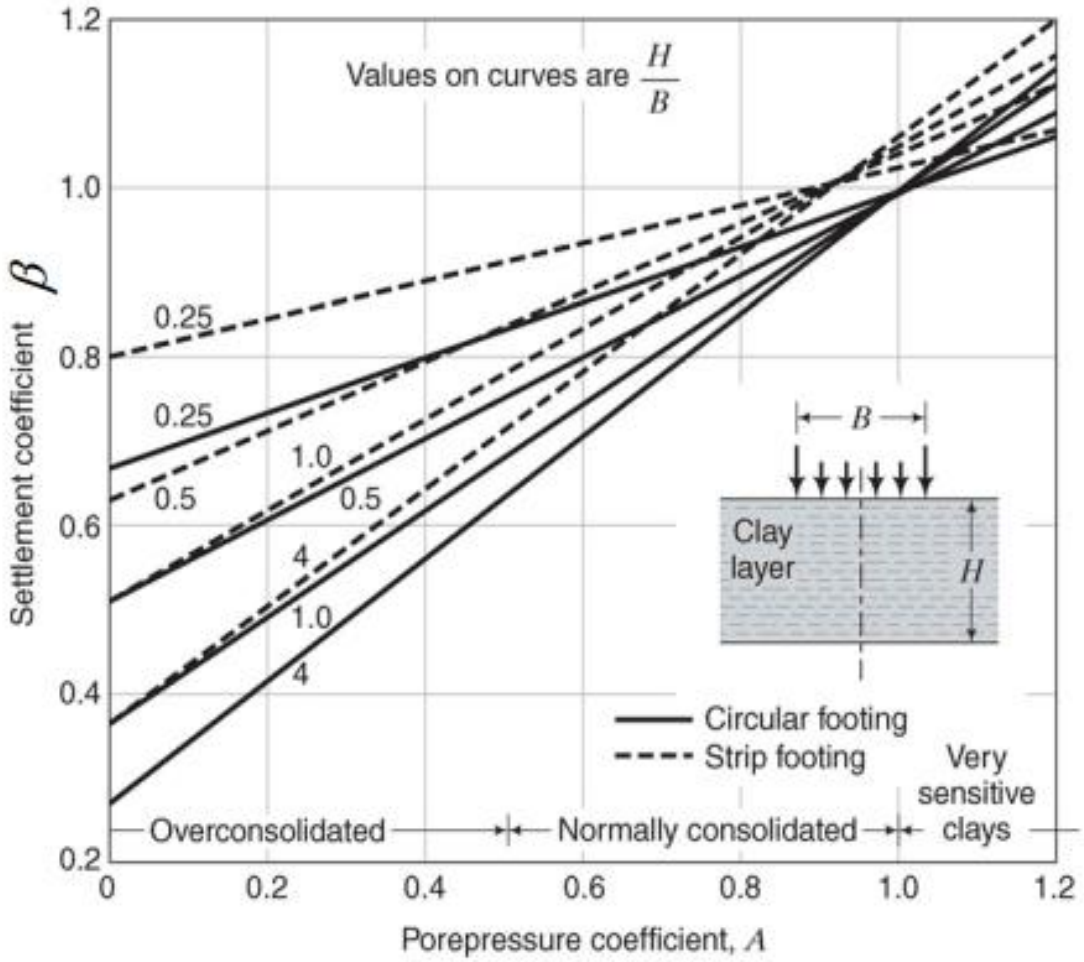

CLAY TYPE	A Value
Sensitive Clays	1.0 ÷ 1.2
NC Clays	0.7 ÷ 1.0
OC Clays	0.5 ÷ 0.7
>> OC Clays	0.2 ÷ 0.5

Appendix 5

Cost estimations for soil section reinforced with PVD

Unit cost of a section of PVD reinforcement section	
No of PVD	26
length of PVD	11 m
Total length of PVD	286 m
PouzaLane Layer	
depth of layer	1 m
width of layer	40 m
unit lenth of layer	1 m
volumn of pouzalane layer	40 m^3
embankment layer	
height of layer(H)	9 m
lager length(A)	40 m
small length of layer(B)	10 m
width of considered section of embankment	1 m
volume of embankment section	225 m^3

Calculation of the volume of section embankment sand

$$\frac{1}{2}(A+B)*W*H$$

Material	unit	total quantity	cost per unit(FCFA)	total cost for a section installation (FCFA)
PVD	**m**	**286**	**15000**	**4290000**
cost of installation	**m**	**286**	**50000**	**14300000**
Embankment sand (installation/ removal)		**225**	**14000**	**3150000**
Pouzalanna		**40**	**21000**	**840000**
Total				**22580000**

Appendix 6

Cost estimation for soil section reinforced with stone columns

Unit cost of a section of the stone column reinforcement section		
No of stone column	18	
length of stone column	20 m	Calculation of the volume of stone columm $L * \pi * \left(\frac{D}{4}\right)^2$
diameter of stone column	1.5 m	
volume of single stone column	35.3429 m^3	
total volumn of stone column	636.173 m^3	
PouzaLane Layer		
depth of layer	1 m	
width of layer	40 m	
unit lenth of layer	1 m	
volumn of pouzalane layer	40 m^3	

Material	unit	total quantity	cost per unit(FCFA)	section installation (FCFA)
stone Column (Gravel 25/63)		**636.1725**	**30000**	**19085175.37**
cost of instalation	**m**	**636.1725**	**30000**	**19085175.37**
Pouzalanna		**40**	**21000**	**840000**
Total				**39010350.74**